Energy-converting [NiFe] hydrogenases in archaea and bacteria: insights into the energy-transducing mechanism

DISSERTATION

zur
Erlangung des Doktorgrades
der Naturwissenschaften
(Dr. rer. nat.)

dem Fachbereich Biologie
der Philipps-Universität Marburg
vorgelegt von

Lucia Forzi
aus Mailand/Italien

Marburg/Lahn im Juni 2005

Die Untersuchungen zur vorliegenden Arbeit wurden von März 2002 bis April 2005 am Max-Planck-Institut für terrestrische Mikrobiologie unter der Leitung von Herrn PD Dr. Reiner Hedderich durchgeführt.

Vom Fachbereich Biologie der Philipps-Universität Marburg als Dissertation
angenommen am: 18.08.2005

Erstgutachter: PD Dr. Reiner Hedderich

Zweitgutachter: Prof. Dr. Wolfgang Buckel

Tag der mündlichen Prüfung am: 24.08.2005

Ein Teil der während der Promotion erzielten Ergebnisse wurde in folgender Originalpublikation veröffentlicht:

Forzi, L., Koch, J., Guss, A. M., Radosevich, C. G., Metcalf, W. W. and Hedderich, R. (2005). Assignment of the [4Fe-4S] clusters of Ech hydrogenase from *Methanosarcina barkeri* to individual subunits via the characterisation of site-directed mutants. *FEBS Journal*, 272, 4741-4753.

Die in dieser Arbeit erzielten Ergebnisse wurde im folgenden Übersichtsartikel dargestellt:

Hedderich, R. and Forzi, L.(2005). Energy-converting [NiFe] hydrogenases: more than just H_2 activation. *Journal of Molecular Microbiology and Biotechnology*, eingereicht.

Dedicated to my family

TABLE OF CONTENTS

LIST OF ABBREVIATIONS

BV	Benzyl viologen
CCCP	Carbonylcyanide-*m*-chlorophenylhydrazone
CoM-S-S-CoB	Heterodisulfide of H-S-CoM and H-S-CoB
DCCD	*N,N'*-dicyclohexylcarbodiimide
DTT	1,4 Dithiothreitol
$\Delta G°'$	Standard Gibbs energy change at pH 7
$\Delta\mu_{H^+}$	Transmembrane electrochemical proton gradient
$\Delta\mu_{Na^+}$	Transmembrane electrochemical sodium ion gradient
ΔpH	Transmembrane gradient of protons
$\Delta\Psi$	Transmembrane electrical gradient (mV)
ε	Molar absorbtion coefficient (mM^{-1} cm^{-1})
E°'	Standard redox potential at pH 7
Ech	Energy converting hydrogenase
EDAC	1-ethyl-3-(3-dimethylaminopropyl)-carbodiimide
EIPA	5-(*N*-ethyl-*N*-isopropyl)-amiloride
ETH-157	*N,N'*–dibenzyl-*N,N'*–diphenyl-1,2-phenylenedioxydiacetamide
Fd	Ferredoxin
Hdr	Heterodisulfide reductase
H-S-CoB	7-mercaptoheptanoylthreonine phosphate (coenzyme B)
H-S-CoM	2-mercaptoethanesulfonate (coenzyme M)
MTZ	Metronidazole
Ni_a-L	Paramagnetic state of the [NiFe] center produced from the EPR-detectable active state (Ni_a-C) upon illumination

Standard abbreviations, indicated in the information for authors in the *European Journal of Biochemistry*, have been used without definition.

I SUMMARY

In recent years a group of multisubunit membrane-bound [NiFe] hydrogenases has been identified in a variety of anaerobic or facultative anaerobic microorganisms. These enzymes share two conserved integral membrane proteins and four conserved hydrophilic proteins with the energy-conserving NADH:quinone oxidoreductases (complex I). Based on experimental evidence derived from physiological and biochemical studies, the various members of this hydrogenase family have been proposed to function as ion pumps being involved in energy-conserving electron transport, reverse electron transport, or both. Therefore these enzymes have been designated energy-converting [NiFe] hydrogenases. In the present work the energy transducing mechanism of energy-converting hydrogenases was studied in comparison to complex I. A particular attention was given to the prosthetic groups involved in the electron transfer pathway, the role of the membrane part and the identification of the coupling ion used by these enzymes. The majority of the experiments were carried out with Ech hydrogenase from *Methanosarcina barkeri*.

The sequence of Ech hydrogenase predicts the binding of three [4Fe-4S] clusters, one by subunit EchC and two by subunit EchF. Previous studies had shown that two of these clusters could be fully reduced under 1 bar of H_2 at pH 7 giving rise to two distinct S ½ EPR signals, designated as the g = 1.89 and the g = 1.92 signal. Redox titrations at different pH values demonstrated that these two clusters had a pH-dependent midpoint potential indicating a function in ion pumping. To assign these EPR signals to the subunits of the enzyme a set of *M. barkeri* mutants was generated in which seven of eight conserved cysteine residues in EchF were individually replaced by serine. EPR spectra recorded from the isolated mutant enzymes revealed a strong reduction or complete loss of the g = 1.92 signal whereas the g =1.89 signal was still detectable as the major EPR signal in five mutant enzymes. It is concluded that the cluster giving rise to the g = 1.89 signal is the proximal cluster located in EchC and that the g = 1.92 signal results from one of the clusters of subunit EchF. The pH-dependent midpoint potential of these two [4Fe-4S] clusters suggests that these clusters simultaneously mediate electron and ion transfer and thus could be an essential part of the ion-translocating machinery.

In the two integral membrane subunits of Ech carboxylic residues are found that are highly conserved within the family of energy-converting hydrogenases and complex I. These residues could be part of a transmembrane ion channel.
In line with this, Ech hydrogenase activity was inhibited by the carboxyl-modifying reagent *N,N'*–dicyclohexylcarbodiimide (DCCD). The inhibition of the enzyme correlated quite well with the incorporation of [^{14}C]DCCD in subunits EchA.

Using a combination of FT-IR difference spectroscopy and electrochemistry it was shown that the electron transfer reaction catalyzed by Ech hydrogenase from *M. barkeri* induces a conformational change of the enzyme and the protonation of amino acid side chains. Oxidized minus reduced spectra in the mid infrared range (1800 to 1200 cm^{-1}) revealed conformational changes in the amide I region and a signal at 1720 cm^{-1} attributed to either an Asp or Glu side chain, protonated in the oxidized state.

To identify the coupling ion used by energy converting hydrogenases studies with the enzyme from *Carboxydothermus hydrogenoformans* were performed. Cell suspensions of *C. hydrogenoformans* were found to couple the oxidation of CO to CO_2 and H_2 with the translocation of protons across the membrane at pH 5.9. This transient acidification was inhibited by the protonophore CCCP but was not affected by the sodium ionophore ETH-157, indicating the generation of a primary electrochemical proton gradient. However, no proton translocation coupled to CO oxidation was observed at pH 6.7. On the other hand, at neutral pH, CO oxidation was coupled to sodium ion translocation. This reaction was protonophore insensitive, indicating a primary Na^+ translocation. These data indicate that the Coo hydrogenase from *C. hydrogenoformans* could be a primary sodium pump, which may also use H^+ at low pH.

I ZUSAMMENFASSUNG

In den letzten Jahren wurden Mitglieder einer Gruppe von membrangebundenen [NiFe]-Hydrogenasen mit deutlicher Sequenzverwandtschaft zu Untereinheiten von NADH:Chinon-Oxidoreduktasen (Komplex I) in verschiedenen anaeroben und fakultativ anaeroben Mikroorganismen identifiziert. Aufgrund physiologischer und biochemischer Untersuchungen wurde für verschiedene Mitglieder dieser Enzymfamilie eine Funktion als Ionenpumpe in energiekonservierenden Elektronentransportketten, eine Beteiligung am revertierten Elektronentransport, oder eine Beteiligung an beiden Prozessen, vorgeschlagen. Aus diesem Grund wurden diese Enzyme als energiekonvertierende [NiFe]-Hydrogenasen bezeichnet. In dieser Arbeit wurde der Mechanismus der Energiekopplung in energiekonvertierenden Hydrogenasen im Vergleich zu Komplex I untersucht. Ein Schwerpunkt wurde dabei auf die Charakterisierung der am Elektronentransfer beteiligten prosthetischen Gruppen, die Funktion des Membranteils des Enzyms und die Identifizierung des Kopplungsions dieser Enzyme, gelegt. Die meisten Experimente wurden mit Ech-Hydrogenase aus *Methanosarcina barkeri* durchgeführt.

Aus der Primärstruktur von Ech-Hydrogenase kann die Bindung von drei [4Fe-4S]-Zentren, eines in Untereinheit EchC und zwei in Untereinheit EchF, vorhergesagt werden. Frühere Studien hatten gezeigt, dass zwei dieser Eisen-Schwefel-Zentren bei pH 7 und unter 1 bar H_2 vollständig reduziert vorliegen und zwei distinkte EPR Signale, die als g = 1.89 Signal und g = 1.92 Signal bezeichnet wurden, hervorrufen. Redox-Titrationen bei verschiedenen pH-Werten zeigten, dass die Mittelpunktspotentiale dieser Eisen-Schwefel-Zentren pH-abhängig sind. Dies deutet auf eine Beteiligung dieser Zentren am Ionentransfer hin. Um diese EPR Signale den Untereinheiten des Enzyms zuzuordnen, wurden verschiedene *M. barkeri* Mutanten hergestellt, in denen sieben der acht konservierten Cysteinreste der Untereinheit EchF jeweils durch Serin ersetzt wurden. Eine Charakterisierung der gereinigten Mutantenenzyme mittels EPR Spektroskopie zeigte eine starke Reduktion bzw. ein völliges Fehlen des g = 1.92 Signals, während das g = 1.89 Signal in fünf der Mutantenenzyme noch als Hauptsignal identifiziert werden konnte. Aufgrund dieser Ergebnisse konnte das g = 1.89 Signal dem proximalen Eisen-Schwefel

Zentrum der Untereinheit EchC und das g = 1.92 Signal einer der beiden Untereinheiten der Untereinheit EchF zugeordnet werden. Die pH-Abhängigkeit des Mittelpunktspotentials dieser beiden [4Fe-4S]-Zentren deutet darauf hin, dass diese Zentren sowohl am Elektronen- als auch Ionentransport beteiligt sind und damit möglicherweise einen wichtigen Teil der Ionenpumpe darstellen.

Die beiden integralen Membranuntereinheiten von Ech Hydrogenase, EchA und EchB, tragen mehrere Glutamat- oder Aspartatreste, die sowohl in anderen Energie-konvertierenden Hydrogenasen als auch in Komplex I hoch konserviert sind. Diese Reste könnten Teil eines transmembranen Ionenkanals sein. Übereinstimmend hiermit konnte gezeigt werden, dass Ech Hydrogenase durch das Carboxylgruppen-modifizierende Reagenz *N*, *N*'-Dicyclohexylcarbodiimid (DCCD) gehemmt wird. [^{14}C]DCCD wurde spezifisch in die beiden hydrophoben Untereinheiten EchA und EchB eingebaut. Die Inaktivierung des Enzyms korrelierte hierbei insbesondere mit dem Einbau von [^{14}C]DCCD in EchA.

Mittels einer Kombination aus FT-IR Differenzspektroskopie und Elektrochemie konnte gezeigt werden, dass der durch Ech-Hydrogenase katalysierte Elektronentransfer eine Konformationsänderung des Enzyms als auch eine Protonierung von Aminosäureseitengruppen induziert. Ox-red Differenzspektren im mittleren Infrarotbereich (1800 bis 1200 cm^{-1}) zeigten insbesondere eine Konformationsänderungen im Amid I Bereich. Ein Signal bei 1720 cm^{-1} wurde Aspartat oder Glutamat Seitengruppen zugeordnet, die im oxidierten Zustand protoniert vorliegen.

Um das Kopplungsion energiekonvertierender Hydrogenasen zu identifizieren, wurden Untersuchungen an *Carboxydothemus hydrogenoformans* durchgeführt. Zellsuspensionen dieses Bakteriums koppeln bei pH 5,9 die Umsetzung von CO zu CO_2 und H_2 mit der Translokation von Protonen über die Cytoplasmamembran. Die transiente Ansäuerung des Mediums wurde durch das Protonophor CCCP, jedoch nicht durch das Natriumionophor ETH-157 gehemmt, was auf die Bildung einen primären elektrochemischen Protonengradienten hindeutet. Bei pH 6,7 konnte hingegen keine Protonentranslokation, gekoppelt an CO-Oxidation, beobachtet werden. Bei neutralem pH-Wert wurde jedoch eine Translokation von Natrium-Ionen beobachtet. Diese Reaktion war Protonophor-insensitiv, was auf eine primäre Natrium-Ionen Translokation hindeutet. Die Daten legen

nahe, dass Coo Hydrogenase aus *C. hydrogenoformans* eine primäre Natrium-Ionen Pumpe ist, die bei niedrigen pH-Werten auch Protonen als Substrat verwendet.

II INTRODUCTION

1. Hydrogenases: general characteristics

In 1931, Stephenson and Stickland proposed the name "hydrogenase" for the enzyme capable of activating H_2 (Stephenson & Stickland, 1931). This enzyme catalyzes the following reversible redox reaction:

$$H_2 \rightleftharpoons 2\,H^+ + 2\,e^-$$

A variety of bacteria were found to possess hydrogenase activity; hence it could be inferred that H_2 plays an important role in microbial metabolism. Most of the enzymes are found in bacteria and archaea, but a few are present in eukarya as well. Molecular hydrogen is an important intermediate in the degradation of organic matter by microorganisms in anaerobic environments such as freshwater and marine sediments, wetland soils and the gastrointestinal tract of animals. Bacteria living in such anaerobic environments gain energy by fermentative processes and use the production of hydrogen to get rid of excess reducing equivalents. The H_2 generated by these microorganisms is generally consumed by both aerobic and anaerobic microorganisms living in the same environment. In anarobic fresh water habitats, the major part of the H_2 produced is used to reduce CO_2 to methane by methanogenic archaea. In order to acquire low-potential reducing equivalents, these bacteria have the capacity to oxidize H_2 to two protons and two electrons. The reducing equivalents obtained in this way enable the bacteria to reduce a variety of substrates and to generate enough energy for ATP synthesis. In marine habitats, sulfate is reduced to sulfide with H_2 as electron donor (Schwarz & Friedrich, 2003).

2. Classes of hydrogenases

Based on their metal content, three phylogenetically distinct classes of hydrogenases can be distinguished: the [FeFe] hydrogenases, the [NiFe] hydrogenases and the iron-sulfur-cluster-free hydrogenases (Vignais *et al.*, 2001).

[FeFe] hydrogenases

[FeFe] hydrogenases contain a binuclear iron-center in the active site and iron-sulfur (Fe-S) clusters (Adams & Stiefel, 2000; Peters, 1999). The active site of those enzymes is a Fe(CO)(CN)Fe(CO)(CN) center, sometimes with a bridging CO (Nicolet *et al.*, 1999) (Peters *et al.*, 1998; Pierik *et al.*, 1998).

[NiFe] hydrogenases

[NiFe] hydrogenases contain a binuclear [NiFe] center and Fe-S clusters (Adams & Stiefel, 2000). The active site of [NiFe] hydrogenases contains a $NiFe(CN)_2(CO)$ group (Happe *et al.*, 1997) (Volbeda *et al.*, 1995; Volbeda *et al.*, 1996). There are also hydrogenases, which have Se-cysteine as ligand to Ni and they are sometimes referred as a separate class ([NiFeSe] hydrogenases), although they can be surely considered as a subclass of [NiFe] hydrogenases.

Iron-sulfur-cluster-free hydrogenases

In some methanogenic archaea there is an hydrogenase that does not contain nickel or iron-sulfur clusters. This enzyme is the H_2-forming methylenetetrahydromethanopterin dehydrogenase (Hmd) and differs from the other types of hydrogenases, which are all iron-sulfur proteins (Buurman *et al.*, 2000; Thauer *et al.*, 1996). Recently it was shown that Hmd contain one iron associated with a low molecular mass cofactor of yet unknown structure (Lyon *et al.*, 2004a); interestingly, infrared spectroscopy studies revealed that in Hmd the iron is bound to CO ligands, similarly to other hydrogenases (Lyon *et al.*, 2004b).

3. Structure of [NiFe] hydrogenases

The presence of nickel in the active site of an hydrogenase, was first described by Graf and Thauer (Graf & Thauer, 1981). Besides in [NiFe] hydrogenases, nickel is found in the active site of other redox enzymes from anaerobic microorganisms: carbon monoxide dehydrogenase, carbon monoxide dehydrogenase/acetyl-coenzyme A synthase, methyl-coenyzme M reductase and superoxide dismutase. In addition nickel is found in the non-redox enzyme urease (Thauer, 2001).

Thus far the three-dimensional structure of [NiFe] hydrogenases from different anaerobic sufate-reducing bacteria have been solved. The *Desulfovibrio gigas* hydrogenase, the first hydrogenase structure that has been determined (Volbeda *et al.*, 1995), can be considered as a prototype of these

enzymes. The basic module conserved in all [NiFe] hydrogenases is formed by two subunits, frequently called “hydrogenase large” and “hydrogenase small” subunit (Fig. 1).

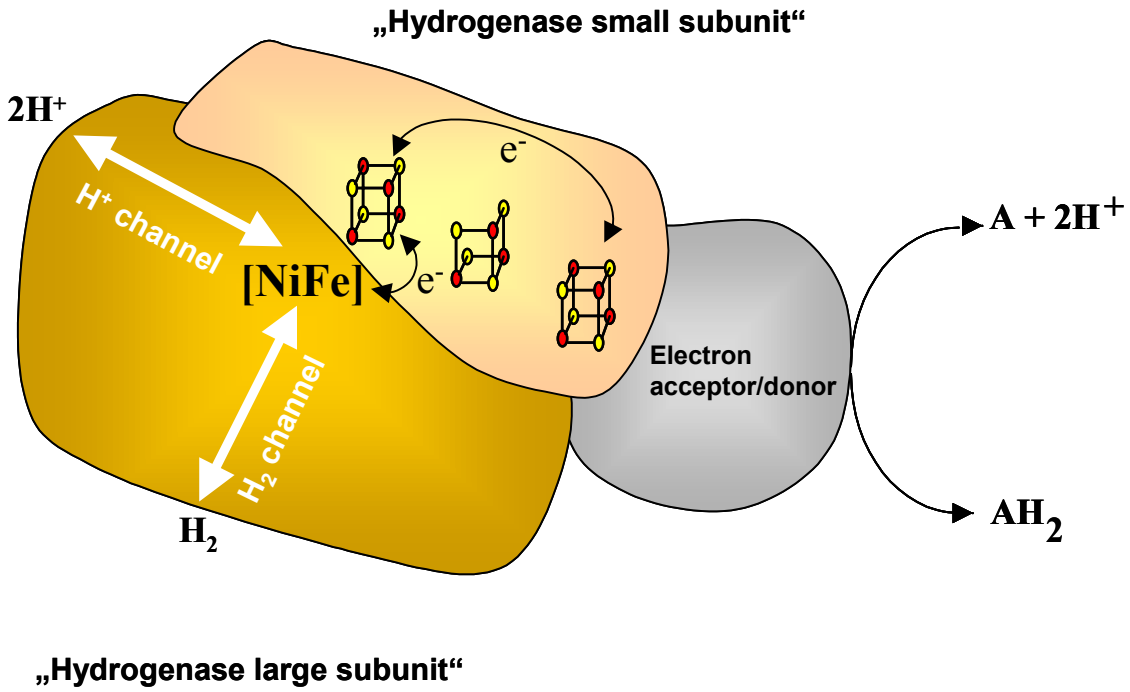

Fig. 1. Schematic representation of the [NiFe] hydrogenase from *Desulfovibrio gigas* based on the structure solved by Volbeda (Volbeda *et al.*, 1995). [NiFe]: binuclear NiFe active site; iron-sulfur clusters red: iron, yellow: sulfur. The [3Fe-4S] is probably not involved in electron transfer (Garcin *et al.*, 1998)**.**

The large subunit harbors the binuclear [NiFe] active site, which is coordinated by two conserved CxxC motifs, one located in the N-terminal region and the second located in the C-terminal region of the polypeptide (Albracht, 1994). Two of the thiolate groups form a bridge between the two metals (Volbeda *et al.*, 1995). The crystal structure together with FT-IR spectroscopy studies reveald the presence of three diatomic nonprotein ligands, one CO and two CN^- ligands, bound to the Fe atom (Happe *et al.*, 1997; Volbeda *et al.*, 1996)(Fig. 2). The active site is buried inside the protein at a distance of about 30 Å from the surface. The small subunit is composed of two domains. The N-terminal domain of the small subunit of all [NiFe] hydrogenases displays a conserved amino-acid sequence pattern, $CxxCx_nGxCxxxGx_mGCPP$ (n=61-106, m=24-61) (Albracht, 1994), binding one [4Fe-4S] cluster. This cluster is within 14 Å from the active site (Volbeda *et al.*, 1995) and is called the proximal cluster. The structure of the C-terminal domain of the small subunit is more variable as indicated by differences in the primary structure between

hydrogenases. In most, but not all enzymes, the small subunit contains six to eight additional cysteine residues, which ligate two more clusters, in the *Desulfovibrio gigas* enzyme being a second [4Fe-4S] cluster (distal cluster) and a [3Fe-4S] cluster (medial cluster). All three clusters are located almost along a straight line at a distance of 12 Å from each other. The combination of the [NiFe] active site and the proximal [4Fe-4S] cluster seem to be essential for the catalytic action of [NiFe] hydrogenases (Garcin *et al.*, 1998).

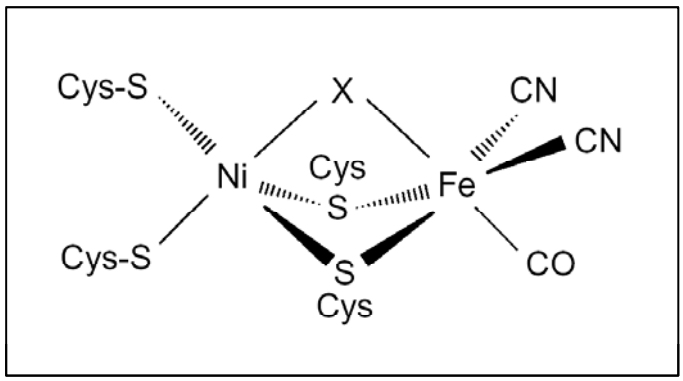

Fig. 2. The structure of the active site of [NiFe] hydrogenases based on the data of X-ray (Volbeda *et al.*, 1995), spectroscopic and chemical analysis (Volbeda *et al.*, 1996; Happe *et al.*, 1997). The bridging ligand X (either an O^{2-}, OH^- or H_2O) in the [NiFe] site is present in inactive forms of hydrogenases and is lost upon reduction of the enzyme (Stein & Lubitz, 2002).

4. Energy-converting [NiFe] hydrogenases

In the recent years a group of multisubunit membrane-bound [NiFe] hydrogenases has been identified in several microorganisms (Hedderich, 2004). These enzymes form a distinct group within the large family of [NiFe] hydrogenases (Vignais *et al.*, 2001). Members of this hydrogenase family include hydrogenases 3 from *Escherichia coli* (Böhm *et al.*, 1990; Sauter *et al.*, 1992), CO-induced hydrogenase from *Rhodospirillum rubrum* and Coo hydrogenase from *Carboxydothermus hydrogenoformans* (Fox *et al.*, 1996; Soboh *et al.*, 2002), Ech hydrogenase from *Methanosarcina barkeri* (Künkel *et al.*, 1998; Meuer *et al.*, 1999) and *Thermoanaerobacter tengcongensis* (Soboh *et al.*, 2004). The hydrogenases large and small subunit of these enzymes show surprisingly little sequence similarity to other (standard) [NiFe] hydrogenases, except for the conserved residues

coordinating the active site and the proximal Fe-S cluster. In addition to the hydrogenase large and small subunit these enzymes contain at least four other subunits, two hydrophilic proteins and two integral membrane proteins. These six subunits form the basic structure of these hydrogenases and are conserved in all members of this hydrogenase subfamily (Fig. 3). Other members of this class of multisubunit membrane-bound [NiFe] hydrogenases have a more complicated structure with additional subunits, like Eha and Ehb hydrogenases from the methanogenic archaeon *Methanothermobacter marburgensis* (Tersteegen & Hedderich, 1999) and Mbh hydrogenase from the hyperthermophilic archaeon *Pyrococcus furiosus* (Sapra *et al.*, 2000; Silva *et al.*, 2000).

These six highly conserved subunits show a striking amino-acid sequence similarity with six subunits of energy conserving NADH:quinone oxidoreductase, also called complex I (Fig. 3) (Albracht & Hedderich, 2000; Friedrich & Scheide, 2000; Friedrich & Weiss, 1997; Yano & Ohnishi, 2001). Complex I is present in the inner mitochondrial membrane and in the cytoplasmic membrane of numerous bacteria. It catalyses electron transfer from NADH to ubiquinone or menaquinone and couples this reaction to the translocation of protons or sodium ions across a membrane (Brandt *et al.*, 2003). The bacterial enzymes are formed by 13 to 14 subunits also conserved in the mitochondrial enzymes (Yagi *et al.*, 1998). These conserved subunits form the catalytic core of complex I. From sequence comparisons it became evident that the catalytic core of complex I has a highly modular architecture (Friedrich & Weiss, 1997). The electron input domain of the enzyme is formed by three subunits catalyzing the oxidation of NADH. This module contains FMN and most of the iron-sulfur clusters of the enzyme. The subunits of this module are sequence related to other $NAD(P)^+$ dependent enzymes. Highest sequence identity has been found to the diaphorase part of NAD^+-reducing [NiFe] hydrogenases (Tran-Betcke *et al.*, 1990) and to $NADP^+$ reducing [FeFe] hydrogenases (Malki *et al.*, 1995).

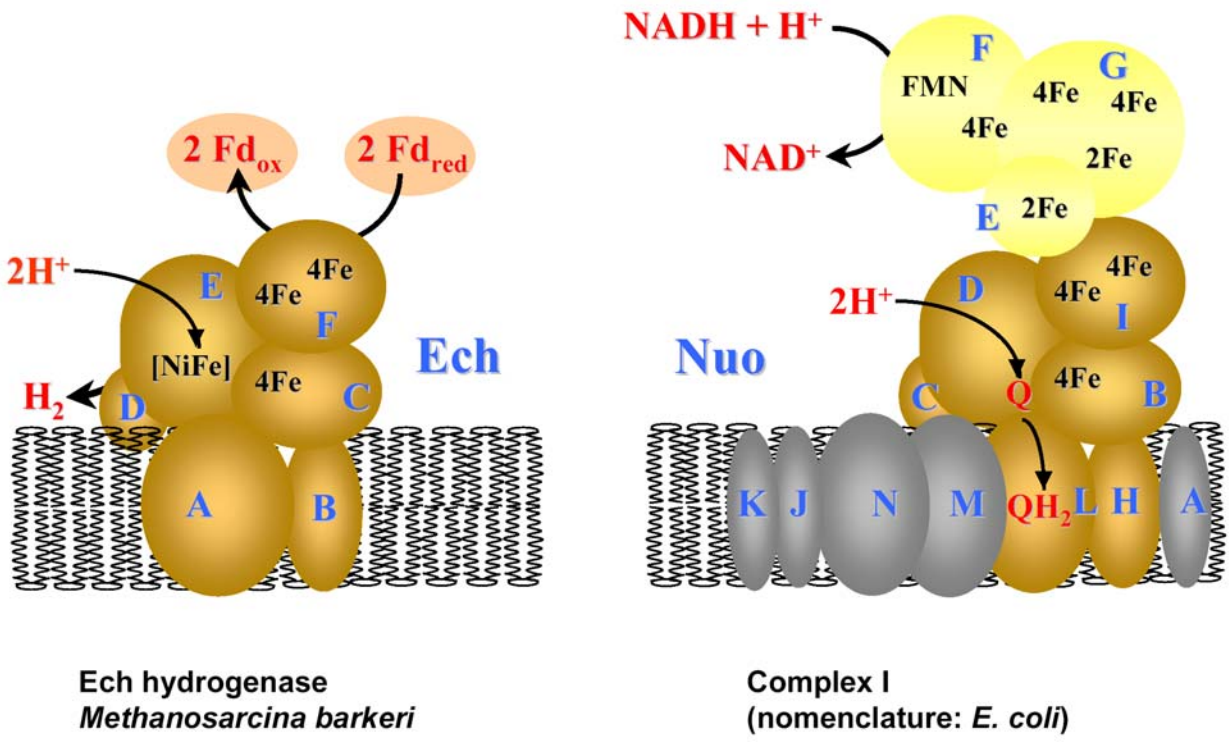

Fig. 3. Schematic representation of the common protein modules in energy-converting [NiFe] hydrogenases and complex I. Ech hydrogenase from *M. barkeri* and complex I from *E. coli* (Friedrich & Scheide, 2000) are shown as examples. Subunits conserved between both enzymes are shown in the same color. Capital letters indicate subunits of the enzymes. Abbreviations: [NiFe]: binuclear NiFe-active site of hydrogenase; 4Fe: [4Fe-4S] cluster; 2Fe: [2Fe-2S] cluster; Fd: 2[4Fe-4S] ferredoxin; FMN: flavin mononucleotide; Q: ubiquinone or menaquinone.

This NADH dehydrogenase module mediates the electron transfer to the central part of the enzyme formed by four hydrophilic subunits. These subunits form the contact site to the membrane part of the enzyme. There is experimental evidence that these subunits participate in the reduction of the quinone (Brandt *et al.*, 2003; Yano *et al.*, 2005). The four hydrophilic subunits in this central part of complex I are highly homologous to the four hydrophilic subunits of membrane-bound [NiFe] hydrogenases. Furthermore, the two membrane-bound subunits present in these hydrogenases are closely related to subunits present in the membrane part of complex I (Fig. 3). The evolutionary relationship between complex I and the membrane-bound [NiFe] hydrogenases has been addressed in recent reviews (Albracht & Hedderich, 2000; Friedrich & Scheide, 2000; Hedderich, 2004; Yano & Ohnishi, 2001). From growth experiments with *R. rubrum* and *C. hydrogenoformans* (Kerby *et al.*, 1995; Svetlichny *et al.*, 1991), from cell-suspension experiments and genetic

studies with *M. barkeri* (Bott & Thauer, 1989; Meuer *et al.*, 2002) and from experiments with inverted vesicles of *P. furiosus* (Sapra *et al.*, 2003) it can be inferred that the [NiFe] hydrogenases in these organisms probably pump protons or sodium-ions as well. They have therefore been designated energy-converting [NiFe] hydrogenases (Vignais *et al.*, 2001).

The members of this hydrogenase family that have been purified so far are: Ech hydrogenase from *M. barkeri* (Meuer *et al.*, 1999) and from *T. tengcongensis* (Soboh *et al.*, 2004), and Coo hydrogenase from *C. hydrogenoformans* (Soboh *et al.*, 2002).

4.1 Ech hydrogenase from *Methanosarcina barkeri*

From a biochemical perspective, the most thoroughly studied member of the family is Ech hydrogenase found in the methanogenic archaeon *M. barkeri*. *Methanosarcina* species are metabolically and physiologically the most versatile methanogens; they can reduce CO_2 to CH_4 with H_2 as electron donor, can reduce methanol or methylamines to CH_4 using H_2 as electron donor, are able to convert methanol or methylamines to CO_2 and CH_4 and can convert acetate to CO_2 and CH_4. In vitro Ech hydrogenase catalyzes the reversible oxidation/reduction of ferredoxin and H_2. Biochemical studies indicate that a 2[4Fe-4S] ferredoxin is the physiological substrate for Ech. The biological role of Ech was recently elucidated using mutational analysis. From the data obtained the following conclusions were made. Under autotrophic growth conditions the enzyme catalyzes the reduction of a low-potential ferredoxin by H_2 (Meuer *et al.*, 1999 and 2002). Reduced ferredoxin generated by Ech hydrogenase donates electrons to different soluble oxidoreductases, e.g. formylmethanofuran dehydrogenase (Fmd) or pyruvate:ferredoxin oxidoreductase (POR). Fmd, for example, catalyzes the reduction of methanofuran and CO_2 to formylmethanofuran. The overall reduction of CO_2 and methanofuran by H_2 is endergonic and *in vivo* is driven by reverse electron transport (Kaesler & Schönheit, 1989a) (Fig. 4). Reduction of the ferredoxin by H_2, the partial reaction catalyzed by Ech hydrogenase, was shown to be the energy driven step (Stojanowic and Hedderich, 2004). In acetoclastic methanogenesis Ech is proposed to catalyze the reverse reaction, the production of H_2 with reduced ferredoxin (produced during the oxidation of the carbonyl group of acetyl-CoA to CO_2, catalyzed by the acetyl-CoA synthase/CO dehydrogenase complex) as electron donor.

Previous studies with cell suspensions of *M. barkeri* have shown that the conversion of CO to CO_2 and H_2 was coupled to the generation of a proton motive force (Bott & Thauer, 1989). This is consistent with the putative ion-translocating activity of Ech. A very similar reaction is catalyzed by C*arboxydothermus hydrogenoformans* (see below).

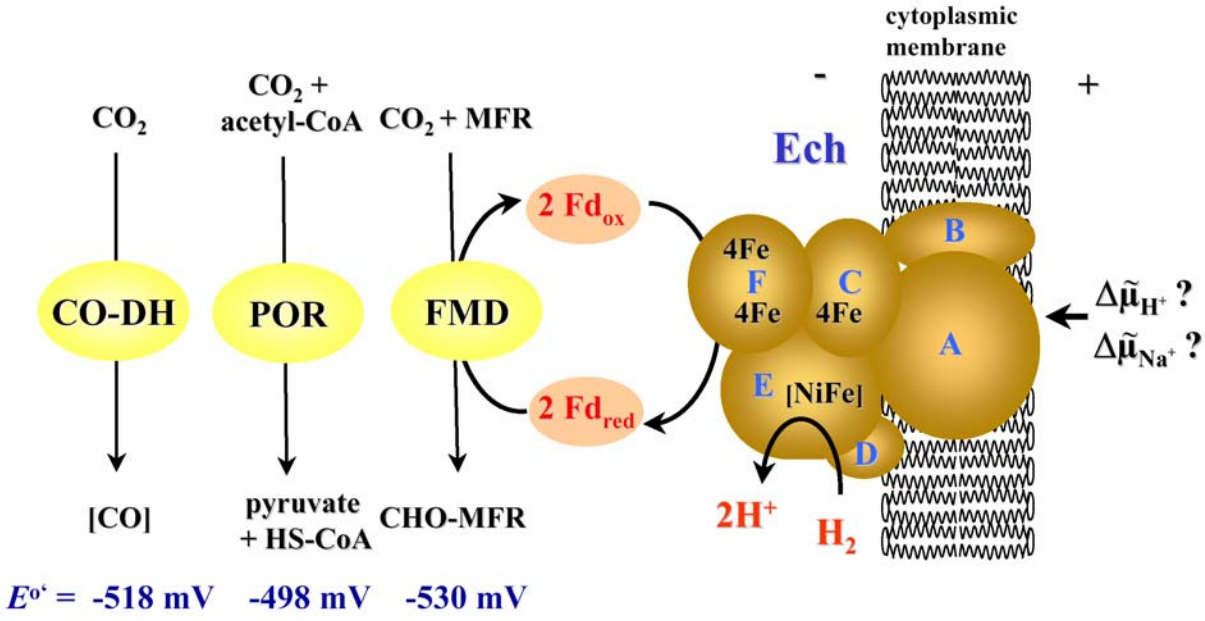

Fig. 4. Proposed function of Ech hydrogenase from *M. barkeri* in endergonic redox-reactions. CO-DH: carbon monoxide dehydrogenase/acetyl-CoA synthase complex; POR: pyruvate:ferredoxin oxidoreductase; FMD: formylmethanofuran deyhrogenase; Fd: 2[4Fe-4S] ferredoxin; [NiFe]: binuclear NiFe-active site of hydrogenase; 4Fe: [4Fe-4S] cluster; MFR: methanofuran; CHO-MFR: formylmethanofuran.

Purified Ech consists of six subunits, encoded by genes organised in the *echABCDEF* operon. The EchA and EchB subunits are predicted to be integral, membrane-spanning proteins, while the other four subunits are expected to extrude into the cytoplasm. Amino-acid sequence analysis of the cytoplasmic subunits points to the presence of two classical [4Fe-4S] clusters in EchF and one [4Fe-4S] cluster in EchC. The EchC subunit belongs to the family of the small subunits in [NiFe] hydrogenases. The EchE subunit shows the characteristic binding motif for the [NiFe] active site found in the large subunits of all [NiFe] hydrogenases. Chemical analysis revealed the presence of Ni, non-heme Fe and acid-labile S in a ratio of 1:12.5:12 (Meuer *et al.*, 1999), corroborating the presence of three Fe-S clusters.

The iron-sulfur clusters of the enzyme have recently been characterized by electron paramagnetic resonance spectroscopy (EPR) (Kurkin *et al.*, 2002). These studies showed that two of these clusters could be fully reduced under 1 bar of H_2 at pH 7 giving rise to two distinct *S* ½ EPR signals, designated as the *g* = 1.89 and the *g* = 1.92 signal. Redox titrations at different pH values demonstrated that these two clusters had a pH-dependent midpoint potential indicating that they could be involved in ion pumping. A third minor EPR signal, designated the *g* = 1.96 signal was only detectable at low-redox potentials. This cluster was tentatively assigned to the third iron-sulfur cluster of the enzyme. Ech hydrogenase is highly homologous to the catalytic core of complex I which is formed by the four hydrophilic subunits NuoB, C, D and I and the membrane subunits NuoH and NuoL, M, N (following the nomenclature of the *E. coli* enzyme), indicating an evolutionary relationship between both enzymes (Brandt, 1997; Friedrich & Scheide, 2000; Friedrich & Weiss, 1997; Yano & Ohnishi, 2001). In this catalytic core of complex I the three binding motifs for [4Fe-4S] centers present in Ech hydrogenase are also conserved. The characterisation of these clusters has been an important issue in the complex I field in the recent years.

NuoB (the homologue of EchC) is thought to harbour the EPR-detectable iron-sulfur cluster N2 (Ahlers *et al.*, 2000; Flemming *et al.*, 2003b). This cluster exhibits a pH-dependent midpoint potential and has therefore been discussed to be involved in H^+ pumping (Ingledew & Ohnishi, 1980). The clusters presumably located on NuoI (the homologue of EchF) were not detectable by EPR spectroscopy but could be detected by UV/Vis redox difference spectroscopy (Rasmussen *et al.*, 2001). The midpoint potentials of these clusters were pH independent. Hence, the properties of the iron-sulfur clusters present in the catalytic core of complex I differ from that of the homologous clusters in Ech hydrogenase. In the latter enzyme two [4Fe-4S] clusters were detected by EPR, both exhibiting a pH-dependent midpoint potential (Kurkin *et al.*, 2002).

Two integral membrane subunits are conserved within the family of energy-converting hydrogenases corresponding to EchA and EchB in the *M. barkeri* enzyme. EchB is a homologue of the complex I NuoH (ND1) protein. EchA is a homologue of the complex I NuoL, NuoM or NuoN (ND2, ND4 or ND5) subunits, which most likely share a common ancestor and arose by gene triplication. These proteins are also related to a distinct type of bacterial K^+ or Na^+/H^+ antiporter found in *Sinorhizobium meliloti* and *Bacillus* sp. C-125 (Hamamoto *et al.*, 1994; Putnoky *et al.*, 1998). Both, EchA and EchB share highly conserved acidic residues, predicted to be located in

transmembrane helices, with the corresponding subunits of complex I. Also the Na^+/H^+ antiporters share the conserved acidic residues present in EchA and its complex I counterparts.

4.2 Related hydrogenases found in non-methanogenic microorganisms

Members of the Ech hydrogenase family are also found in microorganisms that can anaerobically use carbon monoxide as energy substrate. The CO-induced hydrogenase from *Rhodospirillum rubrum* and Coo hydrogenase from *Carboxydothermus hydrogenoformans* catalyzes, together with a carbon monoxide dehydrogenase, the following reaction:

$$CO + H_2O \rightarrow CO_2 + H_2 \qquad \Delta G^{\circ\prime} = -20\ kJmol^{-1}$$

Since *R. rubrum* and *C. hydrogenoformans* can grow anaerobically in the dark with CO as the sole energy source, this reaction should be coupled to energy conservation. The free energy change associated with this reaction does not permit the synthesis of ATP via substrate-level phosphorylation because the energy required for the synthesis of ATP from ADP and P_i in vivo is about 60-80 $kJmol^{-1}$ (Thauer *et al.*, 1977). For this reason, these conditions require ATP to be synthetized via a chemiosmotic mechanism (Mitchell, 1966). Taking into account that the carbon monoxide dehydrogenase is a soluble enzyme, Fox *et al.* (1996) proposed that the hydrogenase is the site of energy conservation with the hydrogenase functioning as an ion-pump. The hydrogenase from *R. rubrum* turned out to be labile preventing its purification and biochemical characterization, which on the other hand was achieved with the enzyme from *C. hydrogenoformans* that was purified in a tight complex with a CO dehydrogenase and a polyferredoxin.

Another well-studied member of this group of energy-converting hydrogenases is hydrogeanse 3 from *E. coli*. This enzyme is part of the formate hydrogenlyase system and was found to be essential for the formation of H_2 in mixed-acid fermentation pathway of *E. coli* (Böhm *et al.*, 1990; Sauter *et al.*, 1992). Hydrogenase 3 catalyses, together with formate dehydrogenase, the following reaction:

$$HCOO^- + H^+ \rightleftharpoons CO_2 + H_2 \qquad \Delta G^{\circ\prime} = -3.5\ kJmol^{-1}$$

Early studies proposed that the physiological function of this enzyme complex is to remove reducing equivalents, generated by the oxidation of formate, and to help offset acidification of the growth medium during fermentative growth (Böck & Sawers, 1996). Under standard substrate concentrations the formate hydrogenlyase reaction is not an exergonic process but under natural conditions (low hydrogen partial pressure and acidic pH) this reaction becomes also exergonic by about –20 $kJmol^{-1}$ (Andrews *et al.*, 1997). Hence, the FHL reaction could also be coupled to energy conservation, from a thermodynamic point of view. The site of energy conservation also in this case would be the hydrogenase since only this enzyme has integral membrane subunits. Experimental evidences for this proposed energy-conserving function have been already obtained (Forzi, 2001). Unfortunately, hydrogenase 3 is unstable and this property prevented its purification and further characterization.

5. Outline of this thesis

All available experimental data deriving from physiological and biochemical studies performed with various members of energy-converting hydrogenases, confirmed the proposal that these enzymes function as ion pumps. The major aim of this work was to get more insights into the mechanism of energy transduction in this group of hydrogenases in comparison to complex I and to identify the prosthetic groups, amino acid residues and the coupling ion that could be involved in this process. Most of the experiments have been performed with Ech hydrogenase from *M. barkeri*.

Based on the modular structure of complex I (see above), it has been proposed that complex I and the energy-converting hydrogenases may have evolved from a common ancestor. Therefore it can be assumed that these two different enzymes may share a common mechanism for coupling an exergonic redox-reaction with the electrogenic translocation of ions across a membrane. For this reason this group of membrane-bound hydrogenases can be used as a model for the study of the more complicated complex I.

For the discussion of how these hydrogenases use exergonic redox-energy to transport charges across the cytoplasmic membrane, it is essential from one side to understand the

electron transfer pathway in these enzymes and from another side to identify the coupling ion used by these enzymes.

Part of this work addresses the assignment of the different EPR signals to the various clusters located in different subunits of Ech hydrogenase and to elucidate which clusters are required for reactivity with the substrate ferredoxin. To answer this question site-directed mutations have been generated in subunit EchF where seven out of eight conserved cysteine residues have been exchanged by serins.

In the two integral membrane subunits of Ech highly conserved acidic residues are found within the family of energy-converting hydrogenases and in complex I. Since these residues could be part of a transmembrane ion channel, their functional importance was tested performing inhibitor and labelling studies with *N,N'*–dicyclohexylcarbodiimide (DCCD).

As mentioned above, the spectroscopic characterization of Ech revealed that two Fe-S clusters have a pH-dependent midpoint potential, like cluster N2 found in complex I. Based on this similarity it was proposed that the clusters found in Ech could also be directly involved in ion pumping. This assumption was further investigated. In order to detect redox-dependent changes in protein structure and protonation states of amino acid side chains associated with the Fe-S clusters, a combination of FT-IR difference spectroscopy and electrochemistry was used.

Recently it has been shown that complex I from *Klebsiella pneumoniae* and from *E. coli* (Steuber, 2001 Gemperli *et al.*, 2002) pumps sodium ions rather than protons. This is in contrast to results obtained elsewhere, at least concerning *E. coli* complex I (Stolpe & Friedrich, 2004). However, this finding opened a new question concerning the coupling ion used by complex I. This question was also extended to the family of energy-converting [NiFe] hydrogenases. In order to investigate this important point the enzyme from *C. hydrogenoformans* was used and ion translocation studies have been performed.

III MATERIALS AND METHODS

1. Materials used

1.1 Chemicals and biochemicals

N,*N'*–dicyclohexylcarbodiimide (DCCD) and *N*,*N'*–dibenzyl-*N*,*N'*–diphenyl-1,2-phenylenedioxydiacetamide (ETH-157) were from Fluka (Buchs, Switzerland); 1-ethyl-3-(3-dimethylaminopropyl)-carbodiimide (EDAC), D-luciferin, luciferase, carbonylcyanide-*m*-chlorophenylhydrazone (CCCP), valinomycin, were from Aldrich-Sigma (Taufkirchen, Germany); dithiothreitol (DTT) was from Roth (Karlsruhe, Germany); Titrisol was from Merck (Darmstadt, Germany). and the dye used for the protein assay according to Bradford (1976) was from BioRad (München, Germany). Vent DNA polymerase and restriction endonucleases were from New England BioLabs (Frankfurt a. M., Germany); n-dodecyl-β-D-maltoside was from Glycon Biochemicals (Luckenwalde, Germany). All other chemicals were from Merck (Darmstadt, Germany) or from Sigma (Taufkirchen, Germany).

1.2 Gases

N_2 (99.996%), H_2 (99.9995%), N_2/H_2 (95:5, 99.99%/99.996%), N_2/CO_2 (80:20, 99.99%/99.995%) and CO (99.997%) were from Air Liquide (Düsseldorf, Germany).

1.3 Radioisotopes

[^{14}C]DCCD (1.99 GBq/mmol) was obtained from Amersham Biosciences (Freiburg, Germany); ^{22}NaCl (1.05 GBq/mmol) was obtained from PerkinElmer (Rodgau, Germany).

1.4 Anaerobic buffers and solutions

Anaerobic buffers were prepared by heating the aqueous solutions until boiling, while N_2 was bubbled simultaneously through the buffer. After two minutes of boiling, the buffer was transferred into a glass bottle equipped with a magnetic stir bar. The bottle was sealed with a rubber-stopper and vacuum pulled, while stirring until the solution cooled to room temperature. The buffer was then loaded into an anaerobic chamber (Coy, Ann Arbor, Michigan, USA), where the rubber stopper was removed, DTT (2 mM) added and the solution stirred overnight to insure that all O_2 was removed. Also, anaerobic solutions were prepared by dissolving the components in solvents already in the anaerobic chamber, which was filled with 95% N_2/5% H_2 and contained a palladium catalyst for the continuous removal of O_2.

1.5 Material used for protein purification

FPLC columns and chromatographic materials (DEAE Sepharose, Q Sepharose HiLoad, DEAE Sephacel and Superdex 75) used were from Amersham Biosciences, with the exception of the ceramic hydroxyapatite material that was from BioRad. The stirred cells (Amicon 8200) and the YM ultrafiltration membranes (cut-off: 50 kDa, 30 kDa and 10 kDa) used for protein concentration or for salt removal and the Amicon Ultra-4 and Microcon Centrifugal Filter Devices (cut-off: 50 kDa, 30 kDa and 10 kDa) used for concentration, desalting and buffer exchange were all from Millipore (Eschborn, Germany).

2. Microorganisms used and growth conditions

2.1 Microorganisms

The different *Methanosarcina barkeri* strains used in this work are listed in table 1.

Table 1. *M. barkeri* strains used in this study

Strain	Genotype	Source
Fusaro (DSM804)	Wild type	DSMZ, Braunschweig, Germany
EchF1	*echF*C42S-*pac*	This study
EchF2	*echF*C45S-*pac*	This study
EchF3	*echF*C48S-*pac*	This study
EchF5	*echF*C73S-*pac*	This study
EchF6	*echF*C76S-*pac*	This study
EchF7	*echF*C79S-*pac*	This study
EchF8	*echF*C83S-*pac*	This study
EchF9	*echF*(wt)-*pac*	This study

Carboxydothermus hydrogenoformans (DSMZ 6008) was from the Deutsche Sammlung für Mikroorganismen und Zellkulturen (Braunschweig, Germany).

2.2 Growth conditions

Methanosarcina barkeri

M. barkeri strain Fusaro was grown on acetate at 37°C as previously described by Karrasch (Karrasch *et al.*, 1989). The cells were grown in 2 l glass flasks or 10 l fermenters (Schott, Mainz, Germany), containing 1 l or 10 l medium, respectively. When an ΔOD_{578} of 0.5 was reached, the cells were harvested under strictly anaerobic conditions at 4°C using a continuous flow centrifuge Heraeus Contifuge 17RS (Heraeus Sepatech GmbH, Osterode, Germany).

The different *echF* mutants were grown in single cell morphology at 37°C in high-salt (HS) medium (table 2) under strictly anaerobic conditions, with a slightly modified version of the procedure described by Sowers (Sowers *et al.*, 1993). Two solutions, Mix A and Mix B, were first separately prepared by dissolving the indicated components in 700 ml and 300 ml distilled water, respectively. Mix A and Mix B were then combined in an anaerobic chamber and then 5 ml of 1 M KH_2PO_4 pH 8.0 (final concentration 5 mM), 1.0 g NH_4Cl (final concentration 19 mM) and 0.5 g cysteine·HCl (final concentration 2.8 mM) were added. The medium was allowed to clear before adding 5 ml of 100% methanol (final

concentration 125 mM) as carbon and energy source. The media were then dispensed into tubes, serum bottles or bottles; the vials were sealed with butyl rubber stoppers and brought out of the anaerobic chamber. The gas phase was then exchanged by repeatedly pulling vacuum and backfilling with N_2/CO_2 (80:20) and the media were then sterilized by autoclaving.

Table 2. Composition of high-salt (HS) medium

Component	Amount per liter	Final concentration
Mix A		
NaCl	23.4 g	400 mM
KCl	1.0 g	13 mM
0.1% resazurin	1 ml	4 μM
Trace elements[a]	10 ml	_
Vitamin solution[b]	10 ml	_
Mix B		
$MgCl_2 \times 6\ H_2O$	11.0 g	54 mM
$CaCl_2 \times 2\ H_2O$	0.3 g	2 mM

a) **Trace elements solution** (amount/liter): 1.5 g EDTA; 0.8 g $Fe(NH_4)_2(SO_4)_2$; 0.2 g $NaSeO_3$; 0.1 g $CoCl_2$ x 6 H_2O; 0.1 g $MnSO_4$ x 2 H_2O; 0.1 g Na_2MoO_4 x 2 H_2O; 0.1 g $NaWO_4$ x 2 H_2O; 0.1 g $ZnSO_4$ x 7 H_2O; 0.1 g $NiCl_2$ x 6 H_2O; 0.01 g H_3BO_3; 0.01 g $CuSO_4$ x 5 H_2O

b) **Vitamin solution** (amount/liter): 10 mg p-aminobenzoic acid; 10 mg nicotinic acid; 10 mg Ca-pantothenate; 10 mg pyridoxine HCl; 10 mg riboflavin; 10 mg thiamine HCl; 5 mg biotin; 5 mg folic acid; 5 mg α-lipoic acid; 5 mg vitamin B_{12}

After the media cooled, 0.4 mM $Na_2S \times 9\ H_2O$ (autoclaved) and 45 mM $NaHCO_3$ (sterilized by filtration) were added. When a 10 l fermenter was used, methanol was also added to the medium after autoclaving. The cells were harvested when an ΔOD_{578} of 1.5-2 was reached. Cultures were either first transferred into 500-ml centrifuge tubes in an anaerobic chamber and the cells were sedimented by centrifugation with a RC 5B centrifuge (Kendro, Hanau, Germany) equipped with a GS3 rotor at 8000 x *g* for 20 minutes at 4°C or in a continuous flow centrifuge (see above).

Escherichia coli

Standard conditions were used for growth of *E. coli* strains (Sambrook *et al.*, 1989).

Carboxydothermus hydrogenoformans

C. hydrogenoformans cells were cultivated as previously described (Soboh, 2001) and were kindly provided by Basem Soboh from our group.

3. Biochemical methods

3.1 Preparation of cell extracts and isolation of membranes from *M. barkeri*

The harvested *M. barkeri* aggregated cells were resuspended in 50 mM MOPS/NaOH buffer pH 7.0 containing 2 mM DTT and disrupted by sonication using a Sonoplus HD 200 sonifier (Bandelin, Berlin, Germany) at a power of 200 W for 7 × 7 min. All the procedures were performed in an anaerobic chamber (Coy, Ann Arbor, Michigan, USA) under a gas phase of 5% H_2/95% N_2. *M. barkeri* single cells were lysed by resuspension in 50 mM MOPS/NaOH buffer pH 7.0 containing 2 mM DTT, to which a few crystals of DNase I were added (spontaneous lysis occurs due to osmotic shock). Complete lysis was ensured by sonication at 200 W for 4 × 3 min. Intact cells and cell debris were removed by centrifugation with an Ultra Pro80 ultracentrifuge (Kendro, Hanau, Germany) at 10000 x *g* for 30 min at 4°C. The supernatant (cell extract) was used for enzyme activity measurements and for Western blot analysis.

Membrane fractions were prepared by centrifugation of cell extracts at 150000 x *g* for 2 h and resuspension of the membrane pellets by gentle homogenization with a teflon potter (Braun Glas, Gruibingen, Germany) in 50 mM MOPS/NaOH buffer pH 7.0 containing 2 mM DTT.

3.2 Purification of Ech hydrogenase from *M. barkeri*

3.2.1 Purification of Ech hydrogenase from acetate grown *M. barkeri* strain Fusaro

All purification steps were performed under strictly anaerobic conditions under an atmosphere of 5% H_2/95% N_2. The crude membrane fraction was isolated from cell extract as described in 3.1, then resuspendend and homogenized in 50 mM MOPS/NaOH buffer pH 7.0 containing 2 mM DTT (buffer A). Membranes thus obtained were solubilized by

dodecyl-β-D-maltoside (15 mM, 4.5 mg detergent per mg protein) for 12 h at 4°C. The suspension was incubated for 12 hat 4°C under light swirling. After centrifugation at 150000 x *g* for 45 min, the solubilized membrane proteins present in the supernatant were loaded on a DEAE Sepharose column (2.6 x 10 cm) equilibrated with buffer A containing 2 mM dodecyl-β-D-maltoside (= buffer A + DDM). The column was washed with 50 ml of buffer A + DDM and proteins were eluted with NaCl in buffer A + detergent using a step gradient: 0.24 M (150 ml) and 0.4 M (150 ml). Ech hydrogenase was recovered in the fractions eluting with 0.24 M NaCl. In order to reduce the salt concentrations, the collected fractions were concentrated by ultrafiltration using a stirred cell (Amicon 8200) with a YM membrane (cut-off: 50 kD), diluted with buffer A and then again concentrated by ultrafiltration. The concentrated sample was then loaded on a Q Sepharose HiLoad column (2.6 x 10 cm) equilibrated with buffer A containing DDM. The column was washed with 50 ml of buffer A + DDM and proteins were eluted with NaCl in buffer A + detergent in a linear gradient form 0.07 M to 0.11 M (450 ml). Ech hydrogenase was recovered in the fractions eluting with 0.1 M NaCl. Most of the heterodisulfidereductase (Hdr) was recovered in the fractions eluting with 0.08 M NaCl. However, some Ech preparation still contained Hdr contaminations. In order to get a complete separation of the last two enzymes, in some cases the concentrated fractions was further purified by chromatography on hydroxyapatite. The column (1.6 x 14 cm) was equilibrated with 30 mM potassium phosphate buffer pH 7.0 containing 2 mM DDM. Protein was eluted using a potassium phosphate step gradient 125 mM (40 ml), 250 mM (40 ml), 375 mM (40 mM), 500 mM (100 ml). Ech hydrogenase was recovered in the fractions eluting with 500 mM potassium phosphate. The protein was concentrated in buffer A + detergent up to a protein concentration of 3-5 mg ml^{-1} and stored under an atmosphere of 5% H_2/95% N_2 (or of 100% H_2 for longer period of time) at 4°C or –20°C.

3.2.2 Purification of Ech hydrogenase from methanol grown *M. barkeri echF* mutant strains

Ech hydrogenase was purified from the *echF* mutant strains using a modified version of the procedure described in 3.2.1. For the isolation of the membrane fraction, cell extracts were loaded on a DEAE Sephacel column (2.6 x 15 cm). The column was washed with 100 ml buffer A. The majority of Ech hydrogenase activity was recovered in the turbid void volume of the column whereas most soluble proteins were bound to the column material.

This procedure resulted in higher Ech yields as compared to an ultracentrifugation step since membranes of methanol-grown *M. barkeri* were difficult to sediment by ultracentrifugation, probably due to their high glycogen content. Membranes thus obtained were solubilized by dodecyl-β-D-maltoside, as described above. Further purification of Ech was carried out by chromatography on DEAE Sepharose, Q Sepharose and hydroxyapatite. As for the acetate grown cells, after the DEAE Sepharose run, Ech hydrogenase was recovered in the fractions eluting with 0.24 M NaCl. The concentrated fractions were loaded on a Q Sepharose HiLoad column (2.6 x 10 cm) and proteins were eluted with a NaCl linear gradient form 0.07 M to 0.11 M (450 ml) followed by a NaCl step gradient at 0.19 M (240 ml). Ech hydrogenase was recovered in the fractions eluting with 0.19 M NaCl. The concentrated fractions were then always loaded on a hydroxyapatite column (1 x 10 cm), the same potassium phosphate step gradient as in 3.2.1 was used and Ech was recovered in the fractions eluting with 500 mM potassium phosphate. These fractions were concentrated and the buffer was exchanged to buffer A + DDM by ultrafiltration using Amicon Ultra-4 Centrifugal Filter Devices (cut-off: 50 kDa). The enzyme was stored under an atmosphere of 100% H_2.

3.3 Purification of ferredoxin from acetate grown *M. barkeri*

The *M. barkeri* ferredoxin was purified under anaerobic conditions from the 150000 x *g* supernatant by anion exchange chromatography on DEAE Sephacel (elution with 0.5 M NaCl) and Q Sepharose HiLoad (elution with 0.75 M NaCl) and by gel filtration on Superdex 75 (elution after 220 ml). The isolated ferredoxin showed absorption maxima at 280 and 390 nm and the ratio of A_{390}/A_{280} ranged from 0.8 to 0.85, which is typical of a pure ferredoxin and further supports the purity of the preparation (Terlesky & Ferry, 1988). An ε_{390} value of 12.8 $mM^{-1} \cdot cm^{-1}$ was used for the determination of ferredoxin concentration.

3.4 Determination of enzyme activities

All spectrophotometric assays were carried out either in butyl rubber stoppered quartz cuvettes or in 8-ml serum bottles. The cuvettes had a pathlength of 1.0 cm, a volume of 1.5 ml and were degassed by repeatedly pulling vacuum and then backfilling with N_2. All

the assay components were injected in the form of anaerobic solutions by using microliter syringes (Unimetrics syringes, Machery-Nagel; Düren, Germany or Hamilton syringes, Bonaduz, Switzerland), where O_2 was previously removed by using anaerobic buffer. To measure the extinction at 578 nm a photometer (model 1101 M, Eppendorf, Hamburg, Germany) and for measurements at 320 nm a spectrophotometer (Ultrospec 2000 or 2100 *pro*, Amersham Biosciences, Freiburg, Germany) were used, respectively. The instruments were connected with a chart recorder or, in the case of the Ultrospec 2100 *pro* spectrophotometer the Swift application software was used. Assays were performed at 37°C with the *M. barkeri* enzyme and at 60°C with *C. hydrogenoformans* enzyme.

Hydrogen evolution activity

Hydrogen evolution activity, with reduced methyl viologen as electron donor, was measured by following the oxidation of reduced methyl viologen at 578 nm under a N_2 atmosphere (120 kPa). The 0.8-ml assays contained 50 mM MOPS/NaOH pH 7.0 in the presence of 2 mM methyl viologen (ε_{578} = 9.8 mM^{-1} cm^{-1}), which was reduced with sodium dithionite to a ΔE_{578} of 2. The reaction was started by injecting the enzyme fraction to be tested. One unit (U) of hydrogenase activity corresponds to the reduction of 2 µmol of protons to produce 1 µmol H_2 per minute, measured by the oxidation of 2 µmol of methyl viologen.

Hydrogen uptake activity

Hydrogen uptake activity, with benzyl viologen as electron acceptor, was determined by following the H_2-dependent benzyl viologen reduction at 578 nm under an H_2 atmosphere (120 kPa). The 0.8 ml assays contained 50 mM MOPS/NaOH pH 7.0, 2 mM DTT and 2 mM benzyl viologen (ε_{578} = 8.6 mM^{-1} cm^{-1}). Before addition of enzyme, the buffer in the cuvette was titrated with a solution of sodium ditihionite (20 mM) to a ΔE_{578} of ≈ 0.3. The reaction was started by adding the enzyme fraction to be tested. One unit (U) of hydrogenase activity corresponds to the oxidation of 1 µmol H_2 to produce 2 µmol of protons per minute, measured by the reduction of 2 µmol of benzyl viologen.

Ech hydrogenase activity

Ech hydrogenase activity was routinely measured with ferredoxin as electron acceptor for H_2 oxidation. The reduction of ferredoxin with H_2 by Ech hydrogenase was determined by following the metronidazole reduction at 320 nm under an H_2 atmosphere (120 kPa). The 0.8 ml assays contained 50 mM MOPS/NaOH pH 7.0, 2 mM DTT, 2 mM dodecyl-*β*-D-maltoside, 20 µM ferredoxin, 150 µM metronidazole (ε_{320} = 9.3 mM^{-1} cm^{-1}) and protein (purified Ech hydrogenase, membrane fraction or cell extract). One unit (U) of hydrogenase activity corresponds to the oxidation of 1 µmol H_2 to produce 2 µmol of protons per minute, measured by the reduction of 1/3 µmol of metronidazole.

Heterodisulfide reductase activity

The activity was determined by following the oxidation of reduced benzyl viologen with CoM-S-S-CoB at 578 nm under a N_2 atmosphere (120 kPa). The 0.8 ml assays contained 50 mM MOPS/NaOH pH 7.0, 2 mM benzyl viologen (ε_{578} = 8.6 mM^{-1} cm^{-1}) and 0.6 mM CoM-S-S-CoB. Benzyl viologen was reduced with sodium dithionite to a ΔE_{578} of 2. The reaction was started by injecting the enzyme fraction to be tested. One unit (U) of enzyme activity corresponds to the reduction of 1 µmol of heterodisulfide per minute, measured by the oxidation of 2 µmol of benzyl viologen.

Conversion of CO to H_2 and CO_2

The CO-dependent production of hydrogen was followed by measuring the H_2 concentration in the gas phase by gas chromatography. The 1-ml assays were performed at 60°C in sealed 8-ml serum bottles, under a 100% CO atmosphere (110 kPa), containing 50 mM MOPS/NaOH pH 7.0 and 50-100 µl cell suspensions from *C. hydrogenoformans* (0.5-2 mg of protein). Reactions were started by injection of cell suspensions. The solution was stirred vigorously with a small magnetic bar; additions and withdrawals were made by syringes. At 1.5-min intervals, samples from the gas phase were withdrawn and H_2 was quantified after separation by gas chromatography. One unit (U) of H_2 formation activity corresponds to 1 µmol of H_2 formed per minute.

3.5 Protein immunodetection by Western blot analysis

After electrophoresis, the protein samples were transferred from an unstained SDS-polyacrylamide gel to polyvinylidene fluoride membrane (ProBlott PVDF-Membran, Applied Biosystems, Weiterstadt, Germany) using a Semy-dry transfer system (Trans-Blot SD, BioRad Laboratories, München, Germany). The discontinuous two-component Tris/glycine buffer system was used as transfer buffer, as indicated in table 3.

Table 3. Transfer buffer used for Western blot

Anode (+) buffer for membrane side	Cathode(-) buffer for gel side
25 mM Tris	25 mM Tris
192 mM glycine	192 mM glycine
0.01% (w/v) SDS	0.1% (w/v) SDS
25% (v/v) methanol	10% (v/v) methanol

The electrotransfer was performed applying a constant current of 0.8 mA/cm^2 for 2 h. Following the electrotransfer of proteins, the membrane was blocked for at least 30 min with 5% (w/v) dried milk in PBS-T (8 mM Na_2HPO_4, 2 mM NaH_2PO_4, 70 mM NaCl, 0.05% (v/v) TWEEN 20) with gentle shaking at room temperature. The membrane was then incubated at room temperature for 2 h with 1:5000 dilutions of a rabbit anti-Ech serum in 2.5 % (w/v) dried milk in PBS-T. After washing 3 × 5 min with PBS-T, in order to remove the unbound primary antibody, the membrane was incubated for 1 h in 2.5 % (w/v) dried milk in PBS-T with 1:10000 dilutions of alkaline phosphatase-conjugated anti-(rabbit IgG) antibody, (Amersham Biosciences, Freiburg, Germany). Excess of conjugates was removed by washing the membrane 3 × 5 min with PBS-T.

Immunodetection was performed with the protocol for the ECF detection kit provided by Amersham Biosciences using a PhosphorImager (Storm 860, Molecular Dynamics, Sunnyvale CA, USA), which can detect the light emitted during the reaction of the substrate ECF with the alkaline phosphatase-linked to the secondary antibody. Signals were analysed using the ImageQuant software (Molecular Dynamics).

4. Analytical methods

4.1 Protein determination

Protein concentrations were determined with the BioRad Protein Microassay (BioRad Laboratories, München, Germany), a dye-binding assay based on the differential colour change of a dye in response to various concentrations of protein (Bradford, 1976). The principle of this method is based on the observation that the absorbance maximum for an acidic solution of Coomassie Brillant Blue G-250 shifts from 465 nm to 595 nm when binding to protein occurs. Each time the assay was performed, a standard curve was prepared using bovine serum albumin as protein standard (0-10 mg ml^{-1}); A_{595} was corrected for the blank. 0.8 ml of appropriately diluted samples or bovine serum albumin were mixed with 0.2 ml dye protein reagent and the absorbance of the solution at 595 nm was measured at room temperature with a spectrophotometer (Ultrospec 2000 or 2100 *pro*, Amersham Biosciences, Freiburg, Germany) after 15 minutes.

4.2 SDS-Polyacrylamide gel electrophoresis (SDS-PAGE)

In order to control the purity of the enzyme preparations or to perform Western blot analysis, polyacrylamide gel electrophoresis under denaturing conditions was performed to separate proteins according to their molecular weights (Laemmli, 1970). The electrophoresis was employed using the BioRad electrophoresis apparatus Mini Protean II cell (BioRad, München, Germany). The gels (80 mm × 65 mm × 0,75 mm) composition is indicated in table 4. Before electrophoresis the protein samples were diluted 1:2 with protein loading buffer (63 mM Tris/HCl pH 6.8, 10% (w/v) SDS, 10% (w/v) glycerin, 16 mM DTT, 0.01% (w/v) bromphenol blue) and denatured for 60 min at room temperature. Subsequently, 3-20 µl (5-15 µg protein) of the samples were loaded to the gel. The electrophoresis chamber was completely filled with Tris/glycine-electrophoresis buffer pH 8.8 (25 mM Tris, 192 mM glycine and 0.1% (w/v) SDS). The electrophoresis was started with a voltage of 70 V until the bromphenol blue marker reached the top of the separating gel then performed at 150 V until the tracking dye reached the bottom of the separating gel. As molecular weights standards in SDS-PAGE the Low Molecular Weight Calibration Kit from AP-Biotech (Freiburg, Germany) composed of phosphorylase b

(94 kDa), albumin (67 kDa), ovalbumin (43 kDa), carbonic anhydrase (30 kDa), trypsin inhibitor (20,1 kDa) und lactalbumin (14,4 kDa) was used.

After the electrophoresis, the proteins were visualized by staining the gel at room temperature for several hours in a solution of 0.05% (w/v) Coomassie Brillant blue R 250, 0.05% (w/v) Crocein Scarlet 7B und 0.5% (w/v) $CuSO_4$ in water/isopropanol/acetic acid (65:25:10). Destaining was carried out at room temperature in a mixture of water/isopropanol/acetic acid (81:12:7), supplemented with 0.5% (w/v) $CuSO_4$.

Table 4. Composition of SDS[a)]-polyacrylamide gels

Solution	Separating gel (14%)	Stacking gel (4%)
Tris/HCl	2.5 ml (1.5 M, pH 8.8)	2.5 ml (0.5 M, pH 6.8)
40% Acrylamide (acrylamide/bisacrylamide 37:1)	3.5 ml	1 ml
H_2O	4 ml	6.5 ml
100 % TEMED[b)]	7 µl	30 µl
10 % APS[c)]	60 µl	60 µl

a) sodium dodecyl sulfate
b) *N, N, N′, N′*-Tetramethylenthylendiamine
c) Ammoniumperoxodisulfate

4.3 Determination of ATP

The ATP content of *C. hydrogenoformans* cells was determined using the luciferin/luciferase assay. The assays were performed at 60°C under an atmosphere of N_2 in 8-ml serum bottles filled with 2 ml 20 mM imidazole/HCl buffer pH 7.0, 2 mM $MgCl_2$, 2 mM KCl, 15 mM NaCl, 2 mM DTT and 150 µl of washed cells (2-6 mg protein). The cells were preincubated at 60°C in a water bath shaker. The reaction was started by changing the gas phase from N_2 to 100 % CO at a pressure of 120 kPa; suspensions were incubated under continuous shaking. At various time intervals, samples of 200 µl of cell suspensions were withdrawn and immediately transferred into tubes containing 600 µl ice-cold ethanol and rapidly mixed. Aliquots of 10 µl of ethanol extracts were immediately analysed for ATP in 1 ml 20 mM Tris/HCl buffer, pH 7.5 containing 100 µM luciferin and 10 µg luciferase in a luminometer (LKB Wallac, Turku, Finnland). For the estimation of the amount of ATP formed, a calibration curve was prepared using standard ATP concentrations.

4.4 Determination of H_2 by gas chromatography

H_2 was determined by gas chromatography with a Carlo Erba Model 6000 GC (Milano, Italy) equipped with a thermal conductivity detector (TCD). The assay conditions are indicated in table 5. A calibration curve was prepared, using gas mixtures of standard H_2 concentrations (5%; 10%; 20%; 35%; 75%; 90%; 100%) in N_2. Withdrawals of samples (0.2-0.3 ml) or of standard gases from the gas phase of various vials were made by a gas-tight syringe. Between the different tests, the syringe was cleaned with 100% N_2.

Table 5. Conditions for the determination of H_2 by gas chromatography.

Parameters for gas chromatography		
Detector		TCD
Carrier gas		N_2
Carrier gas pressure		110 kPa
Column		glass (2.2 m x 2 mm)
Column material		molecular sieve 5 Å
Temperature		
	Injector	80°C
	Column	90°C
	Detector	150°C
Retention time		1 min

5. Measurements of ion translocation

5.1 Determination of proton translocation with a pH electrode

The assays were performed at 60°C in a 11-ml glass vessel with two outlets, which were sealed with rubber stoppers. Proton translocation was followed with a pH electrode (model 8103 Ross, Orion Research, Küsnacht, Switzerland), which was inserted into the vessel from the top through one of the rubber stoppers. The electrode was connected with a compensation pH meter (model 720A, Orion Research) in combination with a chart recorder (Pharmacia Biotech, Freiburg, Germany) (Bott & Thauer, 1989;Deppenmeier *et*

al., 1990; Ide *et al.*, 1999). After gassing with N_2 for 15 minutes, by means of two needles inserted from the side arm of the vessel through a rubber stopper, the vessel was filled with 2.5 ml of 1 mM MES/KOH pH 5.9 or 1 mM MOPS/NaOH pH 6.7 supplemented with 15 µM resazurin, 100 mM KCl and 4 mM DTT. After waiting for 5 min, 50-100 µl of washed cells (10 mg of protein ml^{-1}) and 25 µM valinomycin were added. The mixture was continuously stirred with a small magnetic stir bar. Additions were made with microliter syringes, which were previously degassed by using anaerobic buffer. The pH value was adjusted to about 5.9 with 0.1 M HCl.

5.1 Proton translocation by suspensions of washed cells of *C. hydrogenoformans*

The harvested cells were resuspended in 1 mM MES/KOH pH 5.9 or in 1 mM MOPS/NaOH pH 6.7 supplemented with 15 µM resazurin, 100 mM KCl and 4 mM DTT. The cells were washed twice by centrifugation with a RC 5B centrifuge (Kendro, Hanau, Germany) equipped with GS3 rotor at 7000 x *g* for 20 minutes at 4°C and finally resuspendend in the same buffer used above. Washed cells were added to the glass vessel and allowed to equilibrate, until a straight base line was obtained. Additions of different concentrations of CO-saturated buffer, the protonophore CCCP or the sodium ionophore ETH-157 were made and the associated pH changes were measured. CO-saturated buffer was prepared as follow: a 120-ml serum bottle was filled with 30 ml of desired buffer, the gas phase was 100% CO at 10^5 Pa; the gas phase and the liquid phase were equilibrated at 25°C. Under these conditions the equilibrium CO concentration in solution was calculated to be 0.93 mM (Bott & Thauer, 1989). After completion of the experiments, the pH changes were calibrated with nanomolar additions of a standard solution of HCl (Titrisol).

5.2 Determination of sodium transport

Transmembrane sodium transport was determined by measuring the change of internal Na^+ concentration (Kaesler & Schönheit, 1989a). The assays were performed at 60°C in 8-ml serum bottles filled with 1 ml assay mixture containing 20 mM imidazole/HCl buffer pH 7.0, supplemented with 15 µM resazurin, 20 mM KCl, 2 mM DTT, 50 mM KSCN and 15 mM NaCl. The gas phase was 100% N_2. The assay mixture received 0.37 MBq ^{22}NaCl and was subsequently incubated for 15 min at room temperature to reduce the oxygen introduced. Then washed cells (0.1-0.9 mg protein) were added and incubated at 60°C for

30-45 min until equilibration of the extracellular and intracellular Na^+ was attained. The intracellular Na^+ concentration was calculated from the amount of $^{22}Na^+$ in the cells and the specific radioactivity of the extracellular Na^+. An internal volume of 3.2 µl/mg protein was used for the calculations (Blaut & Gottschalk, 1984). The substrate CO was added to the gas phase with a plastic syringe. Withdrawals of samples (100 µl) from the assay mixture, were made by a syringe previously cooled at 0°C. The samples were transferred into ice-cooled buffer (20 mM imidazole/HCl buffer pH 7.0, 15 µM resazurine, 20 mM KCl, 2 mM DTT, 50 mM KSCN and 15 mM NaCl) and immediately filtered through a cellulose acetate filter (pore size 0.8 µm, SS 68, Schleicher und Schüll, Dassel, Germany). The filters were washed four times with 10 ml ice-cold buffer. The filters had been previously soaked with 2.5 M NaCl to reduce unspecific binding of Na^+ to the filter. The filters were soaked in 10 ml scintillation cocktail Quicksafe A (Zinsser Analytic) and measured for bound radioactivity in a Beckman LS6500 scintillation system.

6. Molecular biology methods

6.1 Construction of *echF* mutants

E. coli DH10B (Invitrogen, Carlsbad, CA, USA) was used as the host strain. *echDEF* was PCR amplified from *M. barkeri* chromosomal DNA using primers GGCGCGCCGGGCCCACGGAGTAGTGGCAGCACTT and GGCGCGCCCTCGAGG GAGAACATTCAGTATTGTTTTTCAAG (restriction sites are underlined), digested with ApaI and XhoI, and ligated into pBluescriptSK (Stratagene) cut with ApaI and XhoI, resulting in pAMG57. Point mutations were generated by the QuickChange™ method (Stratagene) using pAMG57 as the PCR template. The insert of interest was sequenced to verify that the selected clones only contained the desired mutations (see 6.7). The downstream region of *M. barkeri ech* was PCR-amplified using primers GGCGCGCCCTGCAGGGTCTAAATTTGGCAGTTAAGGAA and GGCGCGCCGG ATCCCCTGCACCTTTCCTGATTTT, digested with BamHI and PstI, and ligated into pJK3 (Metcalf *et al.*, 1997) cut with BamHI and PstI, resulting in pAMG77. Each of the seven point mutations generated from pAMG57 and the insert from the original pAMG57 were then subcloned into pAMG77 using the ApaI and XhoI restriction sites, resulting in pCGR1 through pCGR3 and pCGR5 through pCGR9, respectively. These plasmids were

then digested with ApaI and BamHI and transformed into *M. barkeri* using standard techniques (see Fig. 7) (Boccazzi *et al.*, 2000; Metcalf *et al.*, 1997; Pritchett *et al.*, 2004; Zhang *et al.*, 2002), selecting puromycin resistance. After single-colony purification, clones were screened for the correct genotype by PCR amplification and sequenced using primers ACTTATGTTACCGGGCGTCA and CCTCGAGGGAGAACA TTCAG, resulting in the strains listed in Table 1. *M. barkeri* strains were grown in single cell morphology (Sowers *et al.*, 1993) at 37°C in high-salt (HS) medium under strictly anaerobic conditions, as previously described (Metcalf *et al.*, 1996). 125 mM methanol was added to HS media as carbon and energy source. Puromycin was added to 2 $mg \cdot ml^{-1}$ as appropriate.

The construction of the plasmids and the transformation into *M. barkeri* were performed by Adam Guss in the research group of W. Metcalf, University of Illinois at Urbana-Champaign, USA.

6.2 Plasmid and oligonucleotides

The oligonucleotides used in this work were synthesized by Thermo Electron (Ulm, Germany) and are listed in table 6. The plasmid pAMG57 (see 6.1) was kindly provided by Adam Guss from the research group of W. Metcalf, University of Illinois at Urbana-Champaign, USA.

Table 6. Oligonucleotides used for site-directed mutagenesis in pAMG57-*ech*F

oligonucleotide	**sequence**[a)]
*ech*FC42S_for	5'-CCCTGAGAAC**TCT**ATTCTCTGCGGACTATG-3'
*ech*FC42S_rev	5'-CATAGTCCGCAGAGAAT**AGA**GTTCTCAGGG-3'
*ech*FC45S_for	5'-CTGAGAACTGTATTCTC**TCC**GGACTATGTCAAAAGAAATG-3'
*ech*FC45S_rev	5'-CATTTCTTTTGACATAGTCC**GGA**GAGAATACAGTTCTCAG-3'
*ech*FC48S_for	5'-CTCTGCGGACTA**TCT**CAAAAGAAATGCCC-3'
*ech*FC48S_rev	5'-GGGCATTTCTTTTG**AGA**TAGTCCGCAGAG-3'
*ech*FC52S_for	5'-GGACTATGTCAAAAGAAA**TCC**CCGCCTGATGCAATAACAG-3'
*ech*FC52S_rev	5'-CTGTTATTGCATCAGGCGG**GGA**TTTCTTTTGACATAGTCC-3'
*ech*FC73S_for	5'-GGAGCTCAACTTATTTAGA**TCC**ATAATGTGCACTGAATGC-3'
*ech*FC73S_rev	5'-GCATTCAGTGCACATTAT**GGA**TCTAAATAAGTTGAGCTCC-3'
*ech*FC76S_for	5'-GATGCATAATG**TCC**CACTGAATGCGTTAACGGC-3'
*ech*FC76S_rev	5'-GCCGTTAACGCATTCAGT**GGA**CATTATGCATC-3'
*ech*FC79S_for	5'-GCATAATGTGCACTGAA**TCC**GTTAACGGCTGTCC-3'
*ech*FC79S_rev	5'-GGACAGCCGTTAAC**GGA**TTCAGTGCACATTATGC-3'
*ech*FC83S_for	5'-GCACTGAATGCGTTAACGGC**TCT**CCAAAGGGCTGTC-3'
*ech*FC83S_rev	5'-GACAGCCCTTTGGA**GA**GCCGTTAACGCATTCAGTGC-3'

a) Sites of mutations are underlined

6.3 Isolation of plasmid DNA

For purification of small amount of plasmid DNA from 5 ml overnight cultures of *E. coli* the QIAprep Spin Miniprep Kit (Qiagen, Hilden, Germany) was used following the protocol attached.

Large scale preparations of plasmid DNA was perfomed by the "quick and dirty" method (Sambrook *et al.*, 1989), which is based on alkaline lysis of bacterial cells, like the QIAprep principle. 5 ml overnight cultures of *E. coli* were harvested by centrifugation, each pellet was resuspended in 250 µl solution P1 (50 mM Tris/HCl, pH 7.5, 10 mM EDTA, 0.1% Rnase A). Cells were lysed upon addition of 250 µl solution P2 (0.2 M NaOH, 1% SDS) and the lysate was neutralized by addition of 350µl solution P3 (1.5 M potassium acetate, pH 4.8). After 10 min centrifugation at 10000 *g*, the supernatant containing plasmid DNA was transferred into another microfuge tube. DNA was precipitated by addition of 1 volume of 2-propanol (-20°C) and subsequent centrifugation for 10 min at 10000 *g* and 4°C. Then the DNA pellet was washed in ice-cold 70% ethanol, dried and dissolved in H_2O.

6.4 Determination of DNA concentration

DNA concentration was determined by measuring the absorption of the appropriately diluted samples at 260 nm and 280 nm with a spectrophotometer (Ultrospec 3100 pro, Amersham Biosciences, Freiburg, Germany). The reading at 260 nm allows calculation of the concentration of DNA in the sample; an absorption of 1 corresponds to ~50 µg/ml for double-stranded DNA. The ratio between the absorption at 260 nm and 280 nm provides an estimation of the purity of the nucleic acids; pure preparations have A_{260}/A_{280} values of 1.8 (Sambrook *et al.*, 1989).

6.5 Digestion of plasmid DNA with restriction endonucleases

DNA samples were digested with restriction endonucleases using the corresponding reaction buffer (New England Biolabs, Frankfurt/Main, Germany). Generally, digestions were prepared in 20 µl total volume, with 0.5 µl restriction enzyme (20 U/µl) and incubated at 37°C for at least 1 h. The digestion was then controlled by agarose gel electrophoresis.

6.6 Agarose gel electrophoresis

DNA fragments were separated by electrophoresis at 100-135 V using 1% agarose gels in 0.5 TAE buffer (1×: 40 mM Tris-acetate pH 8.0; 1 mM EDTA). Before loading on the gel, the DNA samples were mixed with 1:10 loading buffer (10×: 60% glycerin, 50 mM EDTA, with each 0.25% bromophenol blue, xylene cyanol and orange G). Smart Ladder (Eurogentec, Seraing, Belgium) was used as DNA size standards (200-10,000 bp). After electrophoresis, the gel was stained for 20 min in an ethidium bromide solution (2 μg/ml H_2O). The DNA bands were then visualized using UV light (302 nm) and photos were taken at the same wavelength.

6.7 Preparation and transformation of electrocompetent *E. coli* cells

For the preparation of electrocompetent cells, a flask containing 500 ml LB medium was inoculated at an OD_{578} of 0.1 with an overnight *E. coli* DH5α culture and incubated at 37°C with agitation. When an OD_{578} of 0.6-0.8 was reached, the cultures were rapidly harvested by centrifugation at 5000 g for 10 min at 4°C. The cells were first washed two times in ice-cold sterile water and then in ice-cold sterile 10% glycerol. At the end the cell pellets were resuspended in 10% glycerol, portioned in different microfuge tubes and stored at -80°C until use.

Before transformation the electrocompetent cells were thawed on an ice bath; the electroporation cuvettes (BTX, San Diego, USA) were placed on ice as well. The DNA to be electroporated was dialyzed against H_2O for 30 min, afterwards it was mixed with the electrocompetent cells and the mixture was pipetted into an electroporation cuvette. The transformation was performed using a BioRad Gene Pulser II (BioRad, München, Germany) at 1.8 kV, 250 Ω and 25 μF. As quick as possible after the pulse, 0.75 ml SOC medium (Sambrook *et al.*, 1989) was added, the cells were transferred into tubes and incubated with agitation at 37°C. After 1 h different volumes of the electroporated cells were plated onto LB agar medium containing the appropriate antibiotic and incubated overnight at 37°C. Transformed colonies were screened by isolating the plasmid DNA and performing restriction analysis.

6.8 Site-directed mutagenesis

For the generation of site-directed mutagenesis at desired position of *echF*, the plasmid pAMG57 was used as template, carrying *echDEF* genes as insert of interest. For each point mutation two synthetic oligonucleotide primers, both containing the desired mutation, were used. The mutagenic primers, each complementary to opposite strands of the vector, were extended during temperature cycling by Vent polymerase (New England Biolabs, Frankfurt/Main, Germany). Generally, site-directed mutagenesis were performed in 20 µl total volume, with 20-50 ng template plasmid DNA, 20 pmol of each mutagenic primer, 1 U Vent polymerase and 250 µM of each dNTP. The program used is depicted in table 7. The PCR products were then treated for 2-4 h at 37°C with 20-50 U DpnI (New England Biolabs, Frankfurt/Main, Germany), which was used to digest the methylated parental DNA template and to select for mutation-containing synthesized DNA. After checking the digested samples by electrophoresis on an 1% agarose gel, the DNA containing the desired mutations was transformed into electrocompetent *E. coli* DH5α cells. Following transformation, colonies were screened by isolating the plasmid DNA and performing restriction analysis. Finally, the insert of interest was sequenced to verify that the selected clones contained the desired mutation only at the desired positions.

Table 7. Program used for site-directed mutagenesis.

Step	Cycles	Temperature	Time
1: denaturation	1	95°C	3 min
2: denaturation	30	95°C	30 sec
3: annealing		62-65°C	1 min
4: polymerization		68°C	10 min
5: polymerization	1	68°C	10 min
6: storage	1	4°C	

6.9 DNA Sequencing

DNA sequencing was performed by Agowa (Berlin, Germany). For sequencing the universal SK (CGCTCTAGAACTAGTGGATC), M13-24F (CGCCAGGGTTTTCCCA GTCACGAC) primers, already available by Agowa, have been used.

7. Biophysical methods

7.1 EPR spectroscopy studies

7.1.1 Introduction to EPR spectroscopy

Only the components that have unpaired electrons, such as transition metals or free radicals, are detected by EPR spectroscopy. For simplicity, a paramagnetic substance could be considered to be a substance that has a free unpaired electron (spin S = ½). In the absence of a magnetic field, all of the spins are oriented randomly within the same energy level. When the sample is placed in a magnetic field B, the magnetic moment of unpaired spins will tend to be aligned either anti-parallel or parallel to the direction of the magnetic field (called Zeeman splitting), as shown in Fig. 5. Therefore, spins in the sample are divided into two populations having energies of $-(½)g\beta B$ and $+(½)g\beta B$ (see below). Lower and higher energy levels correspond to spins anti-parallel and parallel to the applied magnetic field, respectively. In EPR spectroscopy the resonance transition between these two induced spin populations is observed. The energy difference (ΔE) between these spin states is dependent on the strength of the applied magnetic field B. When a microwave with an energy $h\nu$ is applied to this system, and B is scanned, a resonance transition takes place when ΔE between the two states ($g\beta B$) becomes equal to $h\nu$ of the applied microwave (h is the Planck's constant, $6.626 \cdot 10^{-34}$ J·s and β is the Bohr magneton, $9.274 \cdot 10^{-28}$ J·G^{-1}). EPR spectra are generally obtained by scanning the magnetic field to find the resonance position with a fixed microwave frequency. The most often used frequency is 9 GHz (called X-band). Since EPR spectroscopy detects a very weak energy absorption, modulation of the magnetic field at 100 kHz and phase-sensitive detection are used to increase signal/noise ratio. Therefore, EPR spectra are routinely recorded as the first derivative of the absorption curve.

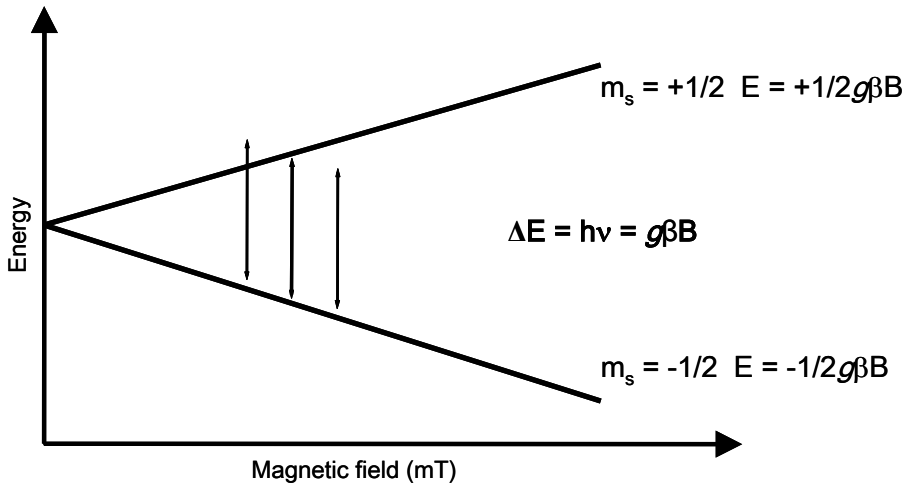

Fig. 5. Dependence of the energies of the m_s = ± ½ states of an electron on the magnetic field. The vertical double-headed arrows signify the energy associated with the microwave quantum and imply that there is a unique value of the magnetic field at which absorption of the microwave energy can occur.

Since the frequency varies somewhat from experiment to experiment, it is better to express the signal position in terms of a value characteristic of the substance. In EPR spectroscopy, a *g* value, which is the constant of magnetization, ($g = h\nu/\beta B = 0.7145 \cdot \nu(MHz)/B(Gauss)$), is used to define the position of resonance. For a free electron, *g* is equal to 2.0023. Since most of the electrons in iron-sulfur clusters are localized in the 3d molecular orbital of the transition metal irons, the *g* value deviates from that of a free electron. This deviation reflects magnetic interactions, which the spin system has with its surroundings. The *g* value of a paramagnetic center can have three values, each corresponding to a value obtained when the magnetic field B is parallel to one of the three spatial directions of the molecule, which are called g_x, g_y and g_z. When spins in the molecule are magnetically isotropic, the *g* value will have a single value; in axial or rhombic symmetry the *g* value is given by two or three parameters, respectively (Fig. 6).

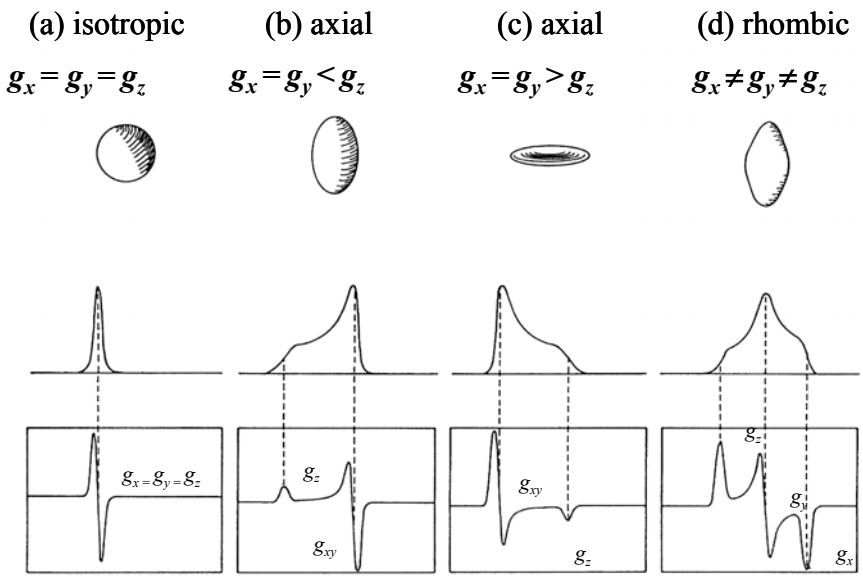

Fig. 6. Schematic representation of the relationship between *g* value anisotropy and the EPR spectral line shapes. Columns (a-d) name each spectral type and immediately below show the associated pattern of *g* anisotropy. Beneath each solid is the idealized lineshape, first in absorption presentation and subsequently in derivative form. The broken vertical lines serve to correlate the features shown in the absorption and derivative presentations. Taken from Palmer, 2000.

7.1.2 Preparation of samples for EPR spectroscopy

Round tubes of very pure quartz (99.99%) with an internal diameter of 0.3 cm were filled with 300 µl of samples, incubated with H_2 for 10 min at 30°C and then rapidly frozen in liquid nitrogen (77K). The EPR tubes were also stored in liquid nitrogen, this did not affect the intensity of the signal.

7.1.3 EPR spectroscopy measurements

EPR spectra at X-band (9 GHz) were obtained with a Bruker EMX spectrometer. All spectra were recorded with a field modulation frequency of 100 kHz. The samples were cooled by an Oxford Instrument ESR 900 helium flow cryostat with an ITC4 temperature controller.

7.1.4 Evaluation of the spectra

For the evaluation of the spectra the WIN-EPR Bruker program as well as a non-commercially available program, created by Simon Albracht (University of Amsterdam, the Netherlands), were used.

Spin quantification was carried out using copper perchlorate as standard (10 mM $CuSO_4$, 2 M $NaClO_4$, 10 mM HCl). By comparing the spin concentration of the copper standard with the spin concentration of the signal of interest, the concentration of that signal can be determined. The area under the absorption spectrum is a direct measure for the concentration of unpaired electrons. Since the EPR spectrum is a first derivative, it is necessary to integrate twice to obtain the intensity. Additional corrections are needed for a number of parameters in order to 'normalize' the spectra; only in this way it is possible to compare double integral values of the copper standard and the unknown sample. The equations needed for calculations are indicated below.

$$C_u = \frac{I_{N(u)} C_{st}}{I_{N(st)}} \qquad I_N = \frac{I_0 d^2 T 10^{dB/20}}{g_p^{av} f a}$$

where

C_U	spin concentration of unknown sample	f	tube calibration factor
C_{st}	spin concentration of standard	a	gain
$I_{N(u)}$	normalized value for the intensity of unknown (normalized double integral)	d	distance between the starting and ending points (in Gauss)
$I_{N(st)}$	normalized value for the intensity of standard	g_p^{av}	$\frac{2}{3}\sqrt{\frac{\left(g_x^2 + g_y^2 + g_z^2\right)}{3}} + \frac{\left(g_x + g_y + g_z\right)}{9}$
I_0	observed intensity	dB	microwave energy
T	temperature in K		

7.1.5 Determination of the temperature-dependency of EPR signals

The temperature-dependency of a sample was determined by measuring the sample at different temperature under non-saturating conditions. Since the observed signal intensity

or amplitude decreases when the temperature increases, it is necessary to normalise the intensity or amplitude, according to the formula:

$$I_N = \frac{I_0 T 10^{dB/20}}{gain}$$

where

I_N normalized value for the intensity

I_0 observed intensity

T absolute temperature in K

dB reading of the attenuator

gain gain

7.2 FT-IR spectroscopy

7.2.1 Introduction to FT-IR spectroscopy

Infrared spectroscopy is a technique based on the interaction of infrared radiation with the vibrations and rotations of the atoms of a molecule; IR radiation does not have enough energy to affect electron excitation but is energetic enough to excite molecular vibration or rotation to higher energy levels. An infrared absorption spectrum can be obtained by passing radiation through a sample and determining what fraction of the incident radiation is absorbed at a particular energy. The energy at which a peak in an absorption spectrum appears corresponds to the frequency of a vibration of a chemical bond within the sample. There are different modes of vibration: variation of the bond length (so-called stretching vibration) or variation of the bond angle (so-called bending vibration). Factors like the strength of chemical bonds or masses of attached atoms influence the absorption frequency.

Fourier transform is a mathematical process for converting an amplitude-time signal to an amplitude-frequency spectrum; data are rapidly collected in the time domain and converted by Fourier transform to a frequency domain.

The combination of FT-IR difference spectroscopy and electrochemistry is a sensitive method to detect redox-dependent changes in protein structure and protonation states of cofactors or amino acid side chains. This method was first evaluated with cytochrome *c* oxidase, since its 3D structure in both redox states was known and its electrochemistry was already well characterized (Moss *et al.*, 1990). This technique was then extended to study other redox proteins. In particular, a difference spectrum of an enzyme in different states (e.g. oxidized minus reduced enzyme) allows the reorganization that occurs in a protein upon the induced reaction to be observed, since the large background absorbance is removed by subtraction.

7.2.2 Electrochemistry

The ultra-thin layer spectroelectrochemical cell for the UV/Vis and IR was used as previously described (Moss *et al.*, 1990). Sufficient transmission in the 1800 cm^{-1} to 1000 cm^{-1} range, even in the region of strong water absorbance around 1645 cm^{-1}, was achieved with the cell pathlength set to 6-8 μm. To avoid protein denaturation, the gold grid working electrode was chemically modified by a 2 mM cysteamine and a 2 mM mercaptopropionic acid solution in a 1:1 ratio. In order to accelerate the redox reaction, the mediators were used at a final concentration of 45 μM each as previously described in (Hellwig *et al.*, 2000). At the given concentrations and with the pathlength below 10 μm, no spectral contributions from the mediators in the IR range used were detected in control experiments with samples lacking the protein. Approximately 6-7 μl of the protein solution were sufficient to fill the spectroelectrochemical cell. To inhibit the enzyme by acetylene the sample and the buffer were purged with 100% acetylene gas.

7.2.3 FT-IR spectroscopy measurements

FT-IR difference spectra as a function of the applied potential were obtained (modified IFS 25, Bruker, Germany) for the 4000 cm^{-1} – 1000 cm^{-1} range as reported previously (Moss *et al.*, 1990; Hellwig *et al.*, 2000). First, the protein was equilibrated with an initial potential at the electrode and single beam spectra in the IR range were recorded. Then a potential step towards the final potential was applied and single beam spectra of this state were again recorded after equilibration. Difference spectra were calculated from the two single beam spectra with the initial single beam spectrum taken as reference. No smoothing or

deconvolution procedures were applied. The equilibration process for each applied potential was followed by monitoring the electrode current and by successively recording spectra in the visible range until no further changes were observed. The equilibration generally took less than 8 min for the full potential step from -0.3 V to 0.1 V. Typically, 128 interferograms at 4 cm^{-1} resolution were coadded for each single beam IR spectrum and Fourier-transformed using triangular apodization. Up to 5 x 20 difference spectra have been averaged.

IV RESULTS

In the first part of the results section the iron sulfur clusters of Ech hydrogenase from *Methanosarcina barkeri* were assigned to its individual subunits. This is based on the biochemical and EPR spectroscopic characterization of site-directed mutants where conserved cysteine residues in subunit EchF of Ech hydrogenase have been replaced by serine residues.

The second section addresses the role of conserved residues, in the membrane part of the enzyme, in ion translocation.

Redox-induced FT-IR difference spectroscopy was used to elucidate if the electron transfer reaction catalyzed by Ech from *M. barkeri* is associated with a conformational change of the enzyme and with protonation of amino acid side chains. The results are described in the third part.

The fourth part addresses the identity of the coupling ion used by energy-converting hydrogenases. Studies were performed with the enzyme from *Carboxydothermus hydrogenoformans*.

1. Site-directed mutagenesis of conserved cysteine residues in subunit EchF of Ech hydrogenase from *Methanosarcina barkeri*

1.1 Generation of *echF* mutants

A set of *M. barkeri* mutants were generated in which seven of eight conserved cysteine residues in subunit EchF, expected to be involved in iron-sulfur cluster coordination, were individually replaced by serine (Fig. 7). The construction of an *M. barkeri* mutant with a deletion of the *echABCDEF* operon has previously been described. The mutant was still able to grow on methanol as the sole energy substrate but failed to grow on H_2/CO_2, H_2/methanol or acetate (Meuer *et al.*, 2002). Methanol-grown cells were therefore used for the generation of *echF* point mutants.

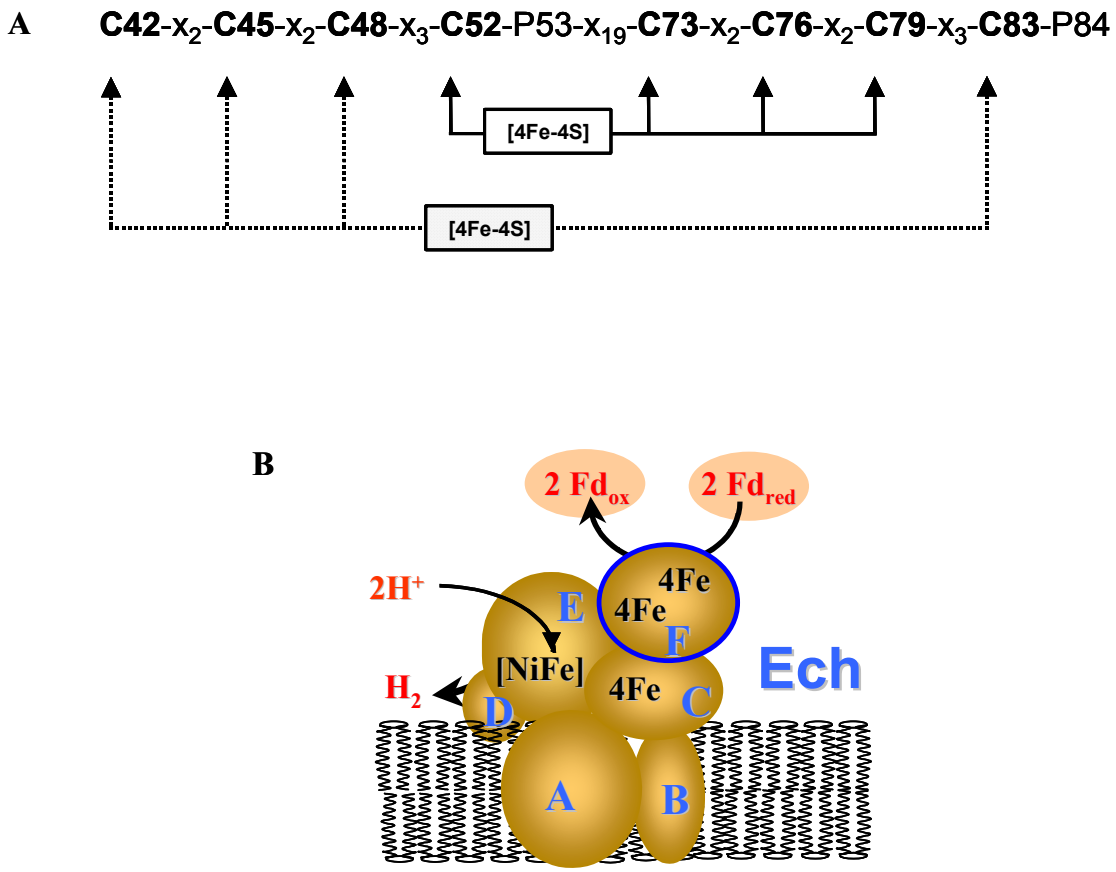

Fig. 7. Representation of the two four-Cys motifs of subunit EchF. The mode of binding of the two putative [4Fe-4S] clusters is indicated (**A**). The F subunit of Ech hydrogenase from *M. barkeri* is highlighted (**B**).

The *echF* mutations were constructed *in vitro* and recombined into the chromosome as described (Fig. 8). *echF* was sequenced from each clone to ensure that it carried the appropriate nucleotide sequence for the individual mutations.

Ech hydrogenase activity in cell extracts of the *echF* mutants and the strain carrying a wild-type copy of *echF* was determined using the ferredoxin assay, which is specific for Ech (table 8). In all *echF* mutants Ech hydrogenase activity was strongly reduced.

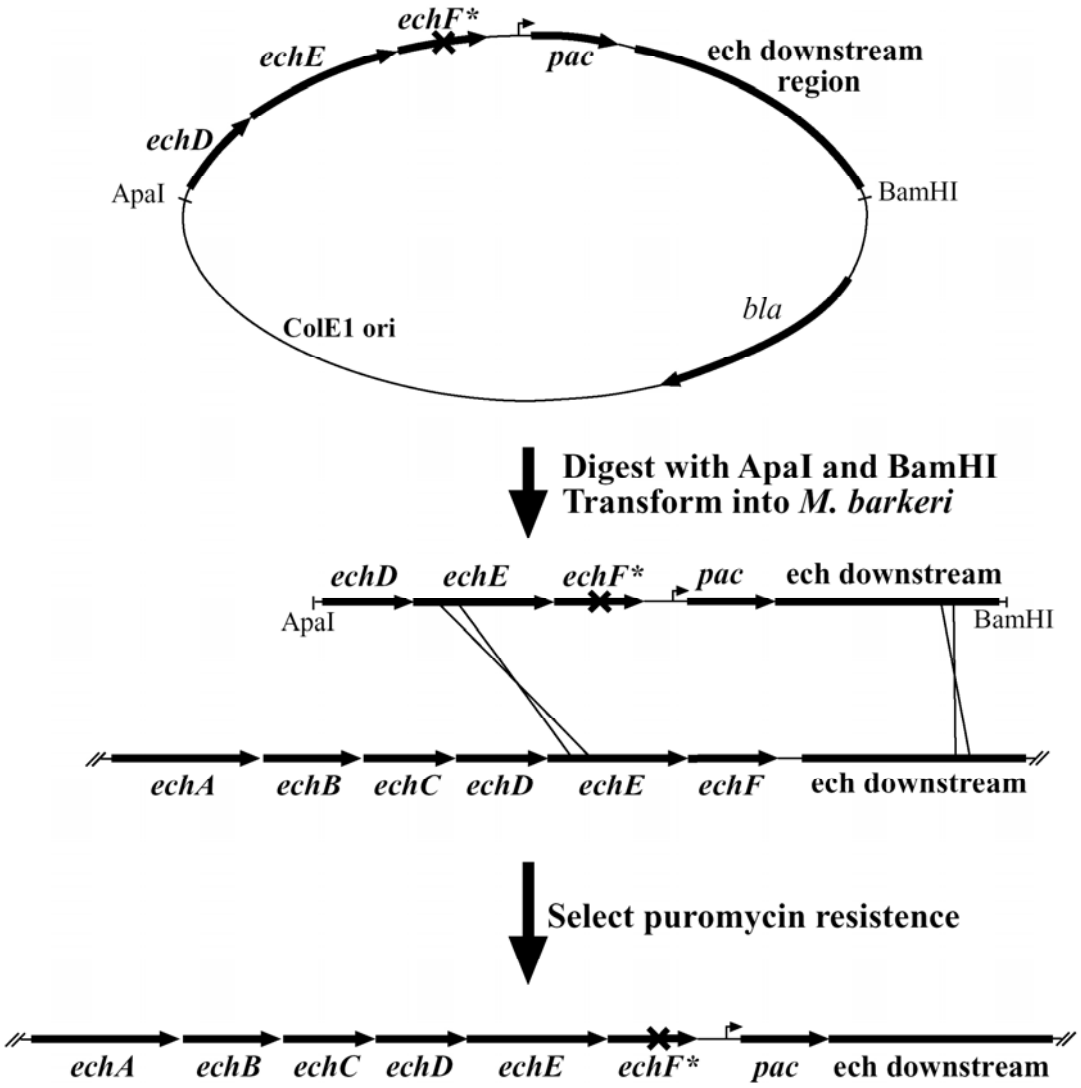

Fig. 8. Generation of *M. barkeri* chromosomal *echF* mutations. Plasmids carrying *echF* point mutations were digested with ApaI and BamHI and then transformed into *M. barkeri*. Each *echF* mutation was stably integrated into the chromosome via two homologous recombination events, which was selected by puromycin resistance.

The highest activities were observed in cell extracts of EchF6, EchF7 and EchF8 mutants. The activity of heterodisulfide reductase, an essential enzyme of the energy metabolic pathway, was determined for internal calibration. The low Ech activity in the mutants was not due to a down regulation of the enzyme as shown by Western blot analysis of total cell

extracts using an antiserum to detect the catalytic subunit EchE (Fig.9). The serum shows cross reactivity with subunit HdrD of heterodisulfide reductase, which was used as an internal standard (Meuer *et al.*, 2002).

Table 8. Ech Hydrogenase and heterodisulfide reductase activity in cell extracts of *echF* mutants and wild type *M. barkeri*. Ech hydrogenase activity was measured by following the H_2- and ferredoxin-dependent reduction of metronidazole and Hdr activity was measured by following the oxidation of reduced benzyl viologen with CoM-S-S-CoB, as described in methods.

Strain	Hydrogenase activity		Hdr activity	
	(U mg^{-1})	(%)	(U mg^{-1})	(%)
EchF9 (WT)	0.340	100	1.7	100
EchF1	0.010	2.9	1.0	59
EchF2	0.009	2.6	1.7	100
EchF3	0.011	3.2	1.1	65
EchF5	0.012	3.5	1.7	100
EchF6	0.038	11.2	1.1	65
EchF7	0.018	5.3	1.4	82
EchF8	0.036	10.6	1.7	100

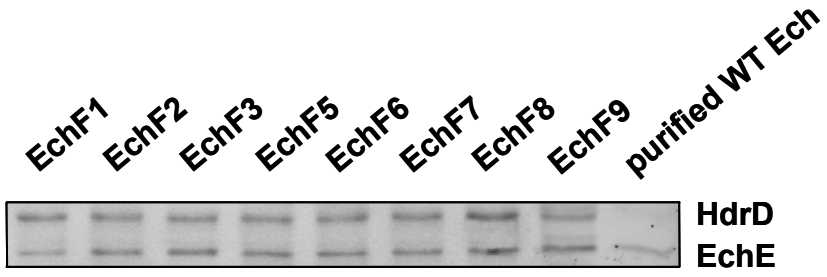

Fig. 9. Western blot detection of EchE subunit in cell extracts of the different *echF* mutants. Immunodetection was performed using rabbit anti-Ech sera, as described in methods. The antiserum also detects HdrD of heterodisulfide reductase, which was used as internal standard. The upper band corresponds to HdrD (43kDa) and the lower band to EchE (39 kDa). In each lane 6 µg protein from cell extract of the *echF* mutant strains were loaded. 40 ng of purified wild-type Ech (WT Ech) was loaded for a comparison.

Cells used in this study were cultivated on methanol in single cell morphology. It was observed that Ech activity in wild-type cells grown under these conditions was approximately 6 to 10-fold lower as compared to Ech activity in cells grown on either methanol or acetate in low salt medium where cells grow as cell-aggregates (Meuer *et al.*, 1999; Meuer *et al.*, 2002)

1.2 Isolation of Ech hydrogenase from the *echF* mutant strains

Ech was purified from wild type and the *echF* mutant strains using a modified version of the procedure described previously (Meuer *et al.*, 1999). After protein solubilisation, purification of Ech was carried out by chromatography on DEAE Sepharose, Q Sepharose and hydroxyapatite. The mutant enzymes studied showed the same chromatographic properties as wild-type Ech throughout all purification steps. Approximately 1.5 mg protein was obtained from 30 g of cells. The preparations thus obtained were analysed by SDS-PAGE (Fig. 10). In preparations obtained from mutant strains EchF2, EchF6 and EchF8 all six subunits of Ech were detectable in Coomassie stained gels (Fig. 10A). The preparations contained contaminating protein bands with apparent molecular masses of 63 kDa, 75 kDa and 90 kDa (only in EchF8). In the preparations obtained from mutant strains EchF1, EchF3, EchF5 and EchF7 the small subunits EchC, EchF and EchD were not clearly detectable in the Commassie stained gel (Fig. 10A), but became detectable after silver staining (Fig. 10B). Subunit EchD was only visible as a fuzzy band migrating directly below EchF. In general the purity of the enzyme from these mutants was lower than the enzyme isolated from the EchF2, EchF6 and EchF8 mutants.

Hydrogenase activity of the purified enzymes was determined by the H_2-uptake assay using the *M. barkeri* ferredoxin, which is the physiological substrate of the enzyme, as electron acceptor. In addition H_2-uptake activity was determined with benzyl viologen as an artificial electron acceptor (table 9). As determined by both assays the EchF8 mutant had the highest activities, with approximately 10% of the activity of the wild-type enzyme. The enzymes from the EchF7, EchF5, and EchF2 mutants showed between 4% and 6% of the wild-type activity. Almost no activity was detectable in the enzymes from the EchF1, EchF3 and EchF6 mutants. The specific activities of the purified enzymes generally correlate with the activities observed in cell extracts. An exception is the EchF6 mutant in which relatively high Ech activity was determined in cell extract but almost no activity

could be detected with the purified enzyme. Wild-type Ech catalysed the reduction of benzyl viologen under the experimental conditions at 4-fold higher rates than the reduction of ferredoxin. This activity ratio was nearly constant in the different mutant enzymes.

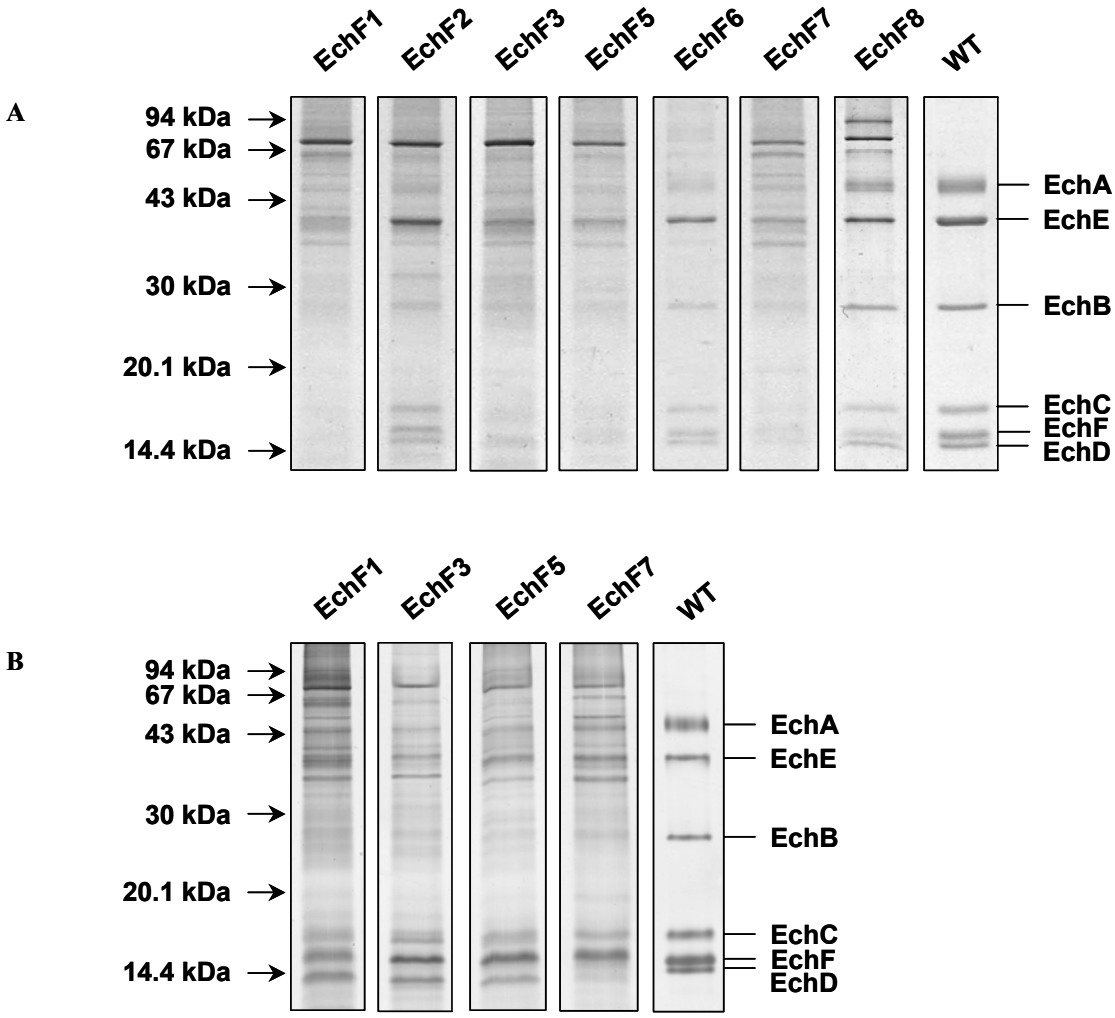

Fig. 10. SDS-PAGE analysis of Ech hydrogenase preparations from *M. barkeri echF* mutants. Proteins were denaturated by incubation in Laemmli-buffer containing 5 mM DTT and 2% SDS for 60 min at room temperature and were subsequently separated in a 14% slab gels (8 × 7 cm). Gels were stained with (**A**) Coomassie Brilliant Blue R250 or (**B**) silver. In each lane 5 µg of protein were loaded. The highly purified enzyme from acetate-grown cells was used as wild-type Ech (WT). The molecular masses of marker proteins are given on the left, the Ech hydrogenase subunits are indicated on the right side.

Table 9. Ech Hydrogenase activity of purified Ech hydrogenase from *echF* mutants and wild-type *M. barkeri*. Hydrogenase uptake activity was measured by following the H_2- and ferredoxin-dependent reduction of metronidazole (Fd assay) or the H_2-dependent reduction of benzyl viologen (BV assay) as described in methods

Strain	Hydrogenase activity			
	Fd Assay		BV Assay	
	(U mg^{-1})	(%)	(U mg^{-1})	(%)
WT	30	100	128	100
EchF1	0.4	1.3	0.7	0.5
EchF2	1.2	4	3.4	3
EchF3	0.2	0.7	0.6	0.5
EchF5	1.9	6	9.9	8
EchF6	0.2	0.7	0.4	0.5
EchF7	1.8	5	4.0	3
EchF8	3.0	10	11.7	9

1.3 EPR analysis of Ech hydrogenase isolated from *echF* mutant strains

The iron-sulfur centres of Ech isolated from the different *echF* mutant strains and the strain carrying a wild-type copy of *echF* were characterized by EPR spectroscopy (Fig. 11). Samples were reduced under an atmosphere of 100% H_2 and EPR spectra were recorded at 10 K and 20 dB (2 mW) microwave power. The wild-type enzyme exhibited a spectrum identical to that described previously (Kurkin *et al.*, 2002). Based on the EPR line shape and differences in temperature dependence this spectrum had been shown to be an overlap of two major EPR signals originating from S = ½ reduced [4Fe-4S] clusters, one signal with g_{xy} = 1.921 and g_z = 2.050 (designated the 1.92 signal) and the second with g_{xy} =1.887 and g_z = 2.078 (designated the 1.89 signal). EPR spectra recorded from the enzyme of the EchF8, EchF7 and EchF2 mutants show a strong signal with g_{xy} = 1.890 and g_z = 2.078, corresponding to the g = 1.89 signal found in the wild-type enzyme. The g = 1.92 signal was still detectable in these mutant enzymes but its spin concentration was strongly reduced relative to the g = 1.89 signal.

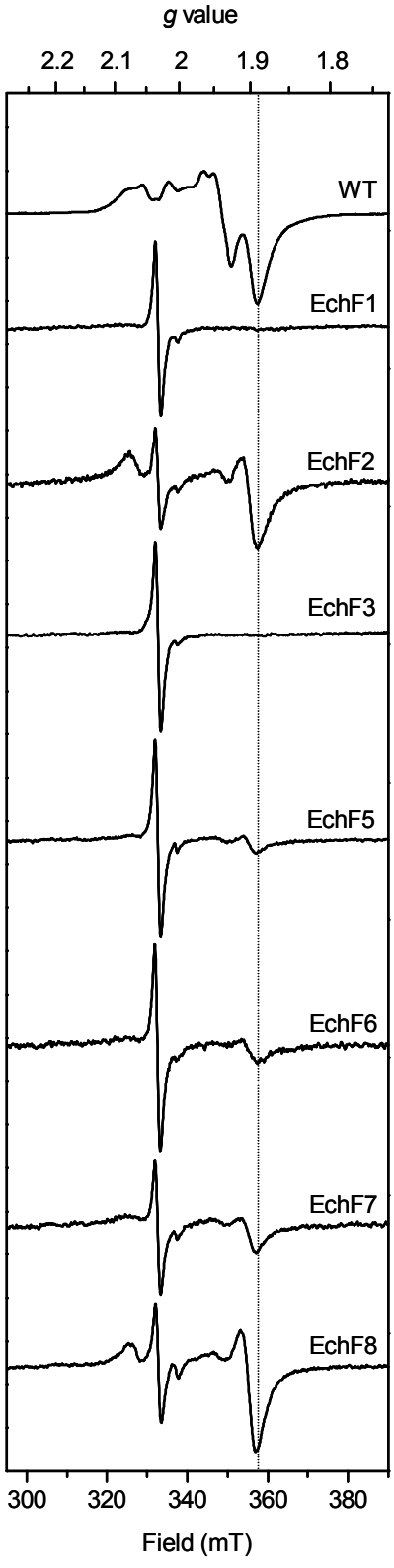

Fig. 11. EPR spectra of Ech hydrogenase isolated from wild type and *echF* mutants. Enzymes (4.6 mg/ml) were dissolved in 50 mM MOPS/NaOH buffer pH 7.0 and reduced by incubation for 10 min at 30°C under 100% H_2 (1.4 x 10^5 Pa). EPR conditions: microwave frequency, 9460 MHz; microwave power, 20 dB (2 mW); modulation amplitude, 0.6 mT; temperature, 10 K. The dotted line indicates the position of the g = 1.89 signal. The intensity of the spectrum of the wild-type enzyme (EchF9) was reduced two-fold.

The EPR spectrum obtained for the enzyme from the EchF8 mutant showed the most intense g = 1.89 signal. Both iron-sulfur signals were simulated (Fig. 12). The parameters for the g = 1.89 signal are slightly different than previously reported (Kurkin *et al.*, 2002) due to the fact that the cluster is not involved in spin-spin interaction with other clusters.

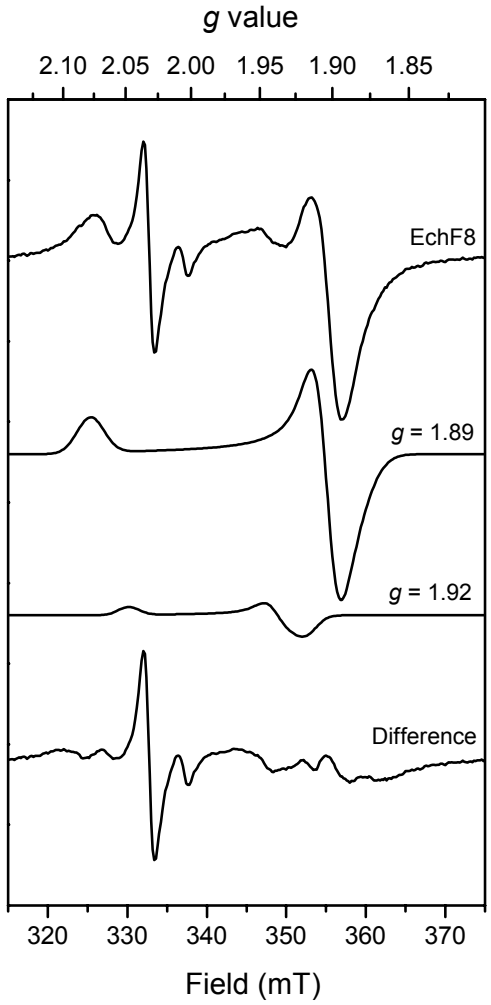

Fig. 12. Simulation of the EPR spectrum of the EchF8 mutant enzyme. The experimental spectrum (EchF8), the simulated g = 1.89 and g = 1.92 spectra and the difference spectrum obtained after subtraction of the two simulated spectra from the experimental spectrum, are shown. Simulation of the g = 1.89 signal of the spectrum from the EchF8 mutant enzyme with parameters g_{zyx} = 2.07750, 1.90223, 1.89000 and widths (zyx) 3.4, 2.6 and 5.9 mT. Simulation of the g = 1.92 signal with parameters g_{zyx} = 2.04721, 1.93799, 1.91821 and widths 2.66, 2.7 and 2.77.

The 1.92 signal was simulated with the same parameters as before since it only has a low contribution to the overall spectrum. The overall spin concentration in the iron-sulfur cluster region, corrected for the g = 2.03/2.00 radical-like signals (see below) was 10 µM, the enzyme concentration was 19 µM. The 1.89 and 1.92 signals are present in a ratio of 9 to 1 as estimated using the simulated EPR spectra. As in the wild-type enzyme the g = 1.92 signal and the g = 1.89 signal showed a different temperature dependence. The g = 1.92 signal was optimally sharpened at 17 K whereas the g = 1.89 signal was already considerably broadened at 17 K as shown for the enzyme from the EchF8 mutant in figure 13.

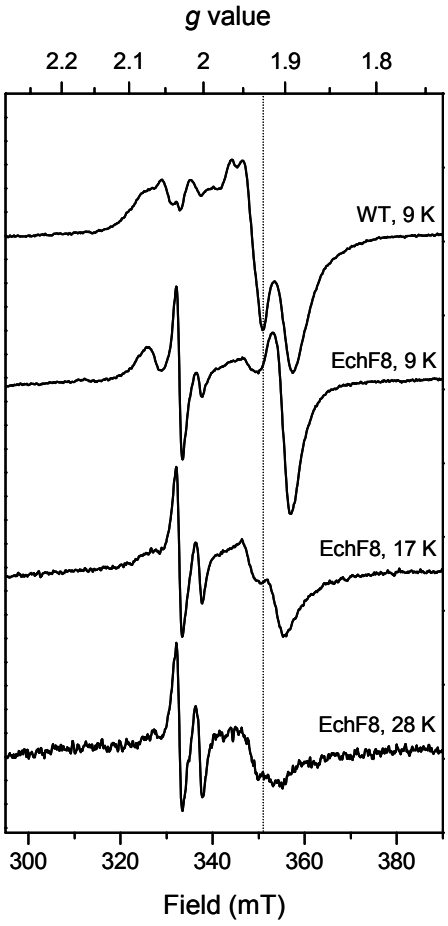

Fig. 13. EPR spectra of the EchF8 mutant enzyme at different temperatures in comparison to the wild-type spectrum. The dotted line indicates the position of the g = 1.92 signal. For EPR conditions, see figure 11.

To determine if the mutations had turned the spin of the ground state of the cluster(s) of subunit EchF to S = 3/2, EPR spectra were recorded in the low field region (50 – 2000 G)

at low temperature (4.5 K) and high power 20 mW. Pronounced signals were only observed at g = 4.3 which could be due to adventitious Fe(III).

EPR spectra recorded from the enzyme of the EchF5 mutant showed only a weak g = 1.89 signal, but the amplitude of the g = 1.92 signal was comparable to that found in the enzyme from the EchF2, EchF7 and EchF8 mutants. The EchF6 mutant also showed a weak g = 1.89 signal but only weak g = 1.92 signal. In EPR spectra recorded from the EchF1 and EchF3 mutant enzymes no iron-sulfur cluster signals could be detected.

EPR spectra of the *echF* mutants all showed signals with g values at 2.033 and 2.003. The two signals showed different saturation properties (Fig. 14).

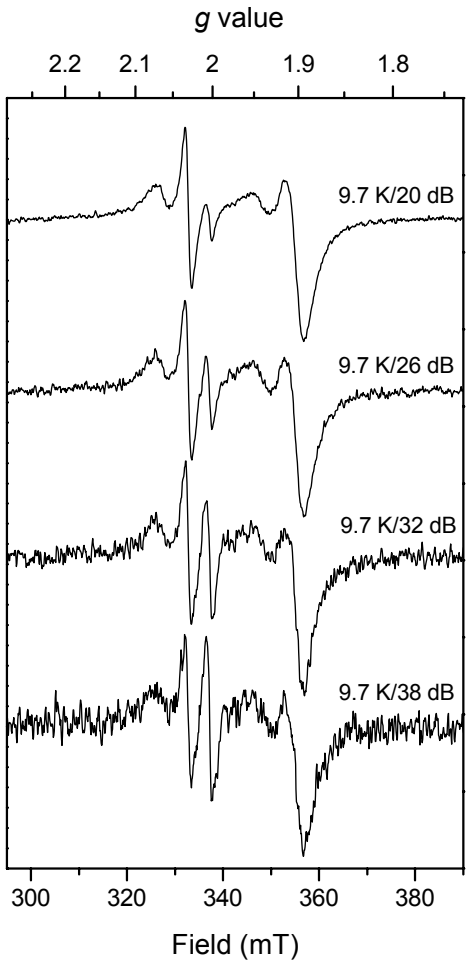

Fig. 14. EPR spectra of the EchF8 mutant enzyme at different power. For EPR conditions, see figure 11.

The 2.03 signal could not be saturated at 4 K and 10 dB (20 mW) whereas the 2.00 signal was already saturated at 10 K and 20 dB (2 mW). The signals could be observed at temperatures up to 130 K without signal broadening. The line width of both signals was approximately 1.2 mT, which is typical for radical species. The identical line width indicates that both signals could belong to the same paramagnetic species. The g = 2.03 signal has been previously detected in wild-type Ech where it is only present at very low intensity. However, this signal is much stronger in the *echF* mutants. The spin concentration of this signal was determined in the EchF1 and EchF3 mutants, which showed no iron-sulfur cluster signal. Here the spin concentration was approximately 0.7 µM, assuming an S ½ species, the enzyme concentration was 19 µM. By comparing the signal amplitudes it could be estimated that the spin concentration of the g = 2.03/2.00 signals in the EchF8 mutant is 0.4 to 0.5 µM corresponding to 4 to 5 % of the spin concentration of the iron-sulfur cluster signals. In general the spin concentration of the g = 2.03/2.00 signals was approximately 1.6 times higher in the enzyme from those mutants which showed no or very low intensity signals for the iron-sulfur clusters. The g = 2.03/2.00 signals shown in figure 8 were observed for the enzyme reduced by 100% H_2. Addition of 20 mM sodium dithionite did not change the intensity of these signals. When 1 mM duroquinone (E_0' = +86 mV) was added to the enzyme under N_2, the g = 1.89 signal was no longer detectable, indicating an oxidation of this iron-sulfur center. The intensities of the g = 2.03/2.00 signals were, however, not altered by duroquinone oxidation.

2. Inhibitor studies with DCCD

N,N'–dicyclohexylcarbodiimide (DCCD), is a carboxyl group modifying reagent, that preferentially attacks acidic amino acid residues in an hydrophobic environment (Fig. 15). DCCD has already been shown to be an inhibitor of the mitochondrial respiratory chain complexes I, III, IV and V (ATP synthase)(Azzi *et al.*, 1984; Solioz, 1984; Yagi, 1987; Yagi & Hatefi, 1988). It has been evidenced that DCCD also inhibits the MV_{red}-dependent H_2 evolution activity of CO-induced hydrogenase from *Rhodospirillum rubrum* (Fox *et al.*, 1996) and of Mbh hydrogenase from *Pyrococcus furiosus* (Silva *et al.*, 2000). Hydrogenase 3 from *E. coli* and Coo hydrogenase from *Carboxydothermus hydrogenoformans* were shown to be inhibited by this compound as well (Forzi, 2001). Preliminary studies showed that also Ech hydrogenase from *Mathanosarcina barkeri* was affected by DCCD (Meuer, 2001); this finding was further investigated within this work.

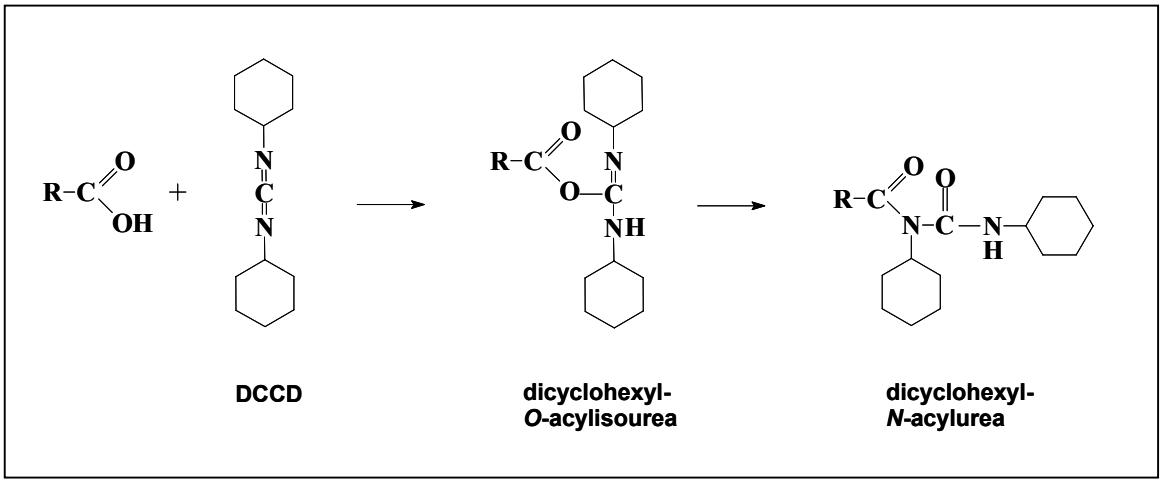

Fig. 15. Reaction of DCCD with a carboxyl residue in a protein, as proposed by Azzi (Azzi *et al.*, 1984). Proton transfer from the acid to one of the imide nitrogens of DCCD is followed by a nucleophilic attack of the carboxylate at the central C-atom of DCCD, yielding the dicyclohexyl-O-acyl-isourea derivative, which subsequently rearranges into the more stable dicyclohexylurea bound via an N-acyl bond to the protein.

2.1 Inhibition of Ech hydrogenase from *M. barkeri* by DCCD

Studies performed with the membrane fraction and purified Ech hydrogenase showed that the enzyme is strongly inhibited by DCCD. Purified Ech hydrogenase was incubated in the presence of DCCD at 30°C and the ferredoxin-dependent reduction of metronidazole by H_2 was assayed. Incubation with 1 mM DCCD for one hour led to an inhibition of 97% of the enzyme activity (Fig 16A). Decreasing the protein concentration resulted in greater percent loss of enzyme activity (Fig. 16B).

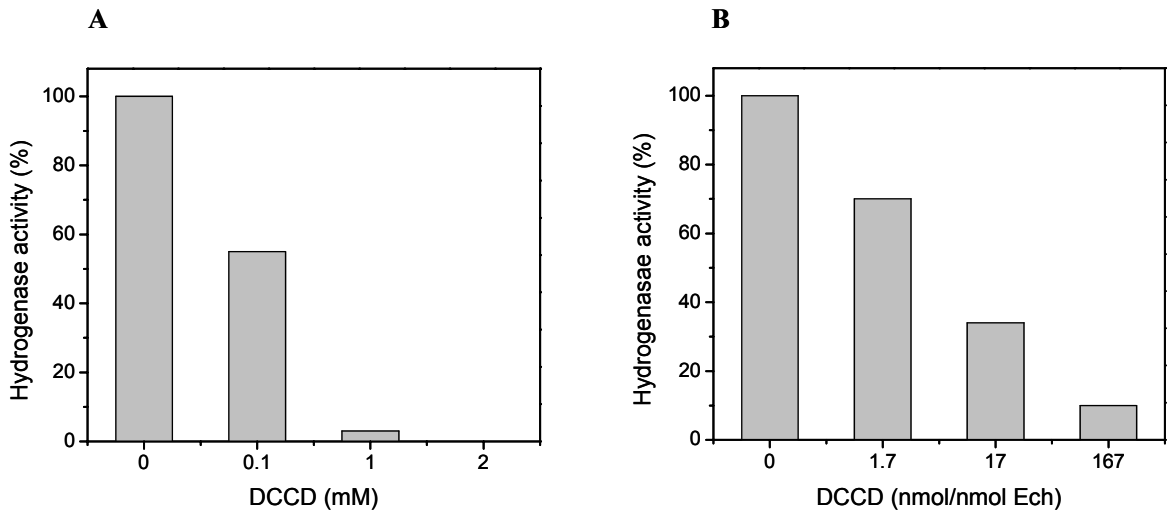

Fig. 16. Inhibition of Ech hydrogenase from *Methanosarcina barkeri* by the carboxyl group modifying reagent *N,N'*-dicyclohexylcarbodiimide (DCCD). Purified hydrogenase at a concentration of 1 mg of protein ml^{-1} in 50 mM MOPS/NaOH, pH 7.0, 2 mM DDM, 2 mM DTT was mixed with different concentrations of DCCD (ethanolic solution), as indicated in figure (**A**). Purified Ech hydrogenase at a concentration of 1-10 mg of protein ml^{-1} was mixed with different DCCD concentrations in order to obtain different inhibitor/protein ratios (**B**). Samples were incubated under an H_2 atmosphere in stoppered vials at 30°C. After an hour, samples from each vial were removed and assayed for ferredoxin-dependent reduction of metronidazole by H_2. The activity of the control sample, which contained ethanol only, was set to 100%.

Moreover, the inactivation rate of the enzyme was pH-dependent: a more rapid inactivation occurred at pH 7, while the increase of pH from 7 to 9 resulted in a continuous reduction of the inactivation rate (Fig. 17). A pH-dependent inactivation rate was also observed with the F_1F_O-ATPase from *Propionigenium modestum* (Kluge & Dimroth, 1993a).

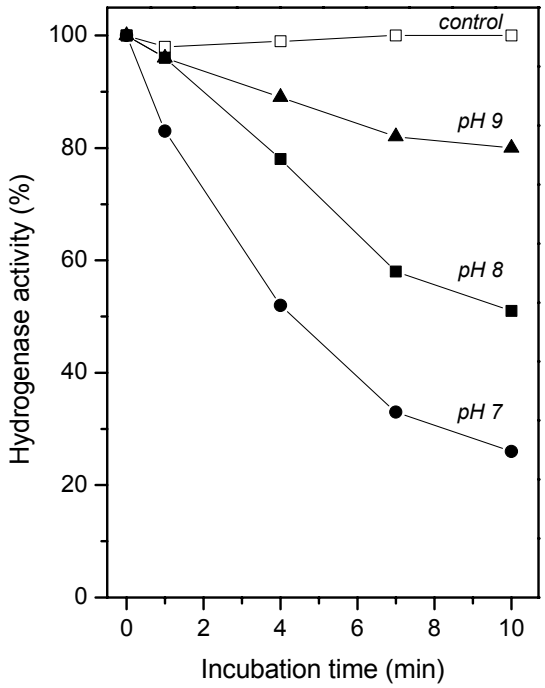

Fig. 17. Kinetics of Ech hydrogenase inhibition by DCCD at different pH values. Purified Ech hydrogenase from *M. barkeri* at a concentration of 4 mg of protein ml^{-1} in 20 mM MES/TRIS/CAPSO at the pH indicated was mixed with 500 µM DCCD (ethanolic solution). Samples were incubated under an H_2 atmosphere in stoppered vials at 30°C. At the time indicated, samples were withdrawn and immediately used for the determination of the ferredoxin-dependent reduction of metronidazole by H_2 at 320 nm, which was performed in 50 mM MOPS/NaOH pH 7.0 supplemented with 2 mM DTT and 2 mM DDM. The activity of the control sample, which contained 1% EtOH, was set to 100%.

Control experiments were performed with 1-ethyl-3-(3-dimethylaminopropyl)-carbodiimide (EDAC), a carbodiimide similarly small as DCCD, but hydrophilic, so that interaction with hydrophilic sites of a protein is expected. The same membrane preparation from *M. barkeri* was incubated either with DCCD or with EDAC at 20°C and the ferredoxin-dependent reduction of metronidazole by H_2 was assayed. Incubation for one hour with EDAC, in the same concentration range used for DCCD, had practically no influence on the activity (Fig. 18). Similar results have been obtained with the purified enzyme.

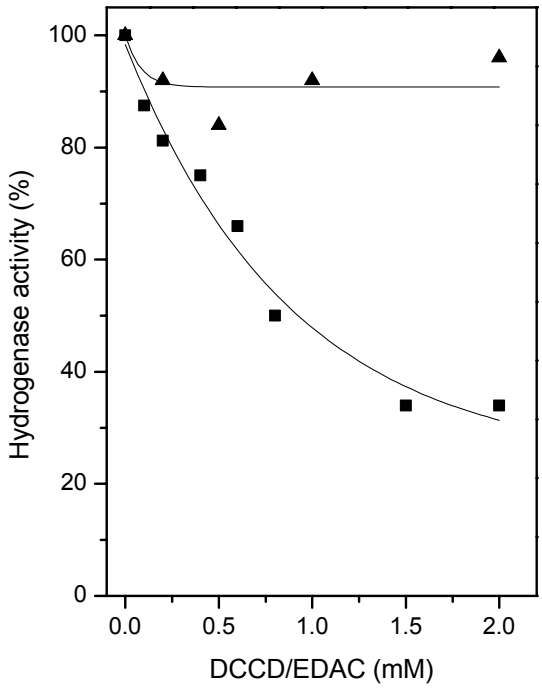

Fig. 18. Effect of DCCD and EDAC on ferredoxin-dependent reduction of metronidazole by H_2 in membranes of *M. barkeri*. Membranes of *M. barkeri* at a concentration of 12 mg of protein ml^{-1} in 50 mM MOPS/NaOH, pH 7.0, 2 mM DTT were mixed with different concentrations of DCCD (ethanolic solution) or of EDAC (dissolved in 50 mM MOPS/NaOH, pH 7.0). Samples were incubated under an H_2 atmosphere in stoppered vials at 20°C. After an hour, samples from each vial were removed and assayed for ferredoxin-dependent reduction of metronidazole by H_2. The activity of the control sample, which contained either ethanol or MOPS buffer, was set to 100%. The symbols indicate samples incubated with DCCD (■) and with EDAC (▲).

2.2 Identification of Ech hydrogenase subunits modified by DCCD

In order to see whether the inhibition of Ech hydrogenase activity by DCCD involves covalent interaction of the inhibitior with the enzyme, labelling studies have been performed. Purified Ech hydrogenase was incubated with [^{14}C]DCCD, followed by SDS-PAGE analysis of the inactivated enzyme (Fig. 19A). Electrophoretic analysis of Ech after incubation with [^{14}C]DCCD at various times revealed no change in the polypeptide pattern or the staining intensity of the polypetides. These results suggest that DCCD inhibition is not due to cross-linking of Ech hydrogenase subunits. Instead, [^{14}C]DCCD was specifically incorporated into the two integral membrane subunits EchA and EchB (Fig. 19B).

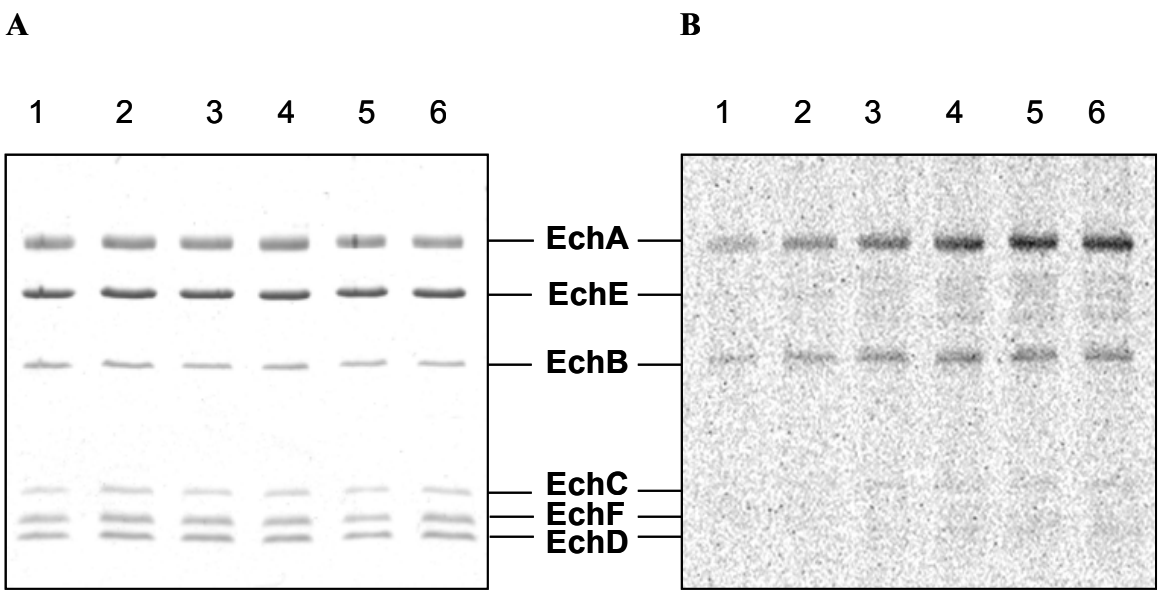

Fig. 19. Time dependence of [^{14}C]DCCD labeling of Ech hydrogenase from *M. barkeri*. Purified Ech hydrogenase from *M. barkeri* at a concentration of 1 mg of protein ml^{-1} in 50 mM MOPS pH 7.0 was incubated with 0.25 mM [^{14}C]DCCD (1 GBq/mmol) at 20°C. At the time indicated, hydrogenase activity was determined and 50 µl of the incubation mixture was withdrawn and mixed with 0.45 ml of cold (0°C) 50 mM CAPSO pH 9.0 in order to stop the reaction with DCCD. The samples were ultrafiltrated at 4°C using microcons devices (cut-off: 50 kDa) for the separation of the labeled protein and unbound [^{14}C]DCCD. Labeled proteins were denatured in SDS sample buffer for 1 hour at room temperature and the samples were separated by elecrophoresis in a 16% slab gel which was subsequentely stained with Coomassie Brilliant Blue R250 (A). The gel was destained, dried under vacuum and exposed to a PhosphorImager Screen. Radioactive bands were detected with a PhosporImager (Molecular Dynamics) after 24 hours of exposure (B). Each lane contains 3 µg of Ech hydrogenase incubated with [^{14}C]DCCD for 15 min (*lane 1*), 30 min (*lane 2*), 1 h (*lane 3*), 2 h (*lane 4*), 3 h (*lane 5*) and 4 h (*lane 6*).

Figure 20 compares the extent of inhibition of hydrogenase activity with the extent of labeling of subunits EchA and EchB with [^{14}C]DCCD at different incubation times. Subunit EchB was labeled rapidly and saturated when inhibition of Ech hydrogenase activity reached about 50% of the maximal value. On the other hand, the extent of labeling of EchA subunit paralleled the inhibition of the enzyme throughout the incubation time, suggesting that inhibition by DCCD is associated with a preferential modification of this subunit. A small amount of radioactivity was also incorporated in other polypeptides. Those with apparent molecular masses of 40 and 18-13 kDa correspond to EchE and EchC,F,D, respectfully. Furthermore, some impurities not visible on the SDS-PAGE were

observed with the radioactive label. However, the protein labeling in these regions did not correlate with the degree of enzyme inhibition.

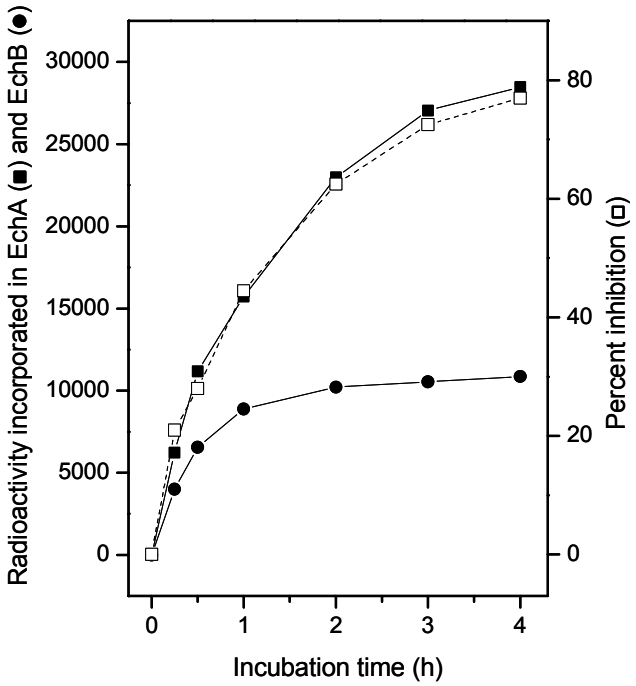

Fig. 20. Time dependence of [^{14}C]DCCD labeling of subunits EchA and EchB from Fig. 19B and inactivation of Ech hydrogenase from *M. barkeri*. The radioactivity incorporated (arbitrary units) was estimated using the ImageQuant software (Molecular dynamics) and was plotted against the incubation time. The incorporation of radioactivity was correlated with the inhibition of Ech hydrogenase activity (which was measured by following the H_2-dependent benzyl viologen reduction at 578 nm).

3. FT-IR spectroscopic characterization of Ech hydrogenase from *Methanosarcina barkeri*

A combination of FT-IR difference spectroscopy and electrochemistry have been used to detect redox-dependent changes in protein structure and protonation states of amino acid side chains, associated with the redox reaction of Fe-S clusters of Ech hydrogenase from *M. barkeri*.

3.1 Electrochemically induced FT-IR difference spectra

Reversible redox induced FT-IR difference spectra could be obtained for Ech hydrogenase from *Methanosarcina barkeri* for a potential step from -0.31 to -0.09 V vs. NHE and reverse. Data could not be measured for potential steps below -0.31 V, due to H_2 production of the enzyme. In case of H_2 production, strong variations of the aqueous background impaired difference spectroscopy. All three iron-sulfur clusters are expected to be partially reduced with this potential step (Kurkin *et al.*, 2002), leading to relatively weak signals in the difference spectra. A larger potential step towards -0.41 V could be applied to the acetylene inhibited enzyme since acetylene binds to the active site and thus prevents H_2 formation (Zorin *et al.*, 1996). The electrochemically-induced FT-IR difference spectra of Ech hydrogenase contained contributions from redox-dependent changes in the protein structure and protonation states of cofactors and individual amino acids.

3.2 Signals in the 2200–1800 cm^{-1} range

Figure 21A shows the oxidized minus reduced FT-IR difference spectrum of Ech hydrogenase for a potential step from -0.31 to -0.09 V vs. NHE at pH 7 in the spectral range from 2200 to 1800 cm^{-1}. In this spectral range the contributions from stretching vibrational modes of the CO and CN ligands of the active site can be expected and have been discussed in detail by several groups for other hydrogenases (De Lacey *et al.*, 2004;

Happe *et al.*, 1997; van der Spek *et al.*, 1996). For the CO vibrational modes, signals at 1920 (minor signal) and 1900 cm^{-1} (major signal) could be identified for the fully oxidized and at 1926 (minor signal) and 1908 cm^{-1} (major signal) for the reduced form. The CN vibrational modes could be seen at 2100 and 2090 cm^{-1} for the oxidized form and at 2104, 2077 and 2068 cm^{-1} for the reduced form. The signals essentially corresponded to signals that were previously obtained with the oxidized form of the enzyme (generated by flushing with argon) and with the form reduced by 100% H_2 (S. Kurkin, R. Hedderich and S.P.J. Albracht, unpublished results). The number of bands is higher than expected for the three ligands, which could be due to the coexistence of different states of the active center. The frequency of the CO and CN vibrations differed from reports on other [NiFe] hydrogenases, i.e., from Chromatium vinosum by up to 50 cm^{-1}, indicating a strong influence of the environment on the vibration (De Lacey *et al.*, 2004; Happe *et al.*, 1997; van der Spek *et al.*, 1996). Samples stored for more than one month at -20°C produced signals with a changed intensity ratio, most prominent in a more intense signal at 1920 cm^{-1}.

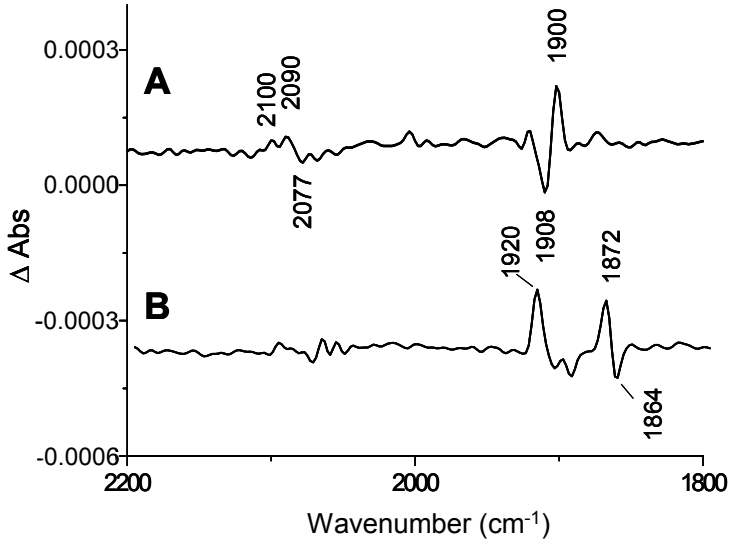

Fig. 21. FT-IR difference spectra of Ech hydrogenase in the spectral range from 2200 to 1800 cm^{-1}. Difference spectrum of oxidized minus reduced spectra of Ech hydrogenase for a potential step from -0.31 to -0.09 V vs. NHE at pH 7 (A) and in the presence of acetylene for a potential step from -0.41 to -0.09 V at pH 8 (B).

In the presence of acetylene (Fig. 21B) additional differential features could be seen at 1872 and 1864 cm^{-1} together with changes in intensity of the other modes. This could be

due to a mixture of two different states of the enzyme. Infrared spectra with ν(CO) = 1920 cm^{-1} and ν(CN) = 2100 cm^{-1} have previously been observed with air-oxidized Ech hydrogenase and most probably represent the inactive oxidized enzyme as evidenced by EPR data (S. Kurkin, R. Hedderich and S.P.J. Albracht, unpublished results).

The nature of the modes at 1872 and 1864 cm^{-1}, which are only observed in the presence of acetylene, is not yet clear. IR spectra of other [NiFe] hydrogenases inhibited by acetylene have not been reported. Binding of acetylene, probably to the Ni, in the form of –C≡CH may donate electron density to the [NiFe] center and this could lead to a shift to lower frequency of ν(CO). Alternatively the modes at 1872 and 1864 cm^{-1} could be assigned to the C≡C vibration of the inhibitor bound to a metal as -C≡C-H. Contributions from non-bound acetylene are not expected in the difference spectra, since it is not redox active. In absorbance spectra contributions would be expected at approximately 1400-1300 cm^{-1}.

3.3 Signals in the 1800–1200 cm^{-1} range

Figure 22 shows the oxidized minus reduced FT-IR difference spectra (oxidized minus reduced) of Ech hydrogenase for a potential step from -0.31 to -0.09 V vs. NHE at pH 7 (A) and pH 9 (B), in the presence of acetylene for a potential step from -0.41 to -0.09 V vs. NHE at pH 8 (C) and of complex I for a potential step from -0.25 to -0.1 V at pH 6 (D) in the spectral range from 1800 to 1200 cm^{-1}. The inset shows the comparison of a sample at pH 7 equilibrated in H_2O (black line) and D_2O buffer (gray line). The data obtained at pH 8 and pH 9 were nearly indistinguishable for a potential step from -0.31 to -0.09 V vs. NHE (data not shown). Generally, in the given spectral range, signals from conformational changes of the protein backbone are expected, as well as protonation/deprotonation reactions of the amino acid side chains. Signals from the buffers can be expected below 1200 cm^{-1}. In addition a small signal at approximately 1410 cm^{-1} was found to be induced in control experiments by the Capso buffer used for the pH 9 data.

Protein backbone

In the so called amide I range from 1700 to 1620 cm^{-1} a broad differential feature could be seen at the typical position for the ν(C=O) mode of the polypeptide backbone. The modes at 1702, 1688, 1678 cm^{-1} seen for the oxidized state and at 1644 and 1634 cm^{-1} for the

reduced state, were present in the spectral range characteristic for β–sheet secondary structure elements and loops (Goormaghtigh *et al.*, 1994). The reorganizations seen at 1664 and 1654 cm^{-1} occured in the spectral range for α-helical elements. In the amide II range from 1570 to 1520 cm^{-1} signals from the coupled CN stretching and NH bending modes are expected to contribute. These vibrational modes uncouple upon H/D exchange inducing a shift to lower wavenumbers. In the inset of Figure 22 the clear decrease of the signal at 1554 cm^{-1} upon H/D exchange allows the assignment to amide II modes.

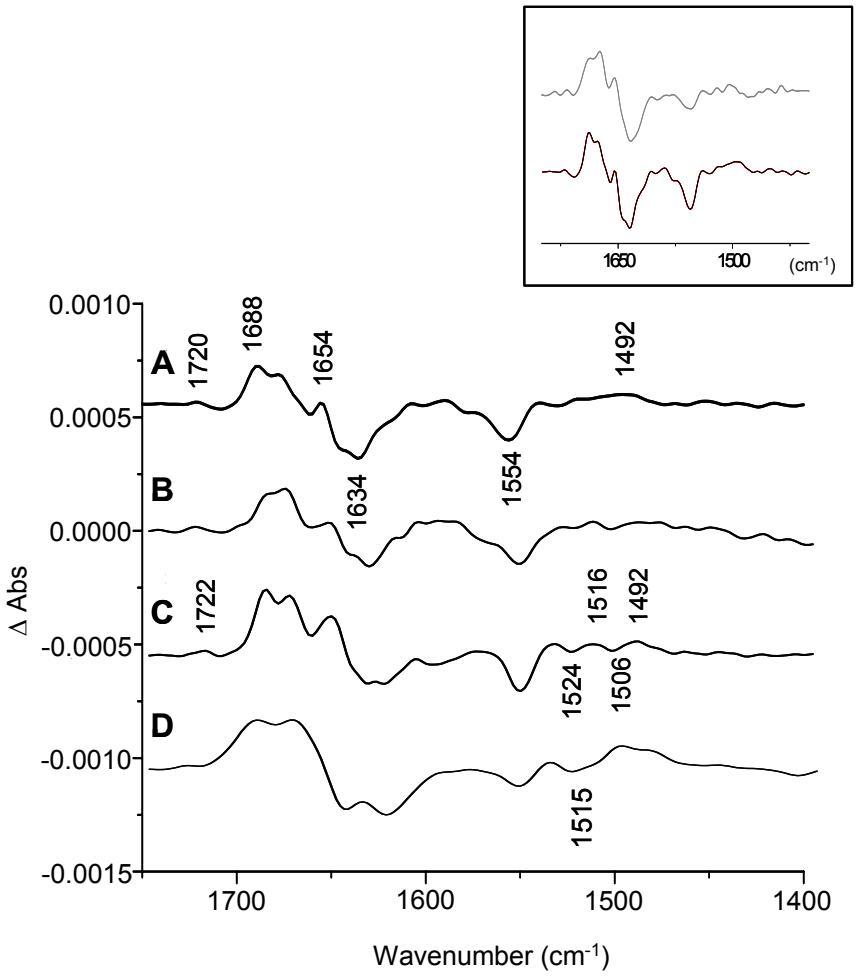

Fig. 22. FT-IR difference spectra of Ech hydrogenase in the spectral range from 1800 to 1200 cm^{-1}. Difference spectrum of oxidized minus reduced spectra of Ech hydrogenase for a potential step from -0.31 to -0.09 V vs. NHE at pH 7 (A) and pH 9 (B), in the presence of acetylene for a potential step from -0.41 to -0.09 V vs. NHE at pH 8 (C) and of complex I for a potentials step from -0.25 to -0.1 V at pH 6 (D). The inset shows the comparison of a sample at pH 7 equilibrated in H_2O (black line) and D_2O buffer (gray line).

Comparing the samples at pH 7 and pH 9 (Fig. 22A and B), minor variations in signal intensity in the amide I range could be found. For the acetylene-inhibited sample (Fig. 22C) a lower redox potential could be applied, allowing to reduce a higher percentage of the iron sulfur clusters. Based on the midpoint potentials determined previously (Kurkin *et al.*, 2002) approximately 50% of the EPR detectable iron-sulfur clusters are reduced under the experimental conditions (pH 8, -0.41 V). This is reflected in higher signal intensities, whereas the data shown were normalized to the same intensities for a clearer comparison.

Individual amino acids

In addition to secondary structure elements, contributions of individual amino acid side chains, in particular Asn, Gln or Arg, are conceivable in the amide I spectral range from 1690 to 1630 cm^{-1} (Venyaminov & Kalnin, 1990). The ν(C=O) modes of protonated aspartic and glutamic acid side chains typically contribute in the spectral range between 1800 and 1710 cm^{-1}. The signal at 1720 cm^{-1} could thus be tentatively assigned to an aspartic or glutamic acid side chain, protonated in the oxidized state. At pH 9 the signal is still present, indicating that the pK_a value of the residue, protonated in the oxidized state exceeds 9.

The protonation or reorganization of tyrosines upon the redox reaction, usually observed between 1530 and 1498 cm^{-1} did not show significant signals for the given experimental conditions at pH 7 (Fig. 22A). In contrast, the oxidized minus reduced FT-IR difference spectra of Ech hydrogenase at pH 9 and in the presence of acetylene, showed differential signals in the region were tyrosines can be expected (Fig. 22B and 22C). A clear assignment to individual amino acids, however, is not possible without mutants.

Comparison to complex I

Figure 22D also shows a direct comparison between the oxidized minus reduced FT-IR difference spectra of Ech hydrogenase and complex I from *E. coli* for a potentials step from –0.25 to –0.1 V (Flemming *et al.*, 2003a; Hellwig *et al.*, 2000), where the analogous iron sulfur clusters N2 and N6A and N6B are involved.

4. Identification of the coupling ion used by Coo hydrogenase from *Carboxydothermus hydrogenoformans*

Carboxydothermus hydrogenoformans is an anaerobic microoragnism with a very simple energy metabolism: it can grow on CO as its sole carbon and energy source. CO in H_2O is converted to CO_2 and H_2 at high rates and this reaction has to be coupled to energy conservation. For this reason *C. hydrogenoformans* has been chosen in order to gain insights on the coupling ion used by energy-converting hydrogenases. H^+ and Na^+ translocation coupled to CO oxidation were investigated.

4.1 Determination of proton translocation with a pH electrode

Washed cells of *C. hydrogenoformans* were tested for their ability to couple the conversion of CO to CO_2 and H_2 with the translocation of protons across the cytoplasmic membrane. The rapid changes in extra cellular pH, upon addition of substrate were measured with a pH electrode. The experimental medium was supplemented with KCl and valinomycin, in order to dissipate the membrane potential.

Proton translocation coupled to CO oxidation at pH 5.9 is shown in Fig. 23. CO was added as CO-saturated solution in 1 mM MES pH 5.9. Upon CO addition to cell suspensions, under an N_2 atmosphere, a rapid transient acidification of the suspension medium was observed. In the second phase, a slower alkalinization was observed due to proton backflow into cells until a stable pH was reached again. The extent of acidification was dependent on the amount of CO added. In control experiments buffer, which contained no CO was used. Here no transient acidification was observed, indicating that H^+ transfer was specifically coupled with CO oxidation. After calibrating the system by the addition of a standard solution of HCl, the extent of reversible acidification was calculated. An average H^+/CO ratio of approximately 1 was obtained, meaning that for every mole of CO oxidized to CO_2, 1 mole of protons were translocated across the membrane. In the evaluation of the H^+/CO stoichiometry the fact that that CO_2, the product of CO oxidation, is a weak acid with an apparent pk_1 of 6.3 ($H_2CO_3 \rightleftharpoons HCO_3^- + H^+$) was taken into consideration. At pH 5.9, only 28% of the H_2CO_3 is dissociated, thus 0.28 mole protons should be generated

and released to the external medium per mole CO oxidized. In order to keep the contributions deriving from the chemical reaction low, experiments have been performed at pH 5.9. The permanent acidification observed is due to the formation of HCO_3^- + H^+ and correlated with the amount of CO added. In the evaluation of the stoichiometry the acidification deriving from CO_2 was subtracted from the total acidification.

In a separate experiment it was shown that cell suspensions from *C. hydrogenoformans* catalyzed H_2 formation, using CO as electron donor, at a good rate (3 μmol min^{-1} mg protein $^{-1}$) even at this low pH.

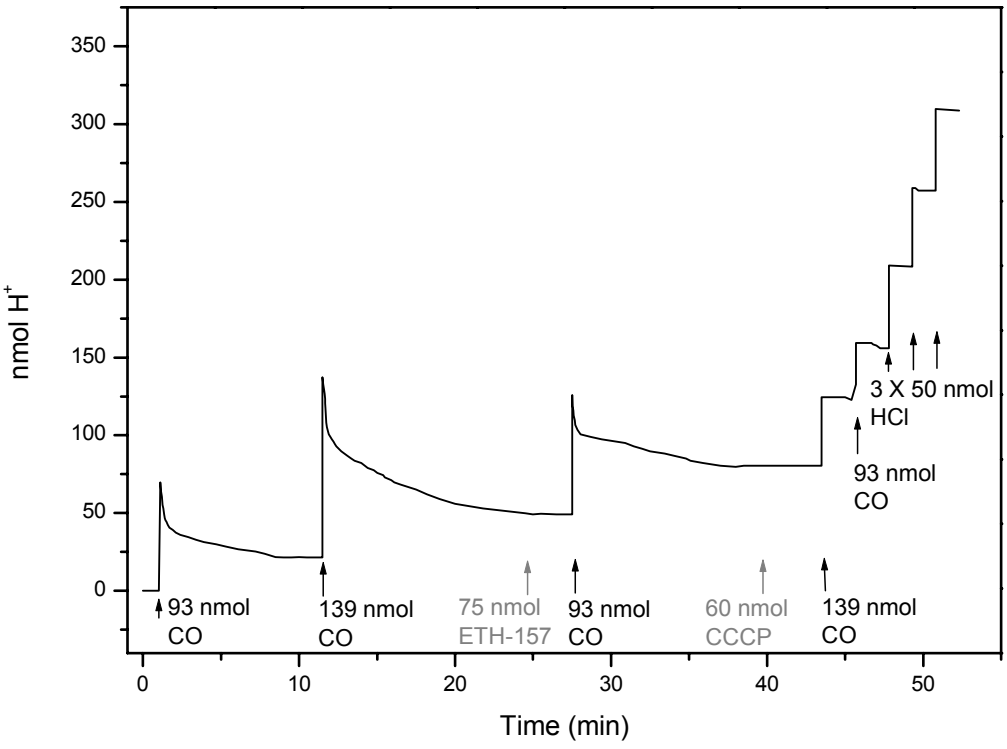

Fig. 23. Proton translocation coupled to the conversion of CO to CO_2 and H_2 at pH 5.9 by cell suspensions of *C. hydrogenoformans*. Washed cells at a concentration of 0.2 mg of protein ml^{-1} were added to 1 mM MES/KOH pH 5.9, 100 mM KCl, 25 μM valinomycin, 4 mM DTT, 15 μM reasazurin. When a stable base line was obtained, different amounts of CO were injected, as indicated. ETH-157 and CCCP were added as ethanolic solutions to a final concentration of 25 μM and 21 μM (corresponding to 150 and 120 nmol mg of $protein^{-1}$, respectively). Experiments were carried out at 60°C under an atmosphere of N_2.

Proton translocation coupled to CO oxidation could proceed via two different mechanisms: CO oxidation is directly coupled with H^+ extrusion (primary H^+ translocation) or CO oxidation is directly coupled with Na^+ extrusion, which drives the extrusion of H^+ via a Na^+/H^+ antiporter (secondary H^+ translocation). In order to discriminate between the two mechanisms, the influence of different uncouplers on proton translocation and CO oxidation by cell suspensions was investigated. In the presence of protonophore CCCP no transient acidification was observed upon CO addition. The proton translocation was, however, not affected by the addition of the sodium ionophore ETH-157 (Fig. 23). It was shown in a separate experiment that H_2 formation was not inhibited in the presence of these uncouplers but even slightly enhanced. Moreover, the effect of ethanol on proton translocation by inverted vesicles was checked, because ethanolic solutions of the inhibitors were used, and it was shown that ethanol did not affect H^+ translocation.
These experiments indicated that upon CO addition, the acidification was mainly due to primary proton translocation.

When experiments were performed with cell suspensions washed in 1 mM MOPS/NaOH pH 6.7 rather than in 1 mM MES/KOH pH 5.9 no protonophore sensitive proton translocation could be observed. In control experiments washed cells at pH 6.7 were injected in the assay mixture at pH 5.9: under these conditions proton translocation coupled to CO oxidation was observed. In other experiments washed cells at pH 5.9 were injected in the assay mixture at pH 6.7: under these conditions no proton translocation could be detected. These results indicated that at pH 6.7 the hydrogenase from *C. hydrogenoformans* is not acting as a proton pump, although the cells are highly active at this pH.

4.2 Determination of sodium translocation with $^{22}Na^+$

Transmembrane sodium transport upon addition of substrate was determined by measuring the change of intracellular Na^+ concentration using $^{22}Na^+$. The experimental medium was supplemented with KSCN in order to dissipate the membrane potential.
The sodium translocating activity of the hydrogenase from *C. hydrogenoformans* upon CO oxidation was tested at pH 7. Addition of CO to cells previously equilibrated with 15 mM $^{22}Na^+$ resulted in a very rapid efflux of Na^+ as indicated by the decrease of the intracellular

Na^+ concentration (Fig. 24). In this case it has not been possible to determine the Na^+/e^- stoichiometry since Na^+ translocation could not be followed directly (e.g. with a Na^+-selective electrode) but was determined discontinuously. Therefore transient Na^+ translocation upon the addition of small amounts of CO could not be determined. Rather, a large excess of CO was added which resulted in a permanent Na^+ extrusion within the first 5-10 min after CO addition. With the intention of discriminating between primary and secondary sodium translocation, the effect of the protonophore CCCP was tested on Na^+ extrusion coupled to CO oxidation.

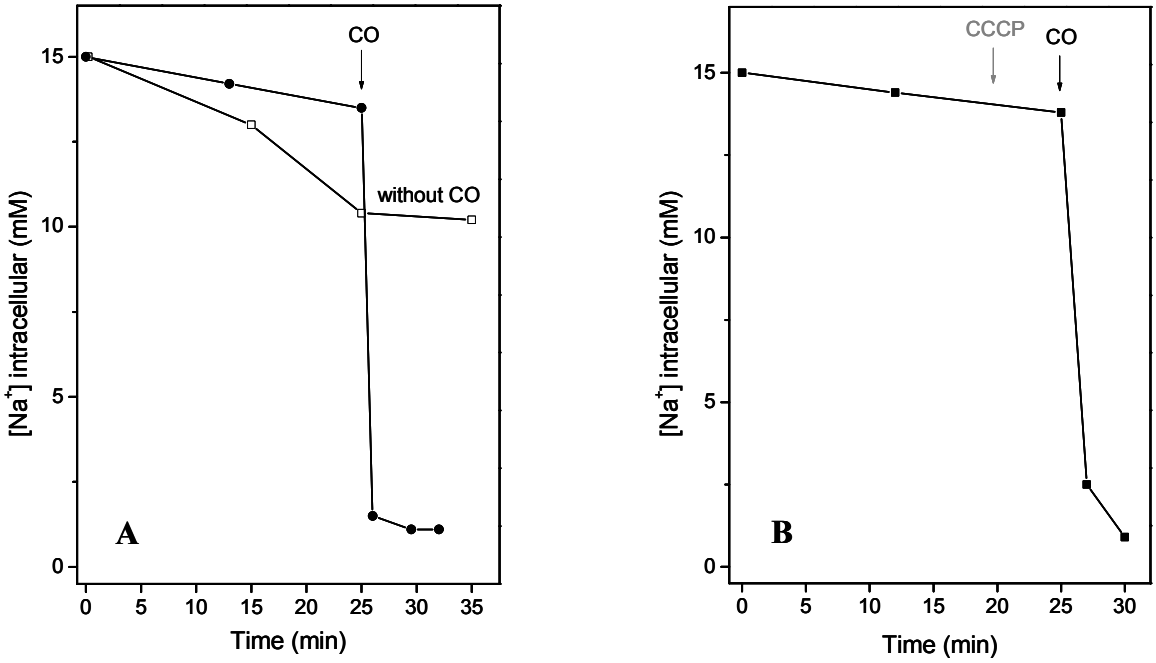

Fig. 24. Sodium translocation coupled to the conversion of CO to CO_2 and H_2 at pH 7.0 by cell suspensions of *C. hydrogenoformans*. The assays were performed at 60°C under an atmosphere of N_2 in 8-ml serum bottles filled with 1 ml assay mixture containing 20 mM imidazole/HCl buffer pH 7.0**,** 15 mM NaCl, 0.37 MBq $^{22}Na^+$, 20 mM KCl, 50 mM KSCN, 15 µM reasazurin, 2 mM DTT and washed cells (0.8 mg protein). The cells were incubated at 60°C for 30-45 min in order to allow the equilibration of the extracellular and intracellular Na^+ (t = 0). Samples were withdrawn to control the Na^+ distribution and the reaction was started by the addition of CO to the gas phase. The control did not receive any CO (**A**). CCCP was added as an ethanolic solution to a final concentration of 25 µM (corresponding to 31 nmol mg of protein^{-1}) (**B**). At the time indicated, the intracellular Na^+ concentration was determined as described in section 5.2 of the materials and methods chapter.

In control experiments it was shown that CO oxidation to CO_2 and H_2 was coupled with the phosphorylation of ADP under the same experimental conditions used for the sodium transport studies. The addition of CO to cell suspensions resulted in synthesis of 3.5-4.5 nmol ATP mg protein^{-1}. When the same experiment was performed either in the presence of CCCP or ETH-157 (in the same concentration range as used for $^{22}Na^+$ extrusion studies), ATP synthesis was inhibited and resulted in less than 5% of the values determined in the absence of uncouplers. These findings indicated that the CCCP concentrations used in previous experiments were sufficient to dissipate the electrochemical proton gradient. Moreover, the results obtained allow the proposal of the following sequence of reactions: CO oxidation is coupled with the generation of a primary electrochemical sodium ion gradient ($\Delta\mu_{Na^+}$), as confirmed by inhibition of ATP synthesis by ETH-157. $\Delta\mu_{Na^+}$ is converted to an electrochemical gradient of protons ($\Delta\mu_{H^+}$) most probably via a Na^+/H^+ antiporter. $\Delta\mu_{H^+}$ drives the synthesis of ATP via a H^+-translocating ATP synthase.

4.3 Inactivation of Coo hydrogenase by DCCD in the presence of sodium ions

Previous studies performed with other Na^+-translocating enzymes such as ATP synthases from *Propionigenium modestum*, *Ilyobacter tartar*icus and *Acetobacterium woodii* and complex I from *Klebsiella pneumoniae* have shown that sodium ions protected the enzyme activity from inactivation by DCCD (Heise *et al.*, 1992; Kluge & Dimroth, 1993a; Neumann *et al.*, 1998; Vgenopoulou *et al.*, 2003). It was therefore proposed that the DCCD-reactive acidic residue represent or is in the vicinity of the Na^+ binding site. With the ATP synthases from *P. modestum* it was also shown that the protective effect of Na^+ ions was most pronounced in the alkaline pH range.

When *C. hydrogenoformans* membranes washed in a sodium-free buffer were incubated with DCCD in the presence of NaCl, a slight but reproducible protective effect was observed. At pH 9, 10 mM NaCl protected 25% of hydrogenase activity from inactivation by 1 mM DCCD during 10 min of incubation (Fig. 25). The specificity of this protective effect was tested using a different alkali ion. Incubation of membranes in the presence of 10 mM KCl had no effect on the reaction of the hydrogenase with DCCD.

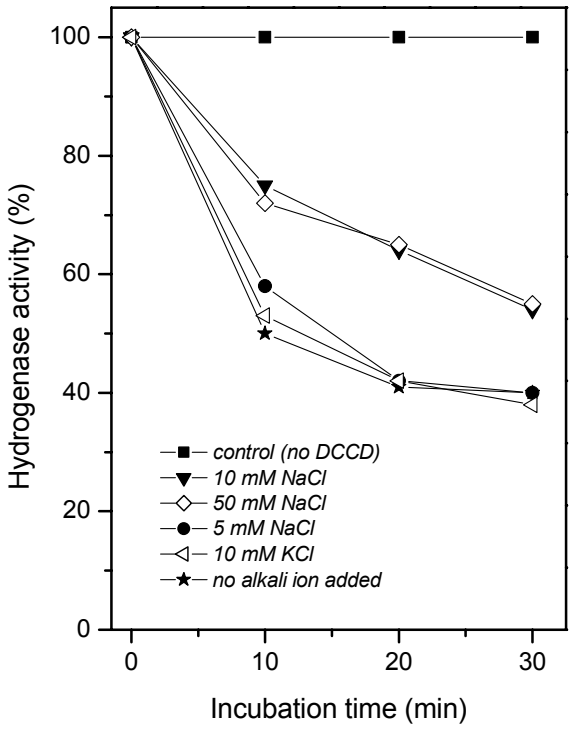

Fig. 25. Inhibition of the *C. hydrogenoformans* hydrogenase by DCCD in the presence of different alkali chlorides. Membranes washed in 50 mM Imidazol/HCl pH 7.0 at a concentration of 0.4 mg protein ml^{-1} were incubated in 50 mM TRIS/HCl pH 9.0, supplemented with 200 µM benzyl viologen and 2 mM DTT. 1 mM DCCD (ethanolic solution) was added. Samples were incubated under an H_2 atmosphere in stoppered vials at 60°C. At the time indicated, samples were withdrawn and immediately used for the H_2-dependent benzyl viologen reduction at 578 nm, which was performed in 50 mM MOPS/NaOH pH 7.0 supplemented with 2 mM DTT. The activity of the control sample, which contained 1% ethanol instead of DCCD, was set to 100%. The Na^+ concentration without extra addition of sodium corresponded to 50-100 µM.

V DISCUSSION

In recent years a group of multisubunit membrane-bound [NiFe] hydrogenases, which are now called energy-converting hydrogenases, was identified. These enzymes share two conserved integral membrane proteins and four conserved hydrophilic proteins with the energy-conserving NADH:quinone oxidoreductases (complex I). As shown by physiological and biochemical studies performed with various members of this hydrogenase family, these enzymes function in energy-conserving electron transport, reverse electron transport, or both. As for complex I, no 3D structure is available for the energy-converting hydrogenases. This work is focused on the characterization of the electron and $H^+(Na^+)$ transfer pathways in energy-converting hydrogenases and the question how these two processes are mechanistically linked to each other. Another part concerns the identification of the coupling ion.

1. Characterisation of the metal centers of Ech hydrogenase from *Methanosarcina barkeri* by site-directed mutagenesis

1.1 Assignment of the [4Fe-4S] clusters of Ech hydrogenase to individual subunits

The characterisation of the iron-sulfur clusters of Ech hydrogenase by EPR spectroscopy, performed previously, revealed the presence of two axial like EPR signals fully reducible under 100% H_2. The two signals were designated as the g = 1.89 and the g = 1.92 signal. Importantly, both species have a pH-dependent midpoint potential. The E_0' value of the g = 1.92 signal decreased by 53 mV per pH unit; that of the g = 1.89 signal decreased by 62 mV per pH unit (Kurkin *et al.*, 2002). These values are reasonably close to the theoretical value of -59 mV per pH unit for a redox titration involving a stoichiometric amount of electrons and protons. The g = 1.89 and the g = 1.92 signal showed slightly different temperature optima, the g = 1.89 signal being optimally sharpened at 12 K and the g = 1.92 signal being optimally sharpened at 17 K. At temperatures below 15 K a two-

fold splitting of the Ni_a-L signal was observed due to the interaction of the Ni-based unpaired electron with the S = ½ system of the reduced proximal [4Fe-4S] cluster. The temperature dependence of the splitting of the Ni_a-L signal paralleled the temperature dependence of the g = 1.89 signal. It was therefore tentatively concluded that the g = 1.89 signal is due to the reduced proximal cluster in EchC (Kurkin *et al.*, 2002). The experiments described in this work substantiate this former assignment. Seven of eight cysteine residues predicted to ligate the iron-sulfur clusters in EchF were systematically changed to serine. For two of the mutant enzymes, EchF2 and EchF8, the g = 1.89 signal was the major signal and only residual spin intensities of the g = 1.92 signal were observed. The spin concentration of the g = 1.89 signal of the EchF8 mutant was highest and accounted for approximately 50% of the enzyme concentration. The determination of the spin concentration is based on the total protein concentration of the sample. Since the preparation still contained three contaminating protein bands (Fig. 10), the spin concentration is probably underestimated. EPR spectra recorded from the enzymes isolated from the EchF5, EchF6 and EchF7 mutants also contained the g = 1.89 signal, however, at lower spin intensities. The formation of the g = 1.89 and the g = 1.92 clusters was not dependent on whether the mutation was in the first (EchF2 and EchF8) or the second (EchF5 and EchF7) iron-sulfur cluster binding motif of EchF (Fig. 7). EPR spectra of the EchF2, EchF5, EchF7 and EchF8 mutant enzymes showed a weak signal in the g = 1.92 region which can be attributed to the g_{xy} of the g = 1.92 signal. Studies with the wild-type enzyme had shown that the third cluster of the enzyme, assigned to the g = 1.96 signal, has a low redox-potential and thus could only be reduced to a low extent under 100% H_2. It is therefore difficult to judge if the intensity of this signal has changed in the mutant enzymes. One possible explanation for the formation of low amounts of the g = 1.92 cluster in some of the *echF* mutants could be ligand exchange. Subunit EchF contains an additional free Cys residue in position 87 which could function as a ligand in some of the mutants (Fig. 26). Likewise, the introduced Ser residues could also function as a ligand of the cluster as suggested for a Cys to Ser mutant of *E. coli* nitrate reductase (Augier *et al.*, 1993). For the *R. capsulatus* NuoI mutants (see below) it was also proposed that in some of the mutants the introduced Ser residue could be a direct ligand to a [4Fe-4S] cluster (Chevallet *et al.*, 2003).

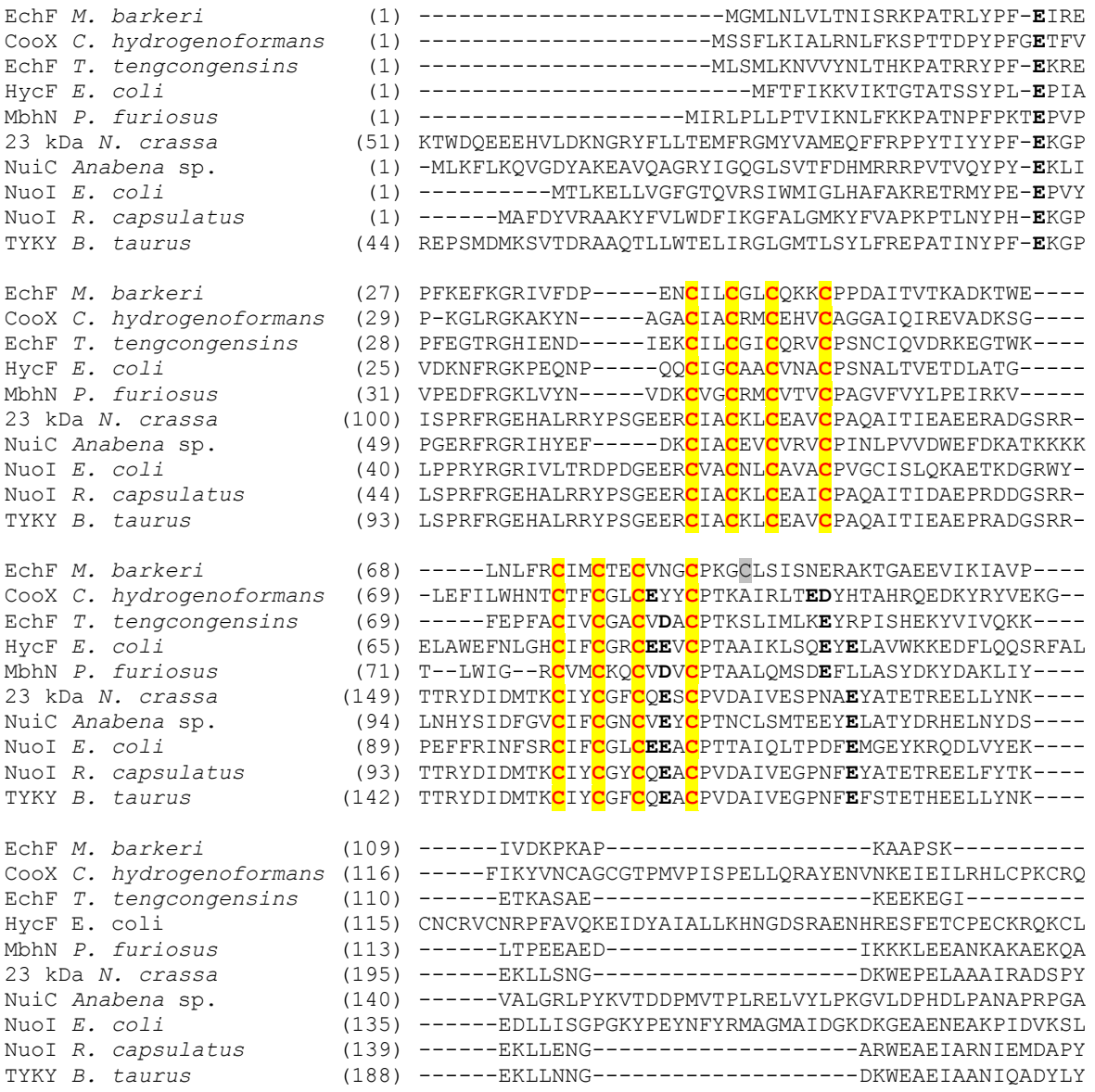

Fig. 26. Primary sequence alignment of EchF from *M. barkeri* Ech hydrogenase with the homologous subunit of other energy-converting hydrogenases (*C. hydrogenoformans* CooX, *T. tengcongensins* EchF, *E. coli* HycF and *P. furiosus* MbhN) and of various complex I enzymes (*N. crassa* 23 kDa, *Anabena* sp. NuiC, *E. coli* NuoI, *R. capsulatus* NuoI and *B. taurus* TYKY). The two four-Cys ferredoxin-like binding motifs are highlighted in yellow; conserved acidic residues are shown in bold. The position of Cys87 of *M. barkeri* is highlighted in gray.

The cluster ligating Cys residues conserved in EchF have also been mutagenized in the homologues subunit of complex I, NuoI, from *Rhodobacter capsulatus* (Chevallet *et al.*, 2003) and *Escherichia coli* (Flemming *et al.*, 2003b). In *R. capsulatus* five Cys residues were individually changed to Ser. Four of these mutants had retained significant amounts

of complex I activity in the membrane fraction (up to 72% of the wild-type activity). Purification of the mutant enzymes was not attempted since even the wild-type enzyme was found to be unstable upon purification. The eight cluster-ligating Cys residues of the closely related *E. coli* complex I were individually mutated to Ala. With the exception of the C102A mutant, which had retained 17% of the wild-type activity, all other mutants had lost complex I activity. The comparison indicates that Cys to Ser mutations are more likely to produce active enzyme in comparison to Cys to Ala mutations.

In most of the EchF mutants the intensity of the g = 1.89 signal was also reduced and in two of the mutants no signal due to an iron-sulfur cluster could be detected indicating that the mutation in EchF also had a strong effect on iron-sulfur cluster assembly in EchC. This is analogous to mutations of the cluster ligating cysteine residues of the NuoI subunit of *E. coli* complex I, which in most cases also resulted in a loss of the iron-sulfur cluster N2 located on subunit NuoB, a homologue of EchC (Flemming *et al.*, 2003b).

The characterisation of the different EchF mutant strains revealed that subunit EchF, homologous to complex I subunit NuoI (or TYKY), contains an EPR-detectable iron-sulfur cluster which exhibits a pH-dependent midpoint potential. In contrast, no EPR signal could be attributed to one of the [4Fe-4S] clusters located on NuoI (or TYKY) of complex I. In studies performed with complex I from *E. coli* and *Neurospora crassa*, a redox-group was identified by means of UV/Vis spectroscopy and was assigned to the two [4Fe-4S] clusters located on NuoI (or TYKY) (Rasmussen *et al.*, 2001). A redox titration of this group, which was followed by UV/Vis spectroscopy, revealed a pH-independent midpoint potential of these clusters with an E_0' value of –270 mV. It is thought that these clusters are magnetically coupled in the reduced state and therefore are difficult to detect by EPR spectroscopy. From these results it was concluded that NuoI (or TYKY) has redox-properties very similar to those of 8Fe-ferredoxins, e.g. the one from *C. pasteurianum*. Therefore, NuoI was proposed to be involved in simple electron transfer. Other studies focusing on the characterisation of the iron-sulfur clusters of NuoI where performed with the homologous protein from *Paracoccus denitrificans*, termed NQ09 (Yano *et al.*, 1999). NQ09 was heterologously produced in *E. coli*. The isolated subunit was found to bind two [4Fe-4S] clusters which when reduced gave rise to a set of two relatively broad axial-type EPR signals at g = 2.08, 2.05 and 1.93 and 1.90. The two sets of EPR signals could either be derived from two distinct species of [4Fe-4S] clusters or alternatively one signal could

be derived from the two *S* = 1/2 [4Fe-4S] clusters in NQ09 which exhibit similar EPR spectra and the second signal could arise from spin-spin interaction between the former two paramagnetic species. The midpoint potentials of these clusters were however < -600 mV indicating that their redox-properties changed considerably in the heterologously produced subunit. In the entire complex I from *P. denitrificans* these signals were not observed.

In Ech the [4Fe-4S] cluster located on subunit EchC and one of the [4Fe-4S] clusters on subunit EchF exhibit a pH-dependent midpoint potential. This indicates that oxidation/reduction of these clusters depends on charge compensation of an acidic residue close to the cluster. These subunits therefore could also play a crucial role in coupling electron transfer to proton translocation. Acidic residues that could be involved in this process have been identified in multiple sequence alignments of EchF or EchC and related subunits from other energy-converting hydrogenases and the corresponding subunit of complex I from various sources. In EchF the second 4xCys-binding motif was found to contain a Glu, Asp or His residue in all members of the protein family (Albracht & Hedderich, 2000). In addition, a highly conserved Glu residue is found in the proximity of the second 4xCys-binding motif (C-X(2)-C-X(2)-C-X(3)-C-P-X(8-10)-**E**) (Fig. 26).
EchC containes Glu, Asp and Tyr residues which are highly conserved in the corresponding subunit of complex I (NuoB or PSST) but not in standard [NiFe] hydrogenases (for more details see section 3 of this chapter).

1.2 Electron transfer pathway in Ech hydrogenase

The hydrogenase activity of the *echF* mutants, with ferredoxin as well as with benzyl viologen as electron acceptor, was strongly reduced. The relative hydrogenase activity, with regards to which electron acceptor was used, indicates that the *echF* mutants and wild-type Ech use the same set of iron-sulfur clusters for the electron transfer from the [NiFe] center. In this context the analysis of the EchF8 mutant is of particular interest. In this mutant the spin concentration of the proximal cluster was highest and accounted for at least 50% of the enzyme concentration. The hydrogenase activity of this mutant enzyme determined with both the physiological and the artificial electron acceptor, however, was only about 10% of that of the wild-type enzyme. This indicates that the *g* = 1.92 cluster

and probably also the g = 1.96 cluster are required not only for the reduction of the ferredoxin but also for the reduction of the artificial electron acceptor benzyl viologen. Reduction of the g = 1.89 cluster by H_2 was still possible in the mutant enzymes, which provides further evidence that this cluster directly interacts with [NiFe] center. Hence, the electron transfer reaction mediated by the enzyme can be summarized as follows: H_2 is activated at the [NiFe] center, and electrons are transferred via the proximal cluster located on subunit EchC (g = 1.89 signal) to the cluster(s) located on subunit EchF, where ferredoxin is reduced. Our studies show that at least the cluster giving rise to the g = 1.92 signal is required for ferredoxin reduction. At the current stage, the exact role of the low-potential g =1.96 signal is not known. Even in the wild-type enzyme, the intensity of this signal is very low because of its very low redox potential. Unlike in complex I, quinones are not involved in the electron transfer reaction pathway mediated by energy-converting hydrogenases. The comparison between complex I and Ech hydrogenase rather indicates that the [NiFe] center and the quinone have complementary functions. The characterisation of several complex I mutants which carry mutations at conserved positions in the NuoD (or 49 kDa) subunit has shown that this subunit of complex I carries a significant part of the quinone binding pocket and that this binding pocket could have evolved directly from the [NiFe] center binding site of the hydrogenases (Brandt *et al.*, 2003). The pH-dependence of the two [4Fe-4S] clusters in Ech suggests that these clusters simultaneously mediate electron and proton transfer and thus could be an essential part of the proton translocating machinery. The protons required for H_2 formation at the active site are thought to be delivered by a distinct proton channel located within the hydrogenase large subunit (Fontecilla-Camps, 2001; Dementin *et al.*, 2004).

1.3 Presence of an additional cofactor?

A question that remains is if the paramagnetic species that gives rise to the 2.03/2.00 signals is an intrinsic part of the enzyme (e.g. a yet unknown redox group) or if this species is artificially generated to a greater extent in the *echF* mutants. The observation that the signals do not respond to oxidation or reduction favours the second possibility. Also the spin concentration is rather low. In freshly prepared wild-type Ech the 2.03 signal is hardly detectable (Fig. 11) whereas the signal becomes more intense upon aging of the enzyme. The line shape and the temperature dependence of the signals could indicate a free radical,

but such high *g*-values have only been described for sulfur based radicals (Lawrence *et al.*, 1999). Such radicals are, however, very unstable and are normally only observed under pre-steady-state conditions. Since the g = 2.03 component of the signal could not be saturated at 4.2 K and full power, it was suggested that the signal could be due to a radical in close proximity to a very rapidly relaxing paramagnet, e.g. high spin Fe^{3+} (Kurkin *et al.*, 2002). EPR spectra with similar *g*-values (g = 2.032 and g = 2.004) and temperature behaviour have been observed for iron-nitrosyl-histidyl complexes which have for example been observed upon disassembly of the [3Fe-4S] cluster of mitochondrial aconitase upon anaerobic NO addition (Kennedy *et al.*, 1997). If such a species is formed upon reaction of a partially assembled iron-sulfur cluster of Ech with NO that could be reductively generated from contaminating amounts of nitrate or nitrite, needs to be shown.

2. Role of the membrane part of energy-converting hydrogenases

2.1 Inhibitor studies with DCCD

DCCD is a covalent carboxyl group-modifying reagent that specifically attacks acidic amino acids in a hydrophobic environment. Modification of these residues is directly responsible for inhibiting ATPase and a number of other enzymes involved in proton translocation across biological membranes by blocking the transmembrane proton channel (Solioz, 1984). Like the other energy-transducing complexes of the mitochondrial respiratory chain, it was demonstrated that complex I activity of several organisms, both prokaryotic and eukaryotic, was inhibited by the addition of DCCD. This inhibition was correlated with the presence of an energy-transducing site in this segment of the respiratory chain. *E. coli* and other bacteria (like *Bacillus subtilis*) also possess a non-proton-pumping NADH:ubiquinone oxidoreductase, which consists of a single subunit located in the cytoplasmic membrane but does not contain transmembrane elements. Its function is simply to oxidize NADH and feed the electrons into the respiratory chain (Gennis & Stewart, 1996). This enzyme was not affected by DCCD. This confirmed that the observed inhibition correlates with the presence of an energy-transducing site in this segment of the respiratory chain (Yagi, 1987). Therefore, DCCD provides a method for the study of ion translocating enzymes at a functional level.

Addition of DCCD resulted in significant inhibition of Ech hydrogenase from *M. barkeri* (Fig. 16). The inactivation of the enzyme was found to be pH-dependent: the inhibition rate increased as the pH was lowered (Fig. 17). This finding was in accord with the reaction mechanism previously proposed (Azzi *et al.*, 1984)(Fig. 15), which implies that the conserved acidic amino acid must be protonated in order to react with DCCD. Moreover, the results obtained are also in accord with the pH dependence for inactivation of other membrane-bound enzymes by DCCD, like the F_1F_O-ATPase from *Propionigenium modestum* (Kluge & Dimroth, 1993a). In particular, in the case of the enzyme from *P. modestum* it was shown that DCCD binds to a conserved glutamate residue (Glu65) located in the middle of the second membrane-spanning helix of subunit c of the hydrophobic F_O moiety (Ludwig *et al.*, 1990). Although the carboxyl group of glutamate in aqueous environment (pK ~ 4) would be hardly protonated at pH 7, the pK of the carboxyl group was estimated to be 7.0 and thus shifted toward the alkaline range (Kluge & Dimroth, 1993b). Also in other enzymes, like the cytochrome *c* oxidase, a glutamate residue has been identified as the amino acid to which DCCD binds (Prochaska *et al.*, 1981) and hence it can be hypothesized that this is a more general feature, which can be extended to other enzymes.

CO-induced hydrogenase from *Rhodospirillum rubrum* (Fox *et al.*, 1996), Mbh hydrogenase from *Pyrococcus furiosus* (Silva *et al.*, 2000), hydrogenase 3 from *E. coli* and Coo hydrogenase from *Carboxydothermus hydrogenoformans* (Forzi, 2001), other members of the energy-converting [NiFe] hydrogenase family, were shown to be inhibited by this compound as well. On the other hand, the F_{420}-non-reducing hydrogenase from *Methanothermobacter marburgensis*, a non-membrane-bound [NiFe]-hydrogenase, was not inhibited by DCCD even after incubation at 60°C for 1 h at DCCD concentrations of up to 5 mM (50 µmol DCCD per mg of protein) (Forzi, 2001). This result showed that, as expected, an energy-coupling site was absent in the latter enzyme and that DCCD did not affect the hydrogenase activity in any unspecific way.

Among different carbodiimides, DCCD has unusual properties due to its hydrophobic nature and its reactivity. When DCCD is added to an aqueous suspension of protein or protein-containing membranes, it will rapidly partition into hydrophobic environments of proteins and lipids; if a protein has hydrophobic pocket that can be occupied by DCCD and this pocket also contains a DCCD-reactive (carboxyl) group, preferential interaction takes place at this site (Solioz, 1984).

This concept was supported by the fact that the water-soluble carbodiimide EDAC did not affect Ech hydrogenase activity (Fig. 18). The high hydrophobic nature of DCCD explained also the higher degree of inhibition observed in experiments performed using the purified enzyme in comparison to experiments performed using membranes.

Likewise complex I, the inhibition of Ech hydrogensase by DCCD indicated that the electron transfer reaction is strictly coupled to cation translocation involving carboxylic side chains located in the membrane part of these enzymes. For this reason it was of interest to identify the DCCD-binding subunit of Ech hydrogenase, especially since this polypeptide may be involved in ion translocation, as already described for other energy-transducing complexes. For bovine complex I, it was proposed that DCCD binds only to subunit ND1 (NuoH with *E. coli* nomenclature) (Yagi, 1987; Yagi & Hatefi, 1988). This subunit corresponds to the small hydrophobic subunit of energy-converting hydrogenases, EchB in the case of the *M. barkeri* enzyme. In Ech, the correlation between DCCD inactivation and incorporation of radioactivity from [^{14}C]DCCD into the enzyme, suggested that inhibition by DCCD is preferentially associated with the modification of subunit EchA, the large hydrophobic subunit (Fig. 20).

2.2 Conserved acidic residues predicted to be located in transmembrane helices

Multiple sequence alignments of the small and the large hydrophobic subunit of different energy-converting hydrogenases and the corresponding subunits of complex I from different organisms revealed the presence of several highly conserved acid residues in or close to transmembrane helices (Fig. 27 and 28). The small hydrophobic subunit (EchB, HycD, NuoH/ND1 protein family) contains one highly conserved glutamate residue predicted to be located in transmembrane helix IV (Fig 27). The large integral membrane protein of the hydrogenases and its homologues in complex I (EchA, HycC, NuoL/ND5, NuoM/ND4, NuoN/ND2 protein family) contain one conserved glutamate residue predicted to be located in helix V. In addition this subunit contains an aspartate residue in the proximity of helix III (Fig. 28). It has been proposed that these highly conserved residues could be part of a transmembrane ion channel and could be the target of DCCD.

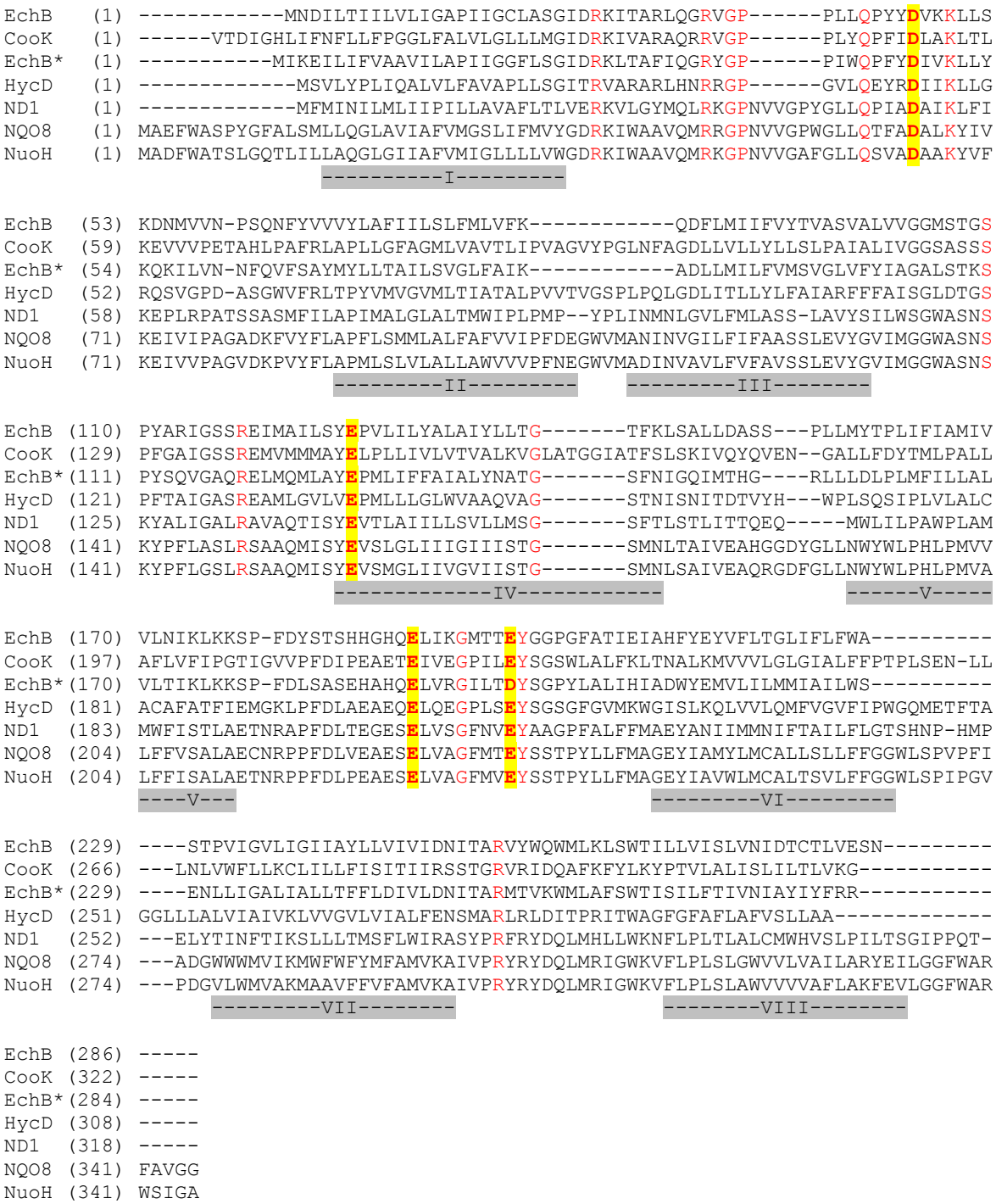

Fig. 27. Primary sequence alignment of proteins homologues to EchB from *M. barkeri* Ech hydrogenase. CooK from the CO-oxidizing:H_2-evolving enzyme complex from *C. hydrogenoformans*, EchB* from *T. tengcongensis* Ech hydrogenase, HycD from *E. coli* hydrogenase 3, ND1 from *B. taurus* complex I, NQO8 from *P. denitrificans* and NuoH from *R. capsulatus* complex I. The transmembrane helices, indicated with roman numbers below the sequence, were derived from an experimentally determined transmembrane topology model of the NuoH subunit from *R. capsulatus* complex I (Roth & Hägerhäll, 2001). Identical residues are shown in red; highly conserved acidic residues are highlighted in yellow.

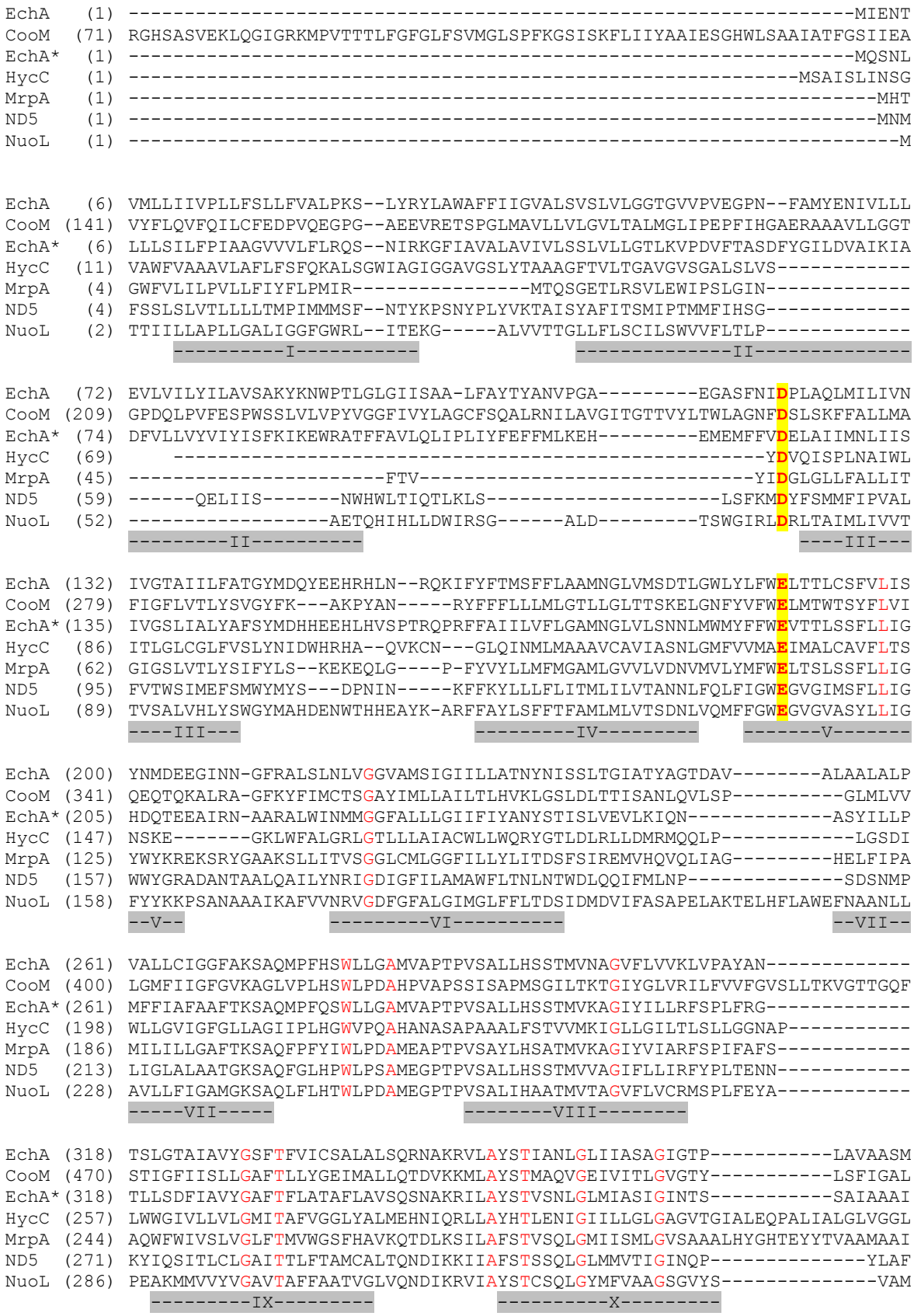
EchA (1) ----------MIENT
CooM (71) RGHSASVEKLQGIGRKMPVTTTLFGFGLFSVMGLSPFKGSISKFLIIYAAIESGHWLSAAIATFGSIIEA
EchA* (1) ----------MQSNL
HycC (1) ----------MSAISLINSG
MrpA (1) ----------MHT
ND5 (1) ----------MNM
NuoL (1) ----------M
EchA (6) VMLLIIVPLLFSLLFVALPKS--LYRYLAWAFFIIGVALSVSLVLGGTGVVPVEGPN--FAMYENIVLLL
CooM (141) VYFLQVFQILCFEDPVQEGPG--AEEVRETSPGLMAVLLVLGVLTALMGLIPEPFIHGAERAAAVLLGGT
EchA* (6) LLLSILFPIAAGVVVLFLRQS--NIRKGFIAVALAVIVLSSLVLLGTLKVPDVFTASDFYGILDVAIKIA
HycC (11) VAWFVAAAVLAFLFSFQKALSGWIAGIGGAVGSLYTAAAGFTVLTGAVGVSGALSLVS----------
MrpA (4) GWFVLILPVLLFIYFLPMIR----------MTQSGETLRSVLEWIPSLGIN----------
ND5 (4) FSSLSLVTLLLLTMPIMMMSF--NTYKPSNYPLYVKTAISYAFITSMIPTMMFIHSG----------
NuoL (2) TTIILLAPLLGALIGGFGWRL--ITEKG-----ALVVTTGLLFLSCILSWVVFLTLP----------
I II
EchA (72) EVLVILYILAVSAKYKNWPTLGLGIISAA-LFAYTYANVPGA---------EGASFNIDPLAQLMILIVN
CooM (209) GPDQLPVFESPWSSLVLVPYVGGFIVYLAGCFSQALRNILAVGITGTTVYLTWLAGNFDSLSKFFALLMA
EchA* (74) DFVLLVYVIYISFKIKEWRATFFAVLQLIPLIYFEFFMLKEH---------EMEMFFVDELAIIMNLIIS
HycC (69) ----------YDVQISPLNAIWL
MrpA (45) ----------FTV----------YIDGLGLLFALLIT
ND5 (59) ------QELIIS-------NWHWLTIQTLKLS----------LSFKMDYFSMMFIPVAL
NuoL (52) ----------AETQHIHLLDWIRSG------ALD---------TSWGIRLDRLTAIMLIVVT
---------II---------- ----III---
EchA (132) IVGTAIILFATGYMDQYEEHRHLN--RQKIFYFTMSFFLAAMNGLVMSDTLGWLYLFWELTTLCSFVLIS
CooM (279) FIGFLVTLYSVGYFK---AKPYAN-----RYFFFLLLMLGTLLGLTTSKELGNFYVFWELMTWTSYFLVI
EchA*(135) IVGSLIALYAFSYMDHHEEHLHVSPTRQPRFFAIILVFLGAMNGLVLSNNLMWMYFFWEVTTLSSFLLIG
HycC (86) ITLGLCGLFVSLYNIDWHRHA--QVKCN---GLQINMLMAAAVCAVIASNLGMFVVMAEIMALCAVFLTS
MrpA (62) GIGSLVTLYSIFYLS--KEKEQLG----P-FYVYLLMFMGAMLGVVLVDNVMVLYMFWELTSLSSFLLIG
ND5 (95) FVTWSIMEFSMWYMYS---DPNIN-----KFFKYLLLFLITMLILVTANNLFQLFIGWEGVGIMSFLLIG
NuoL (89) TVSALVHLYSWGYMAHDENWTHHEAYK-ARFFAYLSFFTFAMLMLVTSDNLVQMFFGWEGVGVASYLLIG
----III--- ---------IV--------- -------V-------
EchA (200) YNMDEEGINN-GFRALSLNLVGGVAMSIGIILLATNYNISSLTGIATYAGTDAV--------ALAALALP
CooM (341) QEQTQKALRA-GFKYFIMCTSGAYIMLLAILTLHVKLGSLDLTTISANLQVLSP----------GLMLVV
EchA*(205) HDQTEEAIRN-AARALWINMMGGFALLLGIIFIYANYSTISLVEVLKIQN-------------ASYILLP
HycC (147) NSKE-------GKLWFALGRLGTLLLAIACWLLWQRYGTLDLRLLDMRMQQLP----------LGSDI
MrpA (125) YWYKREKSRYGAAKSLLITVSGGLCMLGGFILLYLITDSFSIREMVHQVQLIAG---------HELFIPA
ND5 (157) WWYGRADANTAALQAILYNRIGDIGFILAMAWFLTNLNTWDLQQIFMLNP----------SDSNMP
NuoL (158) FYYKKPSANAAAIKAFVVNRVGDFGFALGIMGLFFLTDSIDMDVIFASAPELAKTELHFLAWEFNAANLL
--V-- ---------VI---------- --VII--
EchA (261) VALLCIGGFAKSAQMPFHSWLLGAMVAPTPVSALLHSSTMVNAGVFLVVKLVPAYAN----------
CooM (400) LGMFIIGFGVKAGLVPLHSWLPDAHPVAPSSISAPMSGILTKTGIYGLVRILFVVFGVSLLTKVGTTGQF
EchA*(261) MFFIAFAAFTKSAQMPFQSWLLGAMVAPTPVSALLHSSTMVKAGIYILLRFSPLFRG----------
HycC (198) WLLGVIGFGLLAGIIPLHGWVPQAHANASAPAAALFSTVVMKIGLLGILTLSLLGGNAP----------
MrpA (186) MILILLGAFTKSAQFPFYIWLPDAMEAPTPVSAYLHSATMVKAGIYVIARFSPIFAFS----------
ND5 (213) LIGLALAATGKSAQFGLHPWLPSAMEGPTPVSALLHSSTMVVAGIFLLIRFYPLTENN----------
NuoL (228) AVLLFIGAMGKSAQLFLHTWLPDAMEGPTPVSALIHAATMVTAGVFLVCRMSPLFEYA----------
-----VII----- --------VIII--------
EchA (318) TSLGTAIAVYGSFTFVICSALALSQRNAKRVLAYSTIANLGLIIASAGIGTP----------LAVAASM
CooM (470) STIGFIISLLGAFTLLYGEIMALLQTDVKKMLAYSTMAQVGEIVITLGVGTY----------LSFIGAL
EchA*(318) TLLSDFIAVYGAFTFLATAFLAVSQSNAKRILAYSTVSNLGLMIASIGINTS----------SAIAAAI
HycC (257) LWWGIVLLVLGMITAFVGGLYALMEHNIQRLLAYHTLENIGIILLGLGAGVTGIALEQPALIALGLVGGL
MrpA (244) AQWFWIVSLVGLFTMVWGSFHAVKQTDLKSILAFSTVSQLGMIISMLGVSAAALHYGHTEYYTVAAMAAI
ND5 (271) KYIQSITLCLGAITTLFTAMCALTQNDIKKIIAFSTSSQLGLMMVTIGINQP----------YLAF
NuoL (286) PEAKMMVVYVGAVTAFFAATVGLVQNDIKRVIAYSTCSQLGYMFVAAGSGVYS----------VAM
---------IX--------- ----------X----------

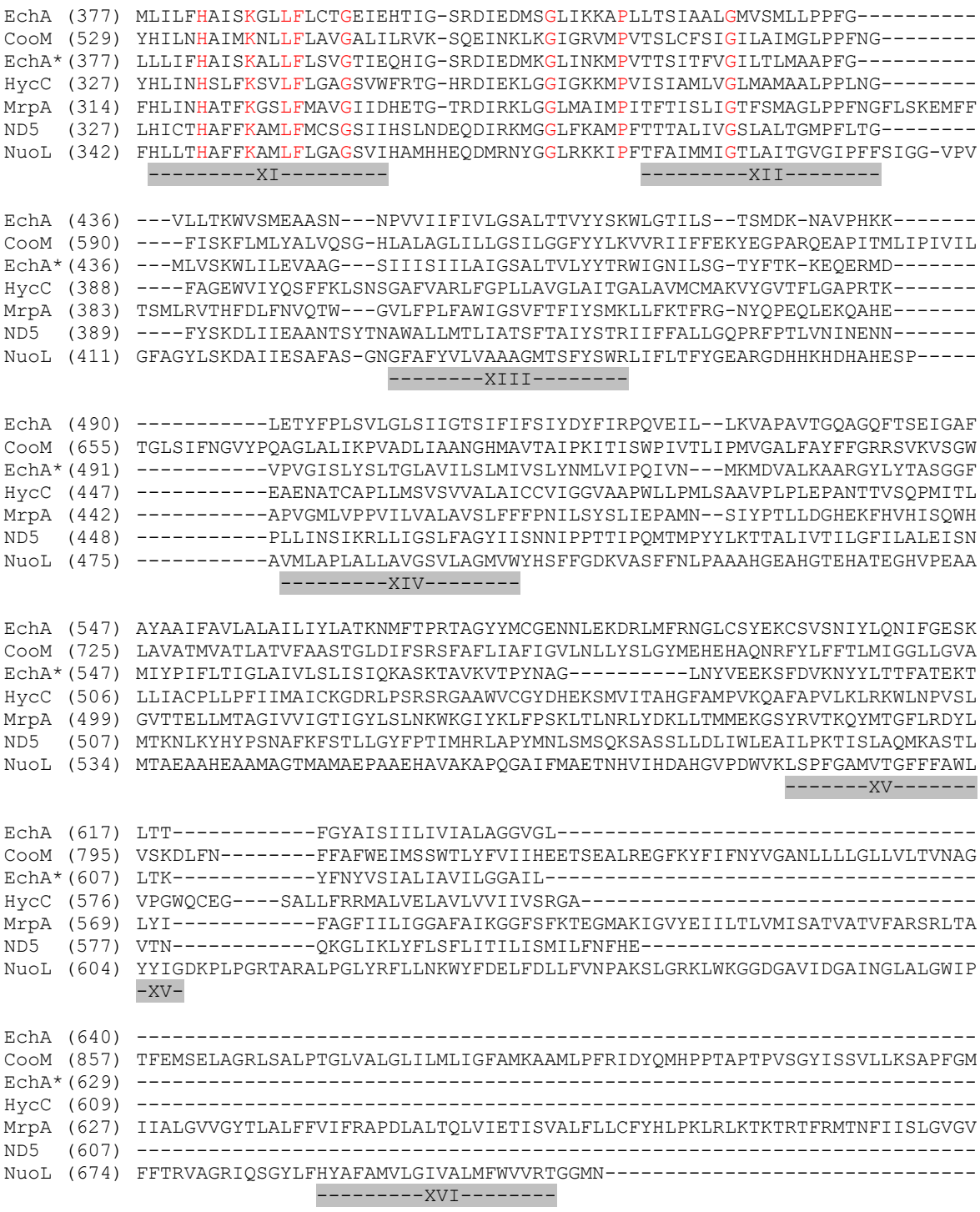

Fig. 28. Primary sequence alignment of proteins homologues to EchA from *M. barkeri* Ech hydrogenase. CooM from the CO-oxidizing:H_2-evolving enzyme complex from *C. hydrogenoformans*, EchA* from *T. tengcongensis* Ech hydrogenase, HycC from *E. coli* hydrogenase 3, MrpA antiporter from *B. subtilis*, ND5 from *B. taurus* complex I and NuoL from *R. capsulatus* complex I. The transmembrane helices, indicated with roman numbers below the sequence, were derived from an experimentally determined transmembrane topology model of the NuoL subunit from *R. capsulatus* complex I (Mathiesen & Hägerhäll, 2002). Identical residues are shown in red; highly conserved acidic residues are highlighted in yellow.

Based on the result of the labeling studies with [^{14}C]DCCD it seems that E188 found in EchA might represent the DCCD-binding amino acid, since radioactivity incorporated in this subunit correlated quite good with the inactivation of the enzyme. However, the small hydrophobic subunit was also labeled by [^{14}C]DCCD (Fig. 19). Therefore, an important function for E127 found in EchB cannot be excluded.

Based on the findings deriving from the labelling studies with DCCD performed with the bovine complex I, the functional role of highly conserved glutamate residues present in the NQO8 subunit (NuoH/ND1 homologue) from *Paracoccus denitrificans* was analysed by site-directed mutagenesis (Kurki *et al.*, 2000). The glutamate residue corresponding to EchB E127 was mutagenized to a non-carboxylic amino acid in complex I from *P. denitrificans* (E158 of subunit NQ08). This mutation resulted in a decreased quinone reductase activity and in an altered K_m value for Q1. The residual quinone reductase activity was however inhibited by DCCD. The authors concluded that E158 could be involved in quinone binding but not in DCCD binding. On the other hand the authors observed that among all the E158 mutants that were selected there was not a single colony without an active NDH-2, which is the non-energy coupled NADH:quinone oxidoreductase. This indicates that *in vivo* the NQ08 E158 mutation is lethal. For this reason these results seem to be somehow contradictory concerning the function of this glutamate residue.

The functional role of the highly conserved glutamate residues present in each membrane subunit of energy-converting [NiFe] hydrogenases were also analysed by constructing site-specific mutants. These experiments were performed with hydrogenase 3 from *E. coli* (Haacke, 2001; Weis, 2004). Both, the HycD E158Q (E158 in HycD corresponds to E127 in EchB) and the HycC E135Q (E135 in HycC corresponds to E188 in EchA) mutation in the small and in the large hydrophobic subunit, respectively, resulted in a complete loss of FHL activity in whole cells and a loss of the hydrogenase activity of isolated membranes after subtraction of residual activities due to the presence of low amounts of other hydrogenases.

The hydrophilic subunits HycE and HycG (the hydrogenase large and small subunit, respectively), which are essential for hydrogenase activity, were still detectable in the membrane fraction. Furthermore the membrane fraction of the HycD E158Q had retained 36% of the H/D exchange activity of a strain carrying wild-type HycD (L. Forzi and

R. Hedderich, unpublished results). These control experiments show that a significant portion of the hydrophilic part of the enzyme is still localized in the membrane fraction of the E158Q mutant although at a reduced level which could result from a destabilization of the mutant enzyme. The data indicate that HycD E158 is indispensable for the electron transfer reaction catalyzed by the hydrophilic portion of the enzyme.

The characterization of the HycC E135Q mutant showed that an acid residue is indispensable at this position. This glutamate residue, which is predicted to be located in transmembrane helix V close to the periplasmic space, could be part of a conserved cation channel since this residue is highly conserved in the homologous subunits of three different enzymes, namely energy-converting hydrogenaes, complex I and Mrp-type Na^+/H^+ antiporters.

The results obtained with [^{14}C]DCCD labeling of the enzyme from *M. barkei* indicated that the large hydrophobic subunit is most likely an important player in the ion translocation machinery of these enzymes. As already mentioned above, this subunit is related to subunits of K^+ and Na^+/H^+ antiporters (Hamamoto *et al.*, 1994; Putnoky *et al.*, 1998). Since recent studies have shown that Na^+ is directly involved in the mechanism of complex I from *K. pneumoniae* and *E. coli* (Steuber, 2001; Gemperli *et al.*, 2002; Gemperli *et al.*, 2003), this would point for a possible ion-translocating function for this subunit. However, a key function cannot be excluded also for the small hydrophobic subunit since the characterization of the *E. coli* hydrogenase 3 mutants in subunits HycD and HycC highlighted the important role of a conserved glutamate residues in each hydrophobic subunit. These residues can be assumed to play a similar role in complex I as well. A disadvantage of the *E. coli* hydrogenase 3 system used in these studies is that the enzyme becomes instable upon solubilisation, which thus far has prevented a purification of the enzyme. It was therefore not possible to study the mutant enzymes at the level of purified enzymes, which would have for example allowed a determination of the subunit stoichiomety or an analysis of the iron-sulfur clusters. From the organisms with energy-converting hydrogenases that can be purified only *M. barkeri* can be genetically manipulated. Methods that allow the construction of nonpolar mutations of individual genes within a transcription are currently developed for *Methanosarcina* species. Hence in future experiments the construction of the mutants described here for *E. coli* hydrogenase 3 will be attempted in *M. barkeri*.

3. FT-IR spectroscopic characterization of Ech hydrogenase from *Methanosarcina barkeri* in comparison to complex I

The combination of FT-IR difference spectroscopy and electrochemistry have already been used to describe other energy transducing complexes, such as cytochrome *c* oxidase (Hellwig *et al.*, 1998; Moss *et al.*, 1990) or more recently also complex I (Flemming *et al.*, 2003a; Hellwig *et al.*, 2000; Hellwig *et al.*, 2004). With this method it is possible to detect redox-dependent changes in protein structure and protonation states of amino acid side chains.

Electrochemically induced FT-IR difference spectra were used to investigate Ech hydrogenase in a spectral range from 2200 to 1000 cm^{-1}; the results obtained are here compared with previous studies performed with complex I. Similarities and dissimilarities are discussed in light of potentially shared energy-coupling mechanism.

In the higher spectral range from 2200 to 1800 cm^{-1}, signals deriving from stretching vibrational mode of the CO and CN ligands of the [NiFe] active site have been detected for the oxidized and reduced form of Ech hydrogenase (Fig. 21). The results obtained were consistent with previous IR spectroscopy studies performed under different conditions (S. Kurkin, R. Hedderich and S.P.J. Albracht, unpublished results). However, the characterization of these ligands was not the major aim of this study.

The region of interest was the mid infrared range from 1800 to 1200 cm^{-1} where usually redox-dependent conformational changes of the proteine backbone and protonation of amino acids side chains can be observed.

The catalytic core of complex I contains three [4Fe-4S] clusters, which are conserved in Ech and related hydrogenases. Different experimental evidences indicated that NuoB (the homologue of EchC) harbour the EPR-detectable iron-sulfur cluster N2. This cluster has a pH-dependent midpoint potential and for this reason it has been discussed to be directly involved in H^+ pumping. Redox induced FT-IR difference spectroscopy on complex I from *E. coli* demonstrated that the oxidation of cluster N2 located on NuoB is accompanied with the protonation of carboxylic side chains and tyrosines. The oxidation of cluster N2 was no longer coupled with protonation of carboxylic residues in the enzyme carrying E67Q and D77N mutations in NuoB (P.Hellwig, personal communication). For Ech hydrogenase a positive signal signal at 1720 cm^{-1} was observed, indicating the presence of a protonated

acidic residue, concomitant with the oxidation of the iron sulfur clusters (Fig. 22). Residues corresponding to E67 and D77 of NuoB of complex I from *E. coli* are conserved in the homologous subunit of energy-converting hydrogenases (Fig. 29).

```
EchC M. barkeri            (1) ------------------------------MSLAKSPWIIHVNCNSCNG-
CooL C. hydrogenoformans   (1) ------------------------MKKILQKIAKKSPWLYRINAGSCNG-
NuoB E. coli               (1) MDYTLTRIDPNGENDRYPLQKQEIVTDPLEQEVNKNVFMGKLNDMVNWGR

EchC M. barkeri           (20) -------------CDIEVVA-CLTPLYDAERFGVLNIGT-PKQADIMVVT
CooL C. hydrogenoformans  (26) -------------CDVELATTACIPRYDVERLGCKYCGS-PKHADIVLIT
NuoB E. coli              (51) KNSIWPYNFGLSCCYVEMVT-SFTAVHDVARFGAEVLRASPRQADLMVVA

EchC M. barkeri           (55) GSVNYKNVNVLKNIYNQIPDPKVVLAVGACASTGGIFHDCYNVIGGVDQV
CooL C. hydrogenoformans  (62) GPLTARVKEKVLRLYEEIPEPKVTVAIGVCPISGGVFRDSYAITGPIDNF
NuoB E. coli             (100) GTCFTKMAPVIQRLYDQMLEPKWVISMGACANSGGMY-DIYSVVQGVDKF

EchC M. barkeri          (105) IPVDAYVPGCCPRPEAILDGVVAALSILENKKK-------------GNIK
CooL C. hydrogenoformans (112) IPVDVNVPGCPPRPQAIIDGIIEAIKIWETRL------------------
NuoB E. coli             (149) IPVDVYIPGCPPRPEAYMQALMLLQESIGKERRPLSWVVGDQGVYRANMQ

EchC M. barkeri          (142) GKEVKLKGNEVPSNA-------
CooL C. hydrogenoformans (144) ----------------------
NuoB E. coli             (199) SERERKRGERIAVTNLRTPDEI
```

Fig. 29. Sequence alignment of complex I subunit NuoB from *E. coli* with the homologous subunits from energy-converting hydrogenases (*Methanosarcina barkeri* EchC and *Carboxydothermus hydrogenoformans* CooL). The four-Cys [4Fe-4S] cluster binding motif is highlighted in yellow; residues corresponding to Y114, Y139, E67 and D77 of NuoB are shown in bold. The four-Cys [4Fe-4S] cluster binding motif for [NiFe] hydrogenases has been demonstrated in the crystal structure of the hydrogenase from *D. gigas* and *D. vulgaris* (Higuchi *et al.*, 1997; Volbeda *et al.*, 1995). In the case of *E. coli* complex I, based on molecular dynamic calculations, it was proposed that Cys63 could be the fourth ligand of the [4Fe-4S] cluster found on NuoB (Gurrath & Friedrich, 2004).

The oxidized minus reduced difference spectra of wild type complex I from *E. coli* displayed a prominent signal at 1515 cm^{-1} which was interpreted as the protonation of one or more tyrosinate residues due to the reduction of cluster N2 as well as the mode at 1500 cm^{-1} interpreted as the deprotonation of the corresponding tyrosine side chain(s) due to the oxidation of cluster N2. The strongest decrease of the modes at 1515 and 1500 cm^{-1} were observed for the NuoB Y114C and Y139C mutants of complex I, demonstrating that Y114 and Y139 were protonated upon reduction of cluster N2. For Ech hydrogenase positive signals were seen at 1516 and 1492 cm^{-1}as well as negative signals at 1524 and 1506 cm^{-1} (Fig.22). Since this spectral range is not perturbed upon H/D exchange, an assignment to

amide II modes is unlikely and tyrosines can be expected to contribute to these signals. Besides the possible protonation of the residues analogous to Y114 and Y139, conserved in the energy-converting hydrogenases (Fig. 29), the additional reorganization of protonated tyrosine residues is possible, which could induce the observed differences in signal shape.

These studies revealed that the redox induced FT-IR difference spectra display similarities and dissimilarities for the redox dependent reorganizations of the three iron-sulfur clusters that are conserved in complex I from *E. coli* as well as in the energy-converting hydrogenase from *M. barkeri*. For both, a noteworthy conformational change in the amide I region was observed. This conformational change was previously suggested to include contributions from a redox driven conformational change ruling proton pumping (Hellwig *et al.*, 2004). The protonation of acidic residues could be seen at approximately 1720-1710 cm^{-1} concomitant with oxidation of both enzymes and reorganizations can be distinguished in the spectral range characteristic for tyrosines. However, variations in signal position, especially concerning the tyrosine modes, were seen. It has to be considered that besides the conserved residues and iron sulfur clusters, we are dealing with two distinct enzymes and that the conserved residues have different environments. In addition signals from the environment of the [NiFe] center cannot be excluded. In future work, the role of distinct residues in Ech hydrogenase will be studied by site directed mutagenesis.

4. Identification of the coupling ion used by Coo hydrogenase from *Carboxydothermus hydrogenoformans*

Recently it has been shown that complex I from *Klebsiella pneumoniae* (Gemperli *et al.*, 2002) pumps sodium ions rather than protons. This finding opened a new question concerning the coupling ion used by complex I. This question was also extended to the family of energy-converting [NiFe] hydrogenases. In order to investigate this important point the enzyme from *C. hydrogenoformans* was used for ion translocation studies.
Different methods were used to measure the translocation of ions coupled to the conversion of CO to H_2 and CO_2 in cell suspensions of *C. hydrogenoformans*. pH electrode measurements were used to test if the reaction catalysed by the CO-oxidizing:H_2-evolving enzyme complex is involved in the generation of a transmembrane proton gradient. In the

results section, it was shown that the conversion of CO to H_2 and CO_2 by cell suspensions at pH 5.9 was associated with an acidification of the suspension medium. This acidification was mainly due to electrogenic proton translocation, because, upon CO addition, it was only transient and it was strongly reduced or abolished in the presence of the protonophore CCCP (Fig. 23). A H^+/CO stoichiometry of approximately 1 was calculated. The sodium ionophore ETH-157 did not affect proton translocation (Fig. 23). This finding indicates that CO oxidation is coupled with the generation of a primary electrochemical proton gradient. However, no proton translocation, coupled to CO oxidation could be observed at pH 6.7, although this value is closer to 7, the physiological pH of this microorganism, and the enzyme complex is highly active at this pH. This brought up the question if the enzyme unspecifically pumps H^+ at low pH and pumps Na^+ at pH 7. The Na^+ translocation studies performed at pH 7.0 indeed showed that the CO oxidation was coupled to sodium ion translocation (Fig. 24). This Na^+ translocation was protonophore insensitive, indicating a primary Na^+ translocation. The possibility that primary Na^+ translocation was driven by a Na^+-translocating ATPase at the expense of ATP hydrolysis was excluded, since the protonophore CCCP was found to uncouple CO oxidation from ATP synthesis without affecting Na^+ extrusion. These findings indicated that ATP synthesis was driven by $\Delta\mu_{H^+}$ rather than by $\Delta\mu_{Na^+}$. Moreover, these control experiments indicated that the CCCP concentrations used in the Na^+ transport studies were sufficient to dissipate the electrochemical proton gradient. Since CO oxidation was coupled with primary Na^+ extrusion, which was also confirmed by the inhibition of ATP synthesis by the sodium ionophore ETH-157, $\Delta\mu_{H^+}$ has to be generated secondarily from $\Delta\mu_{Na^+}$ probably via a Na^+/H^+ antiporter. In order to test this last assumption, the effect of EIPA, an amiloride derivative and Na^+/H^+ antiporter inhibitor, on Na^+ extrusion and on ATP synthesis coupled to CO oxidation was tested. EIPA did not significantly affect either Na^+ translocation or ATP synthesis, indicating primary rather that secondary Na^+ translocation. However, a more careful analysis of the literature concerning Na^+/H^+ antiporters revealed a more complex situation. Previous analysis based on the availability of different genomes and on the elaboration of the DNA sequences allowed to perform phylogenetic analysis that made it possible to identify several families of Na^+/H^+ antiporters (Padan *et al.*, 2001). In addition to the NhaA family, the key antiporter of *E. coli* and of many other enterobacteria that has been most extensively studied, other families of Na^+/H^+ antiporters with little or no homology to NhaA were identified in prokaryotes. These include NapA, NhaP, NhaC,

NhaD and NhaB. Amiloride and its numerous derivatives are competitive inhibitors of various eukaryotic antiporters; the only bacterial antiporter that was found to be sensitive to amiloride was NahB from *E. coli* (Pinner *et al.*, 1995). Previous studies suggested that amiloride inhibits the Na^+/H^+ antiporter of methanogens as well (Schönheit & Beimborn, 1985), but no biochemical characterization of the methanogenic antiporter exists. Nevertheless an effect of EIPA on other Na^+/H^+ antiporters cannot be excluded since most of the transporters have been identified only at a gene level.
In the preliminary genome sequence from *C. hydrogenoformans* genes encoding for two putative Na^+/H^+ antiporter belonging to the NapA and NhaC family were identified. These groups seem not to be affected by EIPA (Padan *et al.*, 2001; Pinner *et al.*, 1995) but any conclusion has to be taken carefully since nothing is known about the antiporters of this microorganism at a biochemical level.

The inhibition of Coo hydrogenase by DCCD was influenced by sodium ions: the presence of Na^+ had a protective effect against inactivation of enzyme activity (Fig. 25). The protective effect was not to as high as the one observed in other Na^+-translocating enzymes but was clearly reproducible. Previous studies performed with the ATPase from *Propionigenium modestum* strongly evidenced that the DCCD-reactive amino acid is part of a Na^+-specific binding site (Kluge & Dimroth, 1993a). It was proposed that occupation of this site by Na^+ interferes with the modification by DCCD and therefore protects the enzyme from inhibition. The lower protective effect with the hydrogenase from *C. hydrogenoformans* could be caused by the preferential interaction of Na^+ with only one of the two integral membrane subunits. The large hydrophobic subunit, which is related to subunits of Na^+/H^+ antiporters, could fulfill such a function. This would be consistent with the fact that the homologue subunit from *M. barkeri* resulted to be preferentially modified by DCCD, as demonstrated by the labeling studies. These studies showed, however, that the small hydrophobic subunit was also labeled by [^{14}C]DCCD, even if the incorporation of radioactivity did not correlate very well with enzyme inactivation. Therefore it cannot be excluded that the inhibition of the enzyme in the presence of Na^+ is mainly due to the interaction of DCCD with the small integral subunit. Mutational studies performed with hydrogenase 3 from *E. coli*, indicate an important functional role of an acidic residue conserved in this subunit (as already discussed in section 2.2 of this chapter).

All the experiments performed with *C. hydrogenoformans* indicate that Coo hydrogenase could be a primary sodium pump, which can use H^+ at low pH. However, these results should be taken carefully, since in some experiments contradictory results were obtained. The activity of the enzyme was stimulated in the presence of Na^+ and even more in the presence of the sodium ionophore ETH-157 in experiments performed with cell suspensions or with the purified enzyme complex (data not shown). However, these results could not be reproduced with all preparations and this was not caused to residual (contaminating) Na^+ in the assay mixture, since the endogenous Na^+ content was determined by atomic absorption spectroscopy to be about 50 µM. The reason for this is not yet known.

In the literature also other examples of contradicting results regarding the coupling ion used by a certain enzyme are found. One of the disputes concerns the first step of methanogenesis from H_2/CO_2. With cell suspensions from *M. barkeri* it was evidenced that reduction of CO_2 to the formaldehyde level (catalyzed by the formylmethanofuran dehydrogenase) by H_2 is driven by a primary electrochemical sodium ion gradient (Kaesler & Schönheit, 1989a; Kaesler & Schönheit, 1989b). However, similar studies performed with *M. barkeri* and *Methanosarcina mazei* strain Gö1 showed that formaldehyde oxidation to CO_2 and H_2 was not sodium-dependent and rather generates a $\Delta\mu_{H^+}$ (Blaut *et al.*, 1992). Experiments performed with cell suspensions of acetate-grown *M. barkeri* indicated that the conversion of CO to CO_2 and H_2 was coupled to the generation of a proton motive force, which did not involve sodium ions (Bott & Thauer, 1989). Recent genetic studies have shown that Ech is the hydrogenase involved in both reactions: the first step of methanogenesis from H_2/CO_2 as well as CO-oxidation during growth on acetate (Meuer *et al.*, 2002). Experiments performed with the Δ*ech* mutant have shown that CH_4 formation could be restored in the presence of CO (or pyruvate). Furthermore, CH_4 formation from H_2/CO_2 plus CO by the Δ*ech* mutant was not inhibited by the protonophore TCS. These data showed that *in vivo* the reduction of CO_2 to formylmethanofuran can be coupled to the oxidation of CO (or pyruvate) via the ferredoxin as electron carrier and that the reduction of the ferredoxin by H_2, catalyzed by Ech hydrogenase, is the energy-driven step in formylmethanofuran synthesis from CO_2, H_2 and methanofuran (Stojanowic & Hedderich, 2004). Moreover, the FT-IR data obtained with Ech indicated protonation reactions associated with the redox reaction of the cofacors of the enzyme (see section 3.3

of the results chapter). These results indicate a proton pump. So far, the reconstitution of Ech into proteoliposomes has not been achieved. For this reason the question if Ech hydrogenase from *M. barkeri* functions as a H^+ or Na^+ pump still remains to be solved, even if the possibility that this enzyme could use different coupling ions cannot be excluded.

Another matter of debate concerns the coupling ion used by *E. coli* complex I. Based on experiments performed with inverted membrane vesicles of a mutant lacking the antiporter genes *nhaA* and *nhaB* it was proposed that the enzyme act as a sodium pump, since the Na^+ uptake was inhibited by rotenone, a specific complex I inhibitor, but not by the protonophore CCCP (Steuber *et al.*, 2000). It was also shown that the overproduced subunit NuoL of *E. coli* complex I mediated Na^+ uptake when reconstituted in to proteoliposomes; the Na^+ transport was inhibited in the presence of EIPA, an inhibitor of Na^+/H^+ antiporters (Steuber, 2003). From other experiments performed with *E. coli* wild-type cells and membrane vesicles it was suggested that complex I works as a proton pump (Bogachev *et al.*, 1996; Matsushita *et al.*, 1987). More recent experiments confirmed this hypothesis. Electrochemically induced FT-IR difference spectra revealed that the redox reaction is associated with the protonation of acidic amino acids and tyrosines (Flemming *et al.*, 2003; Hellwig *et al.*, 2000). Moreover, when the purified complex I was reconstituted into proteliposomes the proton translocation was inhibited by the protonophore CCCP and by complex I inhibitors but not by the sodium ionophore ETH-157 (Stolpe & Friedrich, 2004). These last experiments seem to confirm that *E. coli* complex I is a primary proton pump. However, it has to be considered that the various transport studies have been performed at different pH values, which could have some important consequences on the coupling ion used.

The F_1F_O ATPases is a very large family of enzymes; most of the members of this family use H^+ as the exclusive coupling ion. *Propionigenium modestum* ATP synthase is the prototype of a few enzymes that use Na^+ as the physiological coupling ion and switch to H^+ or Li^+ under certain conditions (Kluge & Dimroth, 1993). Since only a few amino acids determine the coupling ion specificity, the overall mechanism of H^+ or Na^+-translocating F_1F_O ATPases was proposed to be the same (Dimroth *et al.*, 1999). A similar variability of the coupling ion among different NADH:quinone oxidoreductases or energy-converting hydrogenases cannot be excluded. As evidenced from the example of ATP synthase, this would not affect the energy transfer mechanism.

Experiments performed with Mbh hydrogenase from *Pyrococcus furiosus* have provided a direct biochemical demonstration that this member of the energy-converting hydrogenase family represents a site of energy conservation. Addition of reduced ferredoxin to inverted membrane vesicles of *P. furiosus* resulted in the generation of both a ΔpH and a $\Delta\Psi$, which could be coupled to ATP synthesis (Sapra *et al.*, 2003). However, these experiments did not allow a primary H^+ pump or a primary Na^+ pump mechanism to be distinguished. Hence, the H^+ translocation observed could be due to the conversion of a Na^+ gradient into a H^+ gradient by a Na^+/H^+ antiporter.

5. A comparison of energy-converting hydrogenases and complex I

Ech hydrogenase is highly similar to the catalytic core of complex I, which is formed by the four hydrophilic subunits NuoB, C, D, and I and the membrane subunits NuoH and NuoL, M, and N (following the nomenclature of the *E. coli* enzyme). The evolutionary relationship between complex I and energy-converting hydrogenases has been addressed in recent reviews (Brandt *et al.*, 2003; Friedrich & Scheide, 2000; Friedrich & Weiss, 1997; Yano & Ohnishi, 2001). The catalytic core of complex I also contains three binding motifs for [4Fe-4S] centers. The characterization of these clusters has been an important issue in the complex I field in recent years. In NuoB (the homologue of EchC), three of the four Cys residues that ligate a [4Fe-4S] cluster in all [NiFe] hydrogenases are conserved. In NuoB, these Cys residues, together with a fourth unidentified residue, provide the ligands for the EPR-detectable iron-sulfur cluster N2 (Ahlers *et al.*, 2000; Flemming *et al.*, 2003b). Cluster N2 exhibits a pH-dependent midpoint potential and therefore is thought to be involved in H^+ pumping (Ingledew & Ohnishi, 1980). Subunit NuoI shares two conserved four-Cys motifs for the binding of [4Fe-4S] clusters with EchF, which is the homologue of NuoI. In complex I, however, these clusters are not detectable by EPR spectroscopy and could only be detected by UV/Vis redox difference spectroscopy (Rasmussen *et al.*, 2001). The midpoint potentials of these clusters are pH independent. Hence, the properties of the iron-sulfur clusters in the catalytic core of complex I seem to differ from those of the homologous clusters in Ech hydrogenase. In the latter enzyme, the [4Fe-4S] cluster located on EchC and one of the [4Fe-4S] clusters on EchF exhibit a pH-dependent midpoint potential, which indicates that both clusters could be involved in proton translocation. Acidic residues that could be involved in this process have been identified in multiple

sequence alignments of EchF and related subunits from other energy-converting hydrogenases and the corresponding subunit of complex I from different sources (Fig. 26). Likewise, conserved amino acid residues have been identified in the EchC subunit and the corresponding subunit (NuoB or PSST) from complex I. The characterization of *E. coli* complex I carrying site-specific mutations by electrochemically induced FT-IR-difference spectroscopy showed that the reduction of iron-sulfur cluster N2 was accompanied by the protonation of Y114 and Y139 on subunit NuoB (Flemming *et al.*, 2003a; Hellwig *et al.*, 2000). Moreover, the oxidation of cluster N2 was accompanied by the protonation of E67 and D77 (P.Hellwig, personal communication). These residues are also conserved in corresponding subunits of energy-converting hydrogenases (EchC in the case of the *M. barkeri* enzyme) (Fig. 29). The FT-IR data obtained within this work indicated that, the oxidation/reduction of iron-sulfur clusters in Ech are coupled with the protonation/deprotonation of one or more carboxylic amino acids and probably also tyrosines.

In complex I, the electron transfer reaction mediated by the iron-sulfur centers results in the reduction of the quinone, with cluster N2 being the direct electron donor (Yano *et al.*, 2005). In energy-converting hydrogenases, quinones do not function as electron acceptors. A comparison of complex I and Ech hydrogenases rather indicates that the [NiFe] center and the quinone have complementary functions. The characterization of several complex I mutants with mutations at conserved positions in the NuoD (or 49-kDa subunit) has shown that this subunit of complex I carries a significant part of the quinone binding pocket and that this binding pocket could have directly evolved from the [NiFe] center binding site of the hydrogenases (Brandt *et al.*, 2003).

The redox potential of the proximal cluster in EchC is 130 mV more negative than that of the N2 cluster of complex I (Kurkin *et al.*, 2002; Leif *et al.*, 1995). This could be the result of the different coordination spheres of the two iron-sulfur centers. The four-cysteine residues that coordinate the proximal cluster in standard [NiFe] hydrogenases (Albracht, 1993; Volbeda *et al.*, 1995) are also conserved in EchC, whereas in NuoB (PSST), one of these cysteine residues is not conserved (Fig. 29). The fourth ligand of cluster N2 has not yet been identified. The higher redox potential of cluster N2 might be an adaptation of the enzyme to its function in reducing the quinone.

The results presented in this work have confirmed that energy-converting [NiFe] hydrogenases share a conserved module with complex I for coupling an exergonic redox

reaction with the electrogenic translocation of cations across a biological membrane. However, some differences have been found, as already discussed above. The experiments performed with the enzyme from *C. hydrogenoformans* indicated that this hydrogenase could be a primary sodium pump, which may also use H^+ at low pH, even if this requires to be further confirmed. Nevertheless, this must not necessarily be the case for other members of this hydrogenase family. The different members of energy-converting hydrogenases could use different coupling ions. This needs to be more deeply investigated.

The electron transfer pathway in Ech hydrogenases only involves prosthetic groups located in the hydrophilic part of the enzyme (Fig. 30). Unlike complex I, quinones or compounds functionally equivalent to quinones, i.e. the methanogenic methanophenazine, are not involved in the electron transfer reaction catalyzed by the hydrogenases. This has important implications for the discussion of how these hydrogenases use redox energy to transport charges across the cytoplasmic membrane. A conformational energy-transfer mechanism would be most consistent with an electron transfer process not involving membrane-bound electron carriers. Such an indirect coupling is also currently favoured in the field of complex I (Yagi *et al.*, 1998; Friedrich, 2001; Brandt *et al.*, 2003). A large reorganization of the polypeptide backbone accompanied with the reaction of *E. coli* complex I was detected by means of combined electrochemistry and FT-IR spectroscopy (Hellwig *et al.*, 2000; Hellwig *et al.*, 2004). Similar experiments performed with Ech hydrogenase from *M. barkeri* in this work showed that the redox-reaction catalyzed by this enzyme is also associated with a conformational change of the protein backbone. Moreover, complex I and Ech hydrogenase share common properties with those of other indirect coupling enzymes. For example, complex I and Ech hydrogenase, like the ATP synthase, are reversible enzyme catalyzing the reversible reduction of quinone or ferredoxin, respectively. In contrast, other enzymes whose mechanism of energy transduction is based on direct coupling (like the bc_1 complex and the cytochrome *c* oxidase of the respiratory chain) catalyze only forward reactions. Moreover, an indirect coupling of energy transfer mechanism is also favored by the fact that the binding of DCCD to residue(s) in the transmembrane part of the enzyme strongly inhibits the electron transfer reaction, while in bc_1 complex and cytochrome *c* oxidase, DCCD diminishes proton translocation without affecting electron transfer (decoupling) (Yagi & Matsuno-Yagi, 2003).

So far, it is not known which step in the electron transfer pathway could induce such a conformational change. The iron-sulfur clusters could play a key role in this mechanism. The pH-dependence of the midpoint potential of the two [4Fe-4S] clusters in Ech suggests that these clusters simultaneously mediate electron and cation transfer and thus could be an essential part of the cation-translocating machinery.

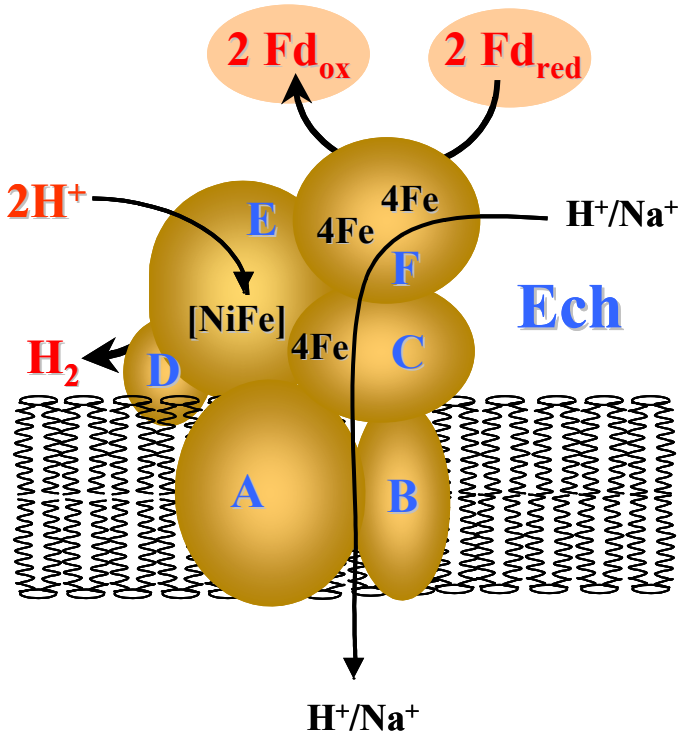

Fig. 30. Schematic representation of the proposed energy-coupling mechanism of energy-converting [NiFe] hydrogenases. Ech from *Methanosarcina barkeri* is shown as an example. The [4Fe-4S] clusters in Ech are proposed to simultaneously mediate electron and proton transfer. Electrons are then transferred to the [Ni-Fe] center, whereas H^+ (Na^+) are guided to a transmembrane H^+ (Na^+) channel. This charge separation could be driven by conformational changes triggered by the exergonic electron transfer process. The H^+ (Na^+)/e^- stoichiometry is not known but for thermodynamic reasons cannot exceed 2 H^+ (2 Na^+)/2e^-.

VI REFERENCES

Adams, M. W. W. & Stiefel, E. I. (2000). Organometallic iron: the key to biological hydrogen metabolism. *Curr. Opin. Chem. Biol.* **4**, 214-220.

Ahlers, P. M., Zwicker, K., Kerscher, S. & Brandt, U. (2000). Function of conserved acidic residues in the PSST homologue of complex I (NADH:ubiquinone oxidoreductase) from *Yarrowia lipolytica*. *J. Biol. Chem.* **275**, 23577-82.

Albracht, S. P. (1994). Nickel hydrogenases: in search of the active site. *Biochim. Biophys. Acta* **1188**, 167-204.

Albracht, S. P. J. (1993). Intimate relationships of the large and the small subunits of all nickel hydrogenases with two nuclear-encoded subunits of mitochondrial NADH: ubiquinone oxidoreductase. *Biochim. Biophys. Acta* **1144**, 221-224.

Albracht, S. P. J. & Hedderich, R. (2000). Learning from hydrogenases: location of a proton pump and of a second FMN in bovine NADH-ubiquinone oxidoreductase (Complex I). *FEBS Lett.* **485**, 1-6.

Andrews, S. C., Berks, B. C., McClay, J., Ambler, A., Quail, M. A., Golby, P. & Guest, J. R. (1997). A 12-cistron *Escherichia coli* Operon (*hyf*) encoding a putative proton-translocating formate hydrogenlyase system. *Microbiology* **143**, 3633-3647.

Augier, V., Guigliarelli, B., Asso, M., Bertrand, P., Frixon, C., Giordano, G., Chippaux, M. & Blasco, F. (1993). Site-directed mutagenesis of conserved cysteine residues within the beta subunit of *Escherichia coli* nitrate reductase. Physiological, biochemical, and EPR characterization of the mutated enzymes. *Biochemistry* **32**, 2013-23.

Azzi, A., Casey, R. P. & Nalecz, M. J. (1984). The effect of *N,N'*-dicyclohexylcarbodiimide on enzymes of bioenergetic relevance. *Biochim. Biophys. Acta* **768**, 209-26.

Blaut, M. & Gottschalk, G. (1984). Coupling of ATP synthesis and methane formation from methanol and molecular hydrogen in *Methanosarcina barkeri*. *Eur. J. Biochem.* **141**, 217-22.

Blaut, M., Müller, V. & Gottschalk, G. (1992). Energetics of methanogenesis studied in vesicular systems. *J. Bioenerg. Biomembr.* **24**, 529-46.

Boccazzi, P., Zhang, J. K. & Metcalf, W. W. (2000). Generation of dominant selectable markers for resistance to pseudomonic acid by cloning and mutagenesis of the ileS gene from the archaeon *Methanosarcina barkeri* fusaro. *J. Bacteriol.* **182**, 2611-8.

Böck, A. & Sawers, G. (1996). Fermentation. In *Escherichia coli* and *Salmonella. Cellular and Molecular Biology*, pp. 262-282. Edited by F. C. Neidhardt. Washington, D.C.: American Society for Microbiology.

Bogachev, A. V., Murtazina, R. A. & Skulachev, V. P. (1996). H^+/e^- stoichiometry for NADH dehydrogenase I and dimethyl sulfoxide reductase in anaerobically grown *Escherichia coli* cells. *J. Bacteriol.* **178**, 6233-7.

Böhm, R., Sauter, M. & Böck, A. (1990). Nucleotide sequence and expression of an operon in *Escherichia coli* coding for formate hydrogenlyase components. *Mol. Microbiol.* **4**, 231-43.

Bott, M. & Thauer, R. K. (1989). Proton translocation coupled to the oxidation of carbon monoxide to CO_2 and H_2 in *Methanosarcina barkeri*. *Eur. J. Biochem.* **179**, 469-72.

Bradford, M. M. (1976). A rapid and sensitive method for the quantitation of microgram quantities of protein utilizing the principle of protein-dye binding. *Analytical Biochemistry* **72**, 248-54.

Brandt, U. (1997). Proton-translocation by membrane-bound NADH:ubiquinone-oxidoreductase (complex I) through redox-gated ligand conduction. *Biochim. Biophys. Acta* **1318**, 79-91.

Brandt, U., Kerscher, S., Drose, S., Zwicker, K. & Zickermann, V. (2003). Proton pumping by NADH : ubiquinone oxidoreductase. A redox driven conformational change mechanism? *FEBS Lett.* **545**, 9-17.

Buurman, G., Shima, S. & Thauer, R. K. (2000). The metal-free hydrogenase from methanogenic archaea: evidence for a bound cofactor. *FEBS Lett.* **485**, 200-204.

Chevallet, M., Dupuis, A., Issartel, J. P., Lunardi, J., van Belzen, R. & Albracht, S. P. (2003). Two EPR-detectable [4Fe-4S] clusters, N2a and N2b, are bound to the NuoI (TYKY) subunit of NADH:ubiquinone oxidoreductase (Complex I) from *Rhodobacter capsulatus*. *Biochim. Biophys. Acta* **1557**, 51-66.

De Lacey, A. L., Pardo, A., Fernandez, V. M., Dementin, S., Adryanczyk-Perrier, G., Hatchikian, E. C. & Rousset, M. (2004). FTIR spectroelectrochemical study of the activation and inactivation processes of [NiFe] hydrogenases: effects of solvent isotope replacement and site-directed mutagenesis. *J. Biol. Inorg. Chem.* **9**, 636-42.

Dementin, S., Burlat, B., De Lacey, A. L., Pardo, A., Adryanczyk-Perrier, G., Guigliarelli, B., Fernandez, V. M. & Rousset, M. (2004). A glutamate is the essential proton transfer gate during the catalytic cycle of the [NiFe] hydrogenase. *J. Biol. Chem.* **279**, 10508-13.

Deppenmeier, U., Blaut, M., Mahlmann, A. & Gottschalk, G. (1990). Reduced coenzyme F_{420}: Heterodisulfide oxidoreductase, a proton-translocating redox system in methanogenic bacteria. *Proc. Natl. Acad. Sci. U S A* **87**, 9449-9453.

Dimroth, P., Wang, H., Grabe, M. & Oster, G. (1999). Energy transduction in the sodium F-ATPase of *Propionigenium modestum*. *Proc. Natl. Acad. Sci. U S A* **96**, 4924-9.

Flemming, D., Hellwig, P. & Friedrich, T. (2003a). Involvement of tyrosines 114 and 139 of subunit NuoB in the proton pathway around cluster N2 in *Escherichia coli* NADH:ubiquinone oxidoreductase. *J. Biol. Chem.* **278**, 3055-62.

Flemming, D., Schlitt, A., Spehr, V., Bischof, T. & Friedrich, T. (2003b). Iron-sulfur cluster N2 of the *Escherichia coli* NADH:ubiquinone oxidoreductase (complex I) is located on subunit NuoB. *J. Biol. Chem.* **278**, 47602-9.

Fontecilla-Camps, J. C., Frey, M., Garcin, E., Higuchi, Y., Montet, Y., Nicolet, Y. & Volbeda, A. (2001). Molecular architecures. In *Hydrogen as a Fuel*, pp. 93-109. Edited by R. Cammack, Frey, M. & Robson, R. London, New York: Taylor & Francis.

Forzi, L. (2001). Probing the proton-pumping function of *Escherichia coli* hydrogenase 3, an enzyme related to energy conserving NADH:quinone oxidoreductase. Marburg and Venice: Philipps University Marburg and Ca' Foscari University Venice.

Fox, J. D., He, Y. P., Shelver, D., Roberts, G. P. & Ludden, P. W. (1996). Characterization of the region encoding the Co-induced hydrogenase of *Rhodospirillum Rubrum*. *J. Bacteriol.* **178**, 6200-6208.

Fox, J. D., Kerby, R. L., Roberts, G. P. & Ludden, P. W. (1996). Characterization of the Co-induced, Co-tolerant hydrogenase from *Rhodospirillum Rubrum* and the gene encoding the large subunit of the enzyme. *J. Bacteriol.* **178**, 1515-1524.

Friedrich, T. & Scheide, D. (2000). The respiratory complex I of bacteria, archaea and eukarya and its module common with membrane-bound multisubunit hydrogenases. *FEBS Lett.* **479**, 1-5.

Friedrich, T. (2001). Complex I: A chimaera of a redox and conformation-driven proton pump? *J. Bioenerg. Biomembr.* **33**, 169-177.

Friedrich, T. & Weiss, H. (1997). Modular evolution of the respiratory NADH-ubiquinone oxidoreductase and the origin of its modules. *J. Theor. Biol.* **187**, 529-540.

Garcin, E., Montet, Y., Volbeda, A., Hatchikian, C., Frey, M. & Fontecilla-Camps, J. C. (1998). Structural bases for the catalytic mechanism of [NiFe] hydrogenases. *Biochem. Soc. Trans.* **26**, 396-401.

Gemperli, A. C., Dimroth, P. & Steuber, J. (2002). The respiratory complex I (NDH I) from *Klebsiella pneumoniae*, a sodium pump. *J. Biol. Chem.* **277**, 33811-7.

Gemperli, A. C., Dimroth, P. & Steuber, J. (2003). Sodium ion cycling mediates energy coupling between complex I and ATP synthase. *Proc. Natl. Acad. Sci. U S A* **100**, 839-44.

Gennis, R. B. & Stewart, V. (1996). Respiration. In *Escherichia coli* and *Salmonella. Cellular and Molecular Biology*, pp. 217-261. Edited by F. C. Neidhardt. Washington, DC: American Society for Microbiology.

Goormaghtigh, E., Cabiaux, V. & Ruysschaert, J. M. (1994). Determination of soluble and membrane protein structure by Fourier transform infrared spectroscopy. III. Secondary structures. *Subcell. Biochem.* **23**, 405-50.

Graf, E. G. & Thauer, R. K. (1981). Hydrogenase from *Methanobacterium thermoautotrophicum*, a nickel-containing enzyme. *FEBS Lett.* **136**, 165-169.

Gurrath, M. & Friedrich, T. (2004). Adjacent cysteines are capable of ligating the same tetranuclear iron-sulfur cluster. *Proteins* **56**, 556-63.

Haacke, A. (2001). Identifizierung von essentiellen Glutamat-Resten in der membranständigen Unereinheit HycD der *Escherichia coli*-Hydrogenase 3 und Erzeugung einer Mutante mit erhöhter CO-Toleranz. Marburg: Philipps University Marburg.

Hamamoto, T., Hashimoto, M., Hino, M., Kitada, M., Seto, Y., Kudo, T. & Horikoshi, K. (1994). Characterization of a gene responsible for the Na^+/H^+ antiporter system of alkalophilic *Bacillus* species strain C-125. *Mol. Microbiol.* **14**, 939-46.

Happe, R. P., Roseboom, W., Pierik, A. J., Albracht, S. P. & Bagley, K. A. (1997). Biological activation of hydrogen. *Nature* **385**, 126.

Hedderich, R. (2004). Energy-converting [NiFe] hydrogenases from archaea and extremophiles: Ancestors of complex I. *J. Bioenerg. Biomembr.* **36**, 65-75.

Heise, R., Müller, V. & Gottschalk, G. (1992). Presence of a sodium-translocating ATPase in membrane vesicles of the homoacetogenic bacterium *Acetobacterium woodii*. *Eur. J. Biochem.* **206**, 553-7.

Hellwig, P., Behr, J., Ostermeier, C., Richter, O. M., Pfitzner, U., Odenwald, A., Ludwig, B., Michel, H. & Mantele, W. (1998). Involvement of glutamic acid 278 in the redox reaction of the cytochrome c oxidase from *Paracoccus denitrificans* investigated by FTIR spectroscopy. *Biochemistry* **37**, 7390-9.

Hellwig, P., Scheide, D., Bungert, S., Mantele, W. & Friedrich, T. (2000). FT-IR spectroscopic characterization of NADH:ubiquinone oxidoreductase (complex I) from *Escherichia coli*: oxidation of FeS cluster N2 is coupled with the protonation of an aspartate or glutamate side chain. *Biochemistry* **39**, 10884-91.

Hellwig, P., Stolpe, S. & Friedrich, T. (2004). Fourier transform infrared spectroscopic study on the conformational reorganization in *Escherichia coli* complex I due to redox-driven proton translocation. *Biopolymers* **74**, 69-72.

Higuchi, Y., Yagi, T. & Yasuoka, N. (1997). Unusual ligand structure in Ni-Fe active center and an additional Mg site in hydrogenase revealed by high resolution X-ray structure analysis. *Structure* **5**, 1671-80.

Ide, T., Baumer, S. & Deppenmeier, U. (1999). Energy Conservation by the H_2: Heterodisulfide oxidoreductase from *Methanosarcina mazei* Gö1: identification of two proton-translocating segments. *J. Bacteriol.* **181**, 4076-4080.

Ingledew, W. J. & Ohnishi, T. (1980). An analysis of some thermodynamic properties of iron-sulphur centres in site I of mitochondria. *Biochem. J.* **186**, 111-117.

Kaesler, B. & Schönheit, P. (1989a). The role of sodium ions in methanogenesis. Formaldehyde oxidation to CO_2 and $2H_2$ in methanogenic bacteria is coupled with primary

electrogenic Na^+ translocation at a stoichiometry of 2-3 Na^+/CO_2. *Eur. J. Biochem.* **184**, 223-232.

Kaesler, B. & Schönheit, P. (1989b). The sodium cycle in methanogenesis. CO_2 reduction to the formaldehyde level in methanogenic bacteria is driven by a primary electrochemical potential of Na^+ generated by formaldehyde reduction to CH_4. *Eur. J. Biochem.* **186**, 309-16.

Karrasch, M., Bott, M. & Thauer, R. K. (1989). Carbonic anhydrase activity in acetate grown *Methanosarcina barkeri*. *Arch. Microbiol.* **151**, 137-142.

Kennedy, M. C., Antholine, W. E. & Beinert, H. (1997). An EPR investigation of the products of the reaction of cytosolic and mitochondrial aconitases with nitric oxide. *J. Biol. Chem.* **272**, 20340-7.

Kerby, R. L., Ludden, P. W. & Roberts, G. P. (1995). Carbon monoxide-dependent growth of *Rhodospirillum rubrum*. *J. Bacteriol.* **177**, 2241-2244.

Kluge, C. & Dimroth, P. (1993b). Kinetics of inactivation of the F_1F_o ATPase of *Propionigenium modestum* by dicyclohexylcarbodiimide in relationship to H^+ and Na^+ concentration: probing the binding site for the coupling ions. *Biochemistry* **32**, 10378-86.

Kluge, C. & Dimroth, P. (1993a). Specific protection by Na^+ or Li^+ of the F_1F_0-ATPase of *Propionigenium modestum* from the reaction with dicyclohexylcarbodiimide. *J. Biol. Chem.* **268**, 14557-60.

Künkel, A., Vorholt, J. A., Thauer, R. K. & Hedderich, R. (1998). An *Escherichia coli* hydrogenase-3-type hydrogenase in methanogenic archaea. *Eur. J. Biochem.* **252**, 467-76.

Kurki, S., Zickermann, V., Kervinen, M., Hassinen, I. & Finel, M. (2000). Mutagenesis of three conserved Glu residues in a bacterial homologue of the ND1 subunit of complex I affects ubiquinone reduction kinetics but not inhibition by dicyclohexylcarbodiimide. *Biochemistry* **39**, 13496-502.

Kurkin, S., Meuer, J., Koch, J., Hedderich, R. & Albracht, S. P. (2002). The membrane-bound [NiFe]-hydrogenase (Ech) from *Methanosarcina barkeri*: unusual properties of the iron-sulphur clusters. *Eur. J. Biochem.* **269**, 6101-11.

Laemmli, U. K. (1970). Cleavage of structural proteins during the assembly of the head of bacteriophage T4. *Nature* **227**, 680-685.

Lawrence, C. C., Bennati, M., Obias, H. V., Bar, G., Griffin, R. G. & Stubbe, J. (1999). High-field EPR detection of a disulfide radical anion in the reduction of cytidine 5'-disphosphate by the E441Q R1 mutant of *Escherichia coli* ribonucleotide reductase. *Proc. Natl. Acad. Sci. USA* **96**, 8979-8984.

Leif, H., Sled, V. D., Ohnishi, T., Weiss, H. & Friedrich, T. (1995). Isolation and characterization of the proton-translocating NADH: ubiquinone oxidoreductase from *Escherichia coli*. *Eur. J. Biochem.* **230**, 538-48.

Ludwig, W., Kaim, G., Laubinger, W., Dimroth, P., Hoppe, J. & Schleifer, K. H. (1990). Sequence of subunit c of the sodium ion translocating adenosine triphosphate synthase of *Propionigenium modestum*. *Eur. J. Biochem.* **193**, 395-9.

Lyon, E. J., Shima, S., Boecher, R., Thauer, R. K., Grevels, F. W., Bill, E., Roseboom, W. & Albracht, S. P. (2004b). Carbon monoxide as an intrinsic ligand to iron in the active site of the iron-sulfur-cluster-free hydrogenase H_2-forming methylenetetrahydromethanopterin dehydrogenase as revealed by infrared spectroscopy. *J. Am. Chem. Soc.* **126**, 14239-48.

Lyon, E. J., Shima, S., Buurman, G., Chowdhuri, S., Batschauer, A., Steinbach, K. & Thauer, R. K. (2004a). UV-A/blue-light inactivation of the 'metal-free' hydrogenase (Hmd) from methanogenic archaea. *Eur. J. Biochem.* **271**, 195-204.

Malki, S., Saimmaime, I., De Luca, G., Rousset, M., Dermoun, Z. & Belaich, J. P. (1995). Characterization of an operon encoding an NADP-reducing hydrogenase in *Desulfovibrio fructosovorans*. *J. Bacteriol.* **177**, 2628-36.

Mathiesen, C. & Hägerhäll, C. (2002). Transmembrane topology of the NuoL, M and N subunits of NADH:quinone oxidoreductase and their homologues among membrane-bound hydrogenases and bona fide antiporters. *Biochim. Biophys. Acta* **1556**, 121-32.

Matsushita, K., Ohnishi, T. & Kaback, H. R. (1987). NADH-ubiquinone oxidoreductases of the *Escherichia coli* aerobic respiratory chain. *Biochemistry* **26**, 7732-7.

Metcalf, W. W., Zhang, J. K., Apolinario, E., Sowers, K. R. & Wolfe, R. S. (1997). A genetic system for Archaea of the genus *Methanosarcina*: liposome-mediated transformation and construction of shuttle vectors. *Proc. Natl. Acad. Sci. U S A* **94**, 2626-31.

Metcalf, W. W., Zhang, J. K., Shi, X. & Wolfe, R. S. (1996). Molecular, genetic, and biochemical characterization of the serC gene of *Methanosarcina barkeri* Fusaro. *J. Bacteriol.* **178**, 5797-802.

Meuer, J. (2001). Zur fentralen Funktion von Ech-Hydrogenase und Ferredoxin in Methanogenese und CO_2-Fixierung in *Methanosarcina barkeri*. Marburg: Philipps University Marburg.

Meuer, J., Bartoschek, S., Koch, J., Künkel, A. & Hedderich, R. (1999). Purification and catalytic properties of Ech hydrogenase from *Methanosarcina barkeri*. *Eur. J. Biochem.* **265**, 325-35.

Meuer, J., Kuettner, H. C., Zhang, J. K., Hedderich, R. & Metcalf, W. W. (2002). Genetic analysis of the archaeon *Methanosarcina barkeri* Fusaro reveals a central role for Ech hydrogenase and ferredoxin in methanogenesis and carbon fixation. *Proc. Natl. Acad. Sci. U S A* **99**, 5632-7.

Mitchell, P. (1966). Chemiosmotic coupling in oxidative and photosynthetic phosphorylation. *Biol. Rev Camb Philos Soc.* **41**, 445-502.

Moss, D., Nabedryk, E., Breton, J. & Mantele, W. (1990). Redox-linked conformational changes in proteins detected by a combination of infrared spectroscopy and protein

electrochemistry. Evaluation of the technique with cytochrome c. *Eur. J. Biochem.* **187**, 565-72.

Neumann, S., Matthey, U., Kaim, G. & Dimroth, P. (1998). Purification and properties of the F_1F_0 ATPase of *Ilyobacter tartaricus*, a sodium ion pump. *J. Bacteriol.* **180**, 3312-6.

Nicolet, Y., Piras, C., Legrand, P., Hatchikian, C. E. & Fontecilla-Camps, J. C. (1999). *Desulfovibrio desulfuricans* iron hydrogenase: the structure shows unusual coordination to an active site Fe binuclear center. *Structure* **7**, 13-23.

Padan, E., Venturi, M., Gerchman, Y. & Dover, N. (2001). Na^+/H^+ antiporters. *Biochim. Biophys. Acta* **1505**, 144-57.

Palmer, G. (2000). Electronparamagnetic resonance of metalloproteins. In *Physical methods in bioinorganic chemistry*, pp. 121-185. Edited by J. Lawrence Que: University Science Books.

Peters, J. W. (1999). Structure and mechanism of iron-only hydrogenases. *Curr. Opin. Struc. Biol.* **9**, 670-676.

Peters, J. W., Lanzilotta, W. N., Lemon, B. J. & Seefeldt, L. C. (1998). X-ray crystal structure of the Fe-only hydrogenase (CpI) from *Clostridium pasteurianum* to 1.8 angstrom resolution. *Science* **282**, 1853-8.

Pierik, A. J., Hulstein, M., Hagen, W. R. & Albracht, S. P. (1998). A low-spin iron with CN and CO as intrinsic ligands forms the core of the active site in [Fe]-hydrogenases. *Eur. J. Biochem.* **258**, 572-8.

Pinner, E., Padan, E. & Schuldiner, S. (1995). Amiloride and harmaline are potent inhibitors of NhaB, a Na^+/H^+ antiporter from *Escherichia coli*. *FEBS Lett.* **365**, 18-22.

Pritchett, M. A., Zhang, J. K. & Metcalf, W. W. (2004). Development of a markerless genetic exchange method for *Methanosarcina acetivorans* C2A and its use in construction of new genetic tools for methanogenic archaea. *Appl. Environ. Microbiol.* **70**, 1425-33.

Prochaska, L. J., Bisson, R., Capaldi, R. A., Steffens, G. C. & Buse, G. (1981). Inhibition of cytochrome c oxidase function by dicyclohexylcarbodiimide. *Biochim. Biophys. Acta* **637**, 360-73.

Putnoky, P., Kereszt, A., Nakamura, T., Endre, G., Grosskopf, E., Kiss, P. & Kondorosi, A. (1998). The *pha* gene cluster of *Rhizobium meliloti* involved in pH adaptation and symbiosis encodes a novel type of K^+ efflux system. *Mol. Microbiol.* **28**, 1091-101.

Rasmussen, T., Scheide, D., Brors, B., Kintscher, L., Weiss, H. & Friedrich, T. (2001). Identification of two tetranuclear FeS clusters on the ferredoxin-type subunit of NADH:ubiquinone oxidoreductase (complex I). *Biochemistry* **40**, 6124-31.

Roth, R. & Hägerhäll, C. (2001). Transmembrane orientation and topology of the NADH:quinone oxidoreductase putative quinone binding subunit NuoH. *Biochim. Biophys. Acta* **1504**, 352-62.

Sambrook, J., Fritsch, E. F. & Maniatis, T. (1989). *Molecular Cloning, a laboratory manual*, 2 edn. New York: Cold Spring Harbor Laboratory Press.

Sapra, R., Bagramyan, K. & Adams, M. W. (2003). A simple energy-conserving system: proton reduction coupled to proton translocation. *Proc. Natl. Acad. Sci. U S A* **100**, 7545-50.

Sapra, R., Verhagen, M. & Adams, M. W. W. (2000). Purification and characterization of a membrane-bound hydrogenase from the hyperthermophilic archaeon *Pyrococcus furiosus*. *J. Bacteriol.* **182**, 3423-3428.

Sauter, M., Böhm, R. & Böck, A. (1992). Mutational analysis of the operon (*hyc*) determining hydrogenase 3 formation in *Escherichia coli*. *Mol. Microbiol.* **6**, 1523-32.

Schönheit, P. & Beimborn, D. B. (1985). Presence of a Na^+/H^+ antiporter in *Methanobacterium thermoautotrophicum* and Its role in Na^+ dependent methanogenesis. *Arch. Microbiol.* **142**, 354-361.

Schwarz, E. & Friedrich, B. (2003). The H_2-metabolizing prokaryotes. In *The prokaryotes: An evolving electronic resource for the microbiological community (http://141.150.157.117:8080/prokPUB/index.htm)*. Edited by M. Dworkin. *et al.* New York: Springer.

Silva, P. J., van den Ban, E. C., Wassink, H., Haaker, H., de Castro, B., Robb, F. T. & Hagen, W. R. (2000). Enzymes of hydrogen metabolism in *Pyrococcus furiosus*. *Eur. J. Biochem.* **267**, 6541-51.

Soboh, B. (2001). Reinigung und Charakterisierung eines CO-oxidierenden/H_2-bildenden Enzymkomplexes aus der Membranfraktion von *Carboxydothermus hydrogenoformans*. Marburg: Philipps University Marburg.

Soboh, B., Linder, D. & Hedderich, R. (2002). Purification and catalytic properties of a CO-oxidizing:H_2-evolving enzyme complex from *Carboxydothermus hydrogenoformans*. *Eur. J. Biochem.* **269**, 5712-21.

Soboh, B., Linder, D. & Hedderich, R. (2004). A multisubunit membrane-bound [NiFe] hydrogenase and an NADH-dependent Fe-only hydrogenase in the fermenting bacterium *Thermoanaerobacter tengcongensis*. *Microbiology* **150**, 2451-63.

Solioz, M. (1984). Dicyclohexylcarbodiimide as a probe for proton translocating enzymes. *Trends Biochem. Sci.* **9**, 309-312.

Sowers, K. R., Boone, J. E. & Gunsalus, R. P. (1993). Disaggregation of *Methanosarcina* spp. and Growth as Single Cells at Elevated Osmolarity. *Appl. Environ. Microbiol.* **59**, 3832-3839.

Stein, M. & Lubitz, W. (2002). Quantum chemical calculations of [NiFe] hydrogenase. *Curr. Opin. Chem. Biol.* **6**, 243-9.

Stephenson, M. & Stickland, L. H. (1931). Hydrogenase: A bacterial enzyme activating molecular hydrogen. I The proprieties of the enzyme. *Biochem. J.* **25**, 205-214.

Steuber, J. (2001). The Na^+-translocating NADH:quinone oxidoreductase (NDH I) from *Klebsiella pneumoniae* and *Escherichia coli*: implications for the mechanism of redox-driven cation translocation by complex I. *J. Bioenerg. Biomembr.* **33**, 179-86.

Steuber, J. (2003). The C-terminally truncated NuoL subunit (ND5 homologue) of the Na^+-dependent complex I from *Escherichia coli* transports Na^+. *J. Biol. Chem.* **278**, 26817-22.

Steuber, J., Schmid, C., Rufibach, M. & Dimroth, P. (2000). Na^+ translocation by complex I (NADH : quinone oxidoreductase) of *Escherichia coli*. *Mol. Microbiol.* **35**, 428-434.

Stojanowic, A. & Hedderich, R. (2004). CO_2 reduction to the level of formylmethanofuran in *Methanosarcina barkeri* is non-energy driven when CO is the electron donor. *FEMS Microbiol. Lett.* **235**, 163-7.

Stolpe, S. & Friedrich, T. (2004). The *Escherichia coli* NADH:ubiquinone oxidoreductase (complex I) is a primary proton pump but may be capable of secondary sodium antiport. *J. Biol. Chem.* **279**, 18377-83.

Svetlichny, V. A., Sokolova, T. G., Gerhardt, M., Kostrikina, N. A. & Zavarzin, G. A. (1991). Anaerobic extremely thermophilic carboxydotrophic bacteria in hydrotherms of Kuril islands. *Microbial Ecology* **21**, 1-10.

Terlesky, K. C. & Ferry, J. G. (1988). Purification and characterization of a ferredoxin from acetate-grown *Methanosarcina thermophila*. *J. Biol. Chem.* **263**, 4080-2.

Tersteegen, A. & Hedderich, R. (1999). *Methanobacterium thermoautotrophicum* encodes two multisubunit membrane-bound [NiFe] hydrogenases. Transcription of the operons and sequence analysis of the deduced proteins. *Eur. J. Biochem.* **264**, 930-43.

Thauer, R. K. (2001). Enzymology. Nickel to the fore. *Science* **293**, 1264-5.

Thauer, R. K., Jungermann, K. & Decker, K. (1977). Energy conservation in chemotrophic anaerobic bacteria. *Bact. Rev.* **41**, 100-80.

Thauer, R. K., Klein, A. R. & Hartmann, G. C. (1996). Reactions with molecular hydrogen in microorganisms - evidence for a purely organic hydrogenation catalyst. *Chem. Rev.* **96**, 3031-3042.

Tran-Betcke, A., Warnecke, U., Bocker, C., Zaborosch, C. & Friedrich, B. (1990). Cloning and nucleotide sequences of the genes for the subunits of NAD-reducing hydrogenase of *Alcaligenes eutrophus* H16. *J. Bacteriol.* **172**, 2920-9.

van der Spek, T. M., Arendsen, A. F., Happe, R. P., Yun, S., Bagley, K. A., Stufkens, D. J., Hagen, W. R. & Albracht, S. P. (1996). Similarities in the architecture of the active sites of Ni-hydrogenases and Fe-hydrogenases detected by means of infrared spectroscopy. *Eur. J. Biochem.* **237**, 629-34.

Venyaminov, S. & Kalnin, N. N. (1990). Quantitative IR spectrophotometry of peptide compounds in water (H_2O) solutions. II. Amide absorption bands of polypeptides and fibrous proteins in alpha-, beta-, and random coil conformations. *Biopolymers* **30**, 1259-71.

Vgenopoulou, I., Gemperli, A. C., Dimroth, P. & Steuber, J. (2003). Inhibition of the Na^+-translocating complex I from *Klebsiella pneumoniae* with *N,N'*-dicyclohexylcarbodiimide. *Biopsektrum* **Sonderausgabe zur VAAM-Jahrestagung 2003**, 79.

Vignais, P. M., Billoud, B. & Meyer, J. (2001). Classification and phylogeny of hydrogenases. *FEMS Microbiol. Rev.* **25**, 455-501.

Volbeda, A., Charon, M. H., Piras, C., Hatchikian, E. C., Frey, M. & Fontecilla-Camps, J. C. (1995). Crystal structure of the nickel-iron hydrogenase from *Desulfovibrio gigas*. *Nature* **373**, 580-7.

Volbeda, A., Fontecilla-Camps, J. C. & Frey, M. (1996). Novel metal sites in protein structures. *Curr. Opin. Struc. Biol.* **6**, 804-12.

Weis, S. (2004). Charakterisierung eines essentiellen Glutamat-Restes in der membranständigen Untereinheit HycC von Hydrogenase 3 aus *Escherichia coli* und Überproduktion von Ech-Hydrogenase aus *Thermoanaerobacter tengcongensis* in *Escherichia coli*. Marburg: Philipps University Marburg.

Yagi, T. (1987). Inhibition of NADH-ubiquinone reductase activity by *N,N'*-dicyclohexylcarbodiimide and correlation of this inhibition with the occurrence of energy-coupling site 1 in various organisms. *Biochemistry* **26**, 2822-8.

Yagi, T. & Hatefi, Y. (1988). Identification of the dicyclohexylcarbodiimide-binding subunit of NADH-ubiquinone oxidoreductase (Complex I). *J. Biol. Chem.* **263**, 16150-5.

Yagi, T. & Matsuno-Yagi, A. (2003). The proton-translocating NADH-quinone oxidoreductase in the respiratory chain: the secret unlocked. *Biochemistry* **42**, 2266-74.

Yagi, T., Yano, T., Di Bernardo, S. & Matsuno-Yagi, A. (1998). Procaryotic complex I (NDH-1), an overview. *Biochim. Biophys. Acta* **1364**, 125-33.

Yano, T., Dunham, W. R. & Ohnishi, T. (2005). Characterization of the $\Delta\mu_{H^+}$-sensitive ubisemiquinone species (SQ_{Nf}) and the interaction with cluster N2: new insight into the energy-coupled electron transfer in complex I. *Biochemistry* **44**, 1744-54.

Yano, T., Magnitsky, S., Sled, V. D., Ohnishi, T. & Yagi, T. (1999). Characterization of the putative 2x[4Fe-4S]-binding NQO9 subunit of the proton-translocating NADH-quinone oxidoreductase (NDH-1) of *Paracoccus denitrificans* - Expression, reconstitution, and EPR characterization. *J. Biol. Chem.* **274**, 28598-28605.

Yano, T. & Ohnishi, T. (2001). The origin of cluster N2 of the energy-transducing NADH-quinone oxidoreductase: comparisons of phylogenetically related enzymes. *J. Bioenerg. Biomembr.* **33**, 213-22.

Zhang, J. K., White, A. K., Kuettner, H. C., Boccazzi, P. & Metcalf, W. W. (2002). Directed mutagenesis and plasmid-based complementation in the methanogenic archaeon

Methanosarcina acetivorans C2A demonstrated by genetic analysis of proline biosynthesis. *J. Bacteriol.* **184**, 1449-54.

Zorin, N. A., Dimon, B., Gagnon, J., Gaillard, J., Carrier, P. & Vignais, P. M. (1996). Inhibition by iodoacetamide and acetylene of the H-D-exchange reaction catalyzed by *Thiocapsa roseopersicina* hydrogenase. *Eur. J. Biochem.* **241**, 675-81.

ACKNOWLEDGEMENTS

First and most of all I would like to express my gratitude to PD Dr. Reiner Hedderich for trusting me and giving me the chance to work on this challenging project, for supporting my research, for the inspiring discussions and for advising my work.

Hence, I would like to thank Prof. Dr. Rudolf K. Thauer for his advice and professionalism and for his readiness to help me. I appreciate to have been allowed to work in his department.

In particular, I would like to express my gratitude to PD Dr. Petra Hellwig for the fruitful collaboration concerning the FT-IR spectroscopic characterization of Ech hydrogenase.

Herewith, I would also like to thank Adam Guss and Prof. Dr. William Metcalf for their crucial help in generating the *echF* mutants.
I would also like to acknowledge Dr. Antonio Pierik and Dr. Evert Duin for their help with EPR spectroscopy and EPR simulations.

Furthermore, I would like to thank each member of the Hedderich, Thauer and Shima working groups for the constructive help, stimulating discussions and good working atmosphere. Special thanks go to Dr. Basem Soboh for providing me with fresh *C. hydrogenoformans* cells whenever I needed and also for the really great time working together and for his friendship. I would like to thank Jürgen Koch, for his support in diverse situations and especially for the huge help in cultivating the various strains. I would like to acknowledge Reinhard Böcher, Dr. Manfred Irmler and Horst Henseling for their technical support. I am also very grateful to Monika Schmidt for her help in many different situations, also outside the lab. I would like to acknowledge Dr. Markus Krüer, Henning Seedorf and Sebastian Weis for their help in molecular biology works. Special thanks go to Dr. Erica Lyon for her patience in going through various manuscripts and above all for her friendship and warm support.

I would also like to take this opportunity to thank the DFG Graduiertenkolleg „Protein function at the atomic level“ and the Max-Planck-Gesellschaft for the financial support.

I would like to thank Henning for his patience during this last gruelling year, for his warm support and for providing contact to the outside world.

Last but not least, I would like to thank my parents and my brother, Tomaso: without their special love, support, patience and encouragement it would have not been possible to get to this point!

LEBENSLAUF

Persönliche Daten

Name:	Lucia Forzi
Geburtsdatum:	08.07.1974
Geburtsort:	Mailand/Italien
Familienstand:	ledig

Schulausbildung

1980–1985	Scuola elementare “Rismondo” (Grundschule)
1985–1988	Scuola media “Favetti” (Mittelschule)
1988–1993	Liceo scientifico “Duca degli Abruzzi” (naturwissenschaftliches Gymnasium)
07.1993	Abitur
Gorizia, Italien	

Studium

11.1993–12.2001	Studium von Scienze ambientali (“Environmental Sciences”) an der Università Urbino (1993-1996) und an der Università Ca’ Foscari Venezia (1996-2001), Italien
03.1999–07.1999	Austauschstudentin innerhalb des EU Erasmus/Socrates Programmes an der Phillipps-Universität Marburg
03.2000–06.2000	Praktikum in der Arbeitsgruppe von PD Dr. R. Hedderich in der Abteilung für Biochemie am Max-Planck-Institut für terrestrische Mikrobiologie, Marburg
07.2000–06.2001	Diplomarbeit am MPI für terrestrische Mikrobiologie unter der Leitung von PD Dr. R. Hedderich zum Thema “Probing the proton-pumping function of *Escherichia coli* hydrogenase 3, an enzyme related to energy conserving NADH:quinone oxidoreductase”
11.12.2001	Verteidigung der Diplomarbeit, Universität Venedig, Italien
seit 03.2002	Dissertation am MPI für terrestrische Mikrobiologie in der Arbeitsgruppe von PD Dr. R. Hedderich zum Thema “Energy-converting [NiFe] hydrogenases in archaea and bacteria: insights into the energy-transducing mechanism”

Erklärung

Ich versichere, dass ich meine Dissertation

„Energy-converting [NiFe] hydrogenases in archaea and bacteria: insights into the energy-transducing mechanism"

selbständig, ohne unerlaubte Hilfe angefertigt und mich dabei keiner anderen als der von mir ausdrücklich bezeichneten Quellen und Hilfen bedient habe.

Die Dissertation wurde in der jetzigen oder einer ähnlichen Form noch keiner anderen Hochschule eingereicht und hat noch keinen sonstigen Prüfungszwecken gedient.

Marburg, _____ _____

(Lucia Forzi)